IMMUNE MODIFYING EFFECT OF DRUG FREE PLGA NANOPARTICLES ON THE COURSE OF EXPERIMENTAL AUTOIMMUNE NEURITIS (EAN)

Dissertation

zur

Erlangung des Doktorgrades (Dr. rer. nat.)

der

Mathematisch-Naturwissenschaftlichen Fakultät

der

Rheinischen Friedrich-Wilhelms-Universität Bonn

vorgelegt von

Ehsan Elahi

aus

Sialkot, Pakistan

Bonn, 2023

Angefertigt mit Genehmigung der Mathematisch-Naturwissenschaftlichen Fakultät der Rheinischen Friedrich-Wilhelms Universität Bonn.

Promotionskommission:
1. Gutachter: Prof. Dr. Marcus Müller
2. Gutachter: Prof. Dr. Alf Lamprecht

Tag der Promotion: 16.01.2024

Erscheinungsjahr: 2024

Dedicated to my beloved Family (especially my daughter, Irha Fatima).
You truly are the greatest gift God has ever given me.

Table of Contents

1. Introduction

1.1. Nanoparticles

Nanotechnology refers to an emerging field of science that deals with the engineering of materials, such as nanoparticles, on the nanoscale (1-1000 nm). The nanoengineering of such materials moulds their structures to interact with biological systems at molecular level, enabling them to play their potent role in unprecedented ways (Srikanth & Kessler, 2012).

Nanoparticles are spherical and solid structures that can be prepared from synthetic and natural sources (Hans & Lowman, 2002; Hillaireau & Couvreur, 2009). Nanoparticles range from 1-1500 nm in size and can be synthesized from almost every compound that is biologically non-degradable such as gold, silver, carbon, iron, and silica, and from biologically degradable compounds like polysaccharides. In 1989, the first nanoparticle-based therapeutics was approved by the FDA. Then with time, more nanoparticle-based therapies have been approved with the main emphasis on dose optimization and pharmacokinetic paradigms of small molecules (Getts et al., 2015; Smith et al., 2013).

Nanoparticles can be synthesized by multiple methods mainly reliant on their application needs (Crucho & Barros, 2017). In the current literature, most commonly used method to prepare polymeric nanoparticles is the solvent evaporation method (Rao & Geckeler, 2011). Briefly, a solution is prepared by dissolving polymer into an organic solvent. Under high homogenization, this solution is added to water phase that usually contains an emulsifying agent or surfactant e.g., polyvinyl alcohol to form an emulsion. Once stable emulsion is prepared, evaporation or removal of organic solvent is carried out by raising the temperature under reduced pressure or constant stirring at room temperature. This results into the preparation of solid nanoparticles. These solid nanoparticles are then collected using ultracentrifugation method and stabilising residue e.g., surfactants are removed by washing with distilled water followed by lyophilisation of nanoparticles for long term storage (Crucho & Barros, 2017; Rao & Geckeler, 2011).

Another widely used method in preparation of polymeric nanoparticles is emulsification-solvent diffusion. This method involves formation of typical oil in water emulsion between a semi miscible solvent which contains the polymer and surfactant bearing aqueous solution. The process involves mutual saturation of water and polymer solvent at room temperature to affirm the thermodynamic equilibrium of both. Then, the polymer-aqueous saturated solvent is mixed with surfactant containing aqueous solution, inducing solvent diffusion to the external phase, and resulting in generation of nanoparticles. Subsequently, the excessive solvent is then evaporated or filtrated depending on its boiling point (Cheaburu-Yilmaz et al., 2019; Crucho & Barros, 2017).

To prepare polymeric nanoparticles in an emulsified system, another common method is salting out technique. This technique is developed to overcome the use of such organic solvents which are toxic to the physiological system and environment as well. To summarize, the desired polymer are added in an organic solvent which is miscible in water phase. The solution obtained is mixed with an aqueous solution comprising of surfactant and a salting out agent under continuous stirring. The frequently used salting out agents are calcium chloride, magnesium acetate and magnesium chloride. The purpose of using salting out agent is to form an emulsion which is carried out by preventing miscibility of organic solvent in water phase. The resulting emulsion is diluted with water leading to precipitation of polymer and formation of nanoparticles. To remove the remaining salting out agents and solvent crossflow filtration method is applied (Krishnamoorthy & Mahalingam, 2015).

Nanoprecipitation method also known as solvent displacement method was established by Fessi et al., for the formulation of polymer-based nanoparticles(Fessi et al., 1989). The basic principle of this method is precipitation followed by solidification of polymers because of interfacial deposition of polymer which is caused by displacement of semipolar solvents miscible with aqueous phase, from a lipophilic solution. In this method polymers can be emulsified in hydrophilic organic solvents and then mixed with aqueous solution containing a surfactant under the continuous stirring. A quick diffusion of organic solvent into water phase occurs due to reduction in interfacial tension between the organic and aqueous phases(Krishnamoorthy & Mahalingam, 2015). During the solvent flow, uniformly sized nanoparticles are formed instantly, which highlights the efficiency and consistency of this technique for producing polymeric nanoparticles(Rao & Geckeler, 2011).

Nanoparticles can be prepared such that, they can either be delivered alone or in conjugation with a variety of substances such as pharmacological drugs, peptides, proteins, DNA (for gene therapy), miRNAs and even the gene editing tools which target the clustered regularly interspaced short palindromic repeat (CRISPR) constituents. Nanoparticles are mainly used to facilitate the delivery of specific drugs to their target site. Secondly, they can also interact with specific targets without carrying an active pharmacological drug. These properties of nanoparticles can play an important role in the development of clinical applications of nanotechnology (Getts et al., 2015).

In addition to the application of nanoparticles as a drug delivery system, recently a novel approach has been carried out in which nanoparticles without any drug or other pharmacological substances were used. Interestingly, drug free nanoparticles exerted their modulating effect on various disease models when applied systemically. This intriguing novel approach has emerged as a new application of nanoparticles in which they can be applied directly as disease modifying

agents, independent of their drug delivery role (Getts et al., 2014; Saito et al., 2019; Sharma et al., 2022; Y. Zhang et al., 2021).

The purpose behind the use of drug free nanoparticles in the medical field is that they have unique feature which makes them favourable in therapeutic application as they don't require an active pharmacological agent to exert their therapeutic effect (Saito et al., 2019).

From previous experimental studies, it is proposed that downstream therapeutic outcome of drug free nanoparticles mainly relies on their physicochemical properties i.e, surface charge and size (Dobrovolskaia et al., 2008; Dobrovolskaia & McNeil, 2007; Getts et al., 2015; Sharma et al., 2022). Nanoparticles can infiltrate deeply into tissue and are generally taken up efficiently by the endothelial cells (Bala et al., 2004). The uptake mechanism and pathways of nanoparticles into the cells have been extensively studied (Fleischer & Payne, 2012; Hillaireau & Couvreur, 2009; Treuel et al., 2013; Wachsmann & Lamprecht, 2012; Walczyk et al., 2010). Nanoparticles are taken up into the cells via endocytic pathways such as phagocytosis (via complement receptor-, Fcγ receptor, scavenger receptor and mannose receptor-mediated pathways)(Dobrovolskaia & McNeil, 2007). During phagocytosis, opsonin proteins tag the nanoparticles enabling them to present to the cells which leads to their phagocytosis (Lu et al., 2009). Other endocytic pathways that may also be involved in the internalization of nanoparticles into the cells include macropinocytosis, caveolae-mediated endocytosis, clathrin-mediated endocytosis and clathrin/caveolin-independent endocytosis (Hillaireau & Couvreur, 2009; Dobrovolskaia & McNeil, 2007). Generally, it is believed that nanoparticles which are less than 100nm size are effectively taken up by calthrin or caveolae mediated pathways. Whereas larger nanoparticles are internalized by phagocytosis (Getts et al., 2015). According to previous preclinical studies on cargo free nanoparticles, it is suggested that surface charge on the nanoparticles plays an important role in the cellular interaction with nanoparticles and influences their disease modulating potential. This emerging approach suggested that, upon entering into biological system, these drug free nanoparticles may influence the immune cell's location thus resulting in modulation of immune response. They selectively impede the infiltration of circulatory immune cells into specific inflammatory loci resulting in disease amelioration (Casey et al., 2019; Getts et al., 2015; Saito et al., 2019; Y. Zhang et al., 2021). Drug-free nanoparticles can be engineered to attain maximal therapeutic efficacy, as the cellular processes and the underlying pathophysiology of the diseases are understood (Sharma et al., 2022). Table 1 describes a brief description of various in vivo studies in which disease modifying role of drug free nanoparticles were investigated.

Table 1. Immune modulatory effects of drug free nanoparticles in animal models (in vivo studies)

Particle type	**Size**	**Zeta potential**	**Experimental disease model**	**Remarks**	**References**
Silver Nanoparticles	15nm	-32.4mV	Wild-type C57BL6/J male mice (9-weeks old)	Increased expression of IL-10	(Botelho et al., 2018)
Gold (Au)	70nm, 140nm	-29.9mV(140nm) -44.4 (70nm)	Skin wound model on C57BL/6 mice (8-weeks old)	Reduced the inflammatory response	(Xu et al., 2021)
Superparamagnetic iron oxide nanoparticles (SPIONs)	21nm	-27.31mV	HT1080 xenograft tumours on female BALB/c mice (female, 4–5 weeks old)	Reduced tumour growth	(Zhang et al., 2020)
Polystyrene	500 nm	-50mV	Mouse model of West Nile virus, encephalitis, (EAE),	Improved survival rate	(Getts et al., 2014)
Polystyrene	500nm	-50mV	triglyceride peritonitis, DSS-induced colitis	Reduction in Inflammation Improvement in disease severity	(Getts et al., 2014)
Polystyrene	500nm	-50mV	cardiac and kidney ischemia-reperfusion models	Reduction in inflammation and infarct size	(Getts et al., 2014)
Polystyrene	500nm	-48.9mV	LPS-instilled acute lung injury. (ALI) model in C57BL/6 and BALB/c mice	Reduction in neutrophil accretion in lungs. Lung injury improved	(Fromen et al., 2017)

1.2. PLGA Nanoparticles

Among the various polymers used to formulate the polymeric nanoparticles, Poly (lactic-co-glycolic acid) (PLGA) is one of the most extensively used polymers. PLGA is a biodegradable polymer, which becomes hydrolysed to its monomer metabolites, lactic acid, and glycolic acid. These two endogenous monomers are metabolized via the Krebs cycle, providing a less systemic toxicity associated with the use of PLGA nanoparticles (Kumari et al., 2010).

When used in drug delivery applications, PLGA nanoparticles ensure a sustained in vitro release of incorporated antigens for a long period (Slutter et al., 2010). For targeted drug delivery, PLGA based nanoparticles have many advantages over other nano formulations. They enhance the stability of the active ingredient and prevent it from degradation. In addition, due to their easy access to specific tissues because of their size, PLGA nanoparticles are able to deliver the active pharmacological agents, proteins, and nucleic acids to the desired site of action. By assuring a steady release of active ingredients at the target site, PLGA nanoparticles enhance the efficacy of treatment. Another important advantage of using PLGA nanoparticles over other types of polymers is that PLGA is approved by Food and Drug Administration (FDA) and European Medicine Agency (EMA) in various options of drug delivery systems, making PLGA based nanoparticles a firm candidate for further clinical trials (Danhier et al., 2012). PLGA nanoparticles can also work as a cargo system when formulated with a single antigen or in combination with other antigens (Brunner et al., 2010). However, PLGA nanoparticles can also be designed to be delivered at the target site and bind to the receptors without formulating with an active pharmacological drug (Casey et al., 2019; Getts et al., 2014, 2015; Saito et al., 2019).

1.3. Immune Modulating Effects of Drug Free PLGA Nanoparticles

Beside their application as a drug delivery system, PLGA nanoparticles can have modulating effects on the immune system when applied systemically. Recent studies in which PLGA nanoparticles have been used for immune modulation have shown promising therapeutic outcomes in pre-clinical disease models. For instance, negatively charged PLGA nanoparticles without any active pharmacological agent or adjuvant have been used to target specific cells of the mononuclear cell system which restored the immune tolerance by regulating the atypical activity of the monocytes during an acute immune response. Inflammatory monocytes are involved in various immune mediated autoimmune disorders. During an immune mediated response, inflammatory monocytes are differentiated into dendritic cells or macrophages which may release proinflammatory mediators such as proteases, cytokines and nitric oxide, resulting in tissue damage (Getts et al., 2014; Saiito et al., 2019).

Experimental studies on the EAE model by Getts et al. revealed that the charge on the nanoparticle surface plays an important role and induces the amelioration of disease. In their studies, they used positive, neutral, and negatively charged nanoparticles in the treatment of EAE in the mice model. From their results, particles with a negative surface charge reduced the severity of the disease and improved the survival rate of animals as compared to other particle treatment groups.

Getts et al., showed that negatively charged drug free PLGA nanoparticles bind with the circulating inflammatory monocytes through the macrophage receptor with collagenous structure (MARCO). As a result, these inflammatory monocytes no longer migrated to the inflammation loci and were sequestered in the spleen, thus abrogating the inflammatory response. They administered negatively charged drug free PLGA nanoparticles in mouse models of various immune mediated diseases such as experimental autoimmune encephalomyelitis (EAE), inflammatory bowel disease, West Nile virus (WNV) encephalitis and acute myocardial infarction (Getts et al., 2014).

It is well known that in EAE, circulating inflammatory monocytes are recruited to the central nervous system for disease induction resulting from the migration of these circulating monocytes through the blood brain barrier and their infiltration into the brain. EAE severity is linked with the intensity of this monocyte infiltration (Saito et al., 2019). Daily intravenous administration of 17.75mg/kg of 500 nm negatively charged drug free PLGA nanoparticles from the onset of disease ameliorated the disease symptoms which was evidenced by the reduced clinical score and less infiltration of monocytes into the brain. Similar results were reported when animals suffering from WNV encephalitis were treated with drug free PLGA nanoparticles (Getts et al., 2014). In addition to EAE model, these drug free PLGA nanoparticles were used in the mouse models of spinal cord injury, where they exerted their immunomodulatory effect with improvement in motor function (Jeong et al., 2017).

Other than neurological disease models, drug free PLGA nanoparticles played a role in other immune mediated disease models. For instance, treatment with drug free PLGA nanoparticles in an anterior descending artery occlusion model in mice significantly reduced the cardiac inflammation and promoted tissue repair. Treatment with drug free PLGA nanoparticles also reduced the symptoms of inflammatory bowel disease, which was evidenced by the reduced trafficking of inflammatory monocytes into the colon (Getts et al., 2014). A reduction in growth rate of tumour resulting in increased survival rates has been observed with the treatment of drug free PLGA nanoparticles(Zhang et al., 2021). Treatment with drug free PLGA nanoparticles downregulated the release of cytokines and expression of TLR-induced costimulatory molecule,

thereby playing their role in the treatment of animal model of sepsis (Casey et al., 2019). Taken together, the immunomodulatory effects of PLGA-particles appear promising in the treatment of a variety of diseases in which the immune system is pathophysiologically relevant.

A summary of their findings from the use of negatively charged drug free PLGA nanoparticles in various experimental disease models is presented in the table (Table 2.) below.

Table 2. Efficacy of drug free PLGA nanoparticles in various experimental disease models

Experimental disease model	**Remarks**	**Zeta Potential**	**Reference**
Acute myocardial infarction	Reduction in inflammation and infarct size	-50mV	(Getts et al., 2014)
Inflammatory bowel disease (IBD)	Reduction in Inflammation, improvement in clinical symptoms	-50mV	(Getts et al., 2014)
WNV encephalitis	Improvement in survival rate	-50mV	(Getts et al., 2014)
Experimental autoimmune encephalitis	Reduction in inflammation and demyelination, improvement in symptoms	-50mV	(Getts et al., 2014)
Experimental autoimmune encephalitis	Reduction in inflammation and demyelination, improvement in symptoms	-40.6	(Saito et al., 2019)
Spinal cord injury model	Improvement in the recovery of motor function	-30mV	(Jeong et al., 2017)
Sepsis	Downregulation of TLR-induced costimulatory molecule expression and cytokine secretion.	-40mV	(Casey et al., 2019)
Metastatic breast cancer	Reduction in tumour growth and improved survival rate.	-20.1mV	(Zhang et al., 2021)

1.4. Guillain-Barre Syndrome (GBS)

Guillain-Barré Syndrome (GBS) is an acute paralytic autoimmune disease that mainly affects the axons and myelin, specifically causing demyelination and axonal nerve damage in the peripheral nervous system (PNS). It is considered as one of the most commonly occurring paralytic autoimmune diseases that accounts for a large number of deaths and morbidity (van den Berg et al., 2014). GBS was first defined by Guillain, Strohl and Barré in 1916 with symmetrical, rapid onset-paraparesis and areflexia (Guillain et al., 1916).

The mechanism and pathogenesis of GBS is not completely understood. The histopathology of GBS is characterized by demyelination and inflammation of the PNS, which points towards an autoimmune attack against antigens of the PNS. This results in injury to the axons or myelin sheaths (Hughes & Cornblath, 2005; Schwerer, 2002).

Before the onset of GBS, most of the patients typically show the symptoms of gastrointestinal tract or respiratory tract infections. One hypothesis that describes the triggering of the autoimmune response in GBS is the mechanism of molecular mimicry. In the molecular mimicry process, infectious or exogenous agents such as Campylobacter jejuni, Epstein-Barr virus, Mycoplasma pneumoniae, cytomegalovirus, Haemophilus influenzae and non-infectious agents such as vaccination (Influenza), chemotherapy and bone marrow transplant may initiate an immune response against autoantigens (van den Berg et al., 2014). In this mechanism, the host is infected with an infectious agent containing antigens which are immunologically similar to the host's antigens but are adequately different enough to generate an autoimmune response when they interact with the T cells. This results in the reduction of tolerance to autoantigens, and the infectious agent-specific immune response which is initiated reacts with the host structures leading to tissue damage. However, the molecular mimicry hypothesis does not completely explain the underlying immunological mechanism of GBS (Hartung et al., 2001). In the immunopathogenesis of GBS, humoral and cellular responses are involved. Antibodies and activated autoreactive T cells breach the blood nerve barrier, which triggers an inflammatory response resulting in axonal damage and demyelination (van Doorn et al., 2008).

The major issues in the management and treatment of GBS are, good ICU management comprising respiratory care, anticoagulant therapy, early treatment and monitoring of autonomic ailments. Two disease modifying therapies, high dose of intravenous immunoglobulin (IVIG) and plasma exchange, have proved to be effective in improving motor recovery (Hartung et al., 2001). The first effective treatment in speeding recovery in GBS patients was plasma exchange. Its therapeutic effectiveness was more profound when administered within the first two weeks of disease onset in patients with impaired walk. In comparison to plasma exchange, IVIG treatment

administered within the first two weeks of disease onset was found to be as efficacious as plasma exchange. However, concomitant treatment with plasma exchange followed by administration of IVIG does not significantly provide a better treatment option than plasma exchange or IVIG alone. Moreover, the use of steroidal drugs such as methylprednisolone or prednisolone do not significantly improve the recovery in GBS patients (Yuki & Hartung, 2012).

1.5. Experimental Autoimmune Neuritis (EAN)

Experimental autoimmune neuritis is an immunological animal model which resembles many clinical, immunological, histological as well as electrophysiological aspects of Guillain-Barre syndrome. Therefore, due to aforementioned aspects of EAN, this disease model has been widely used to study the demyelinating diseases of the peripheral nervous system (Kieseier et al., 2004).

1.5.1. Induction of EAN

In 1955, experimental autoimmune neuritis was first described by two scientists Waksmann and Adams, who inoculated the peripheral nerve antigen in rabbits (Waksman & Adams, 1955). Moreover, less uniformity in the motor impairment of EAN was observed in rabbits as compared to Lewis rats. Therefore, rabbit models are not often used to study EAN. Alternatively, Lewis rat models are more commonly used to study EAN because of their higher susceptibility and ease of handling (Fujioka, 2018).

Active induction of experimental autoimmune neuritis in rats can be done by bovine P2 protein, peptides containing neuritogenic peptides with amino acid sequence 53-78 or human recombinant P2 protein emulsified in complete freund's adjuvant (Mäurer & Gold, 2002). Today, this is the most examined and standardized animal model of GBS.

Principally, it is widely accepted that a number of PNS-antigens can also exert their neuritogenic effects and can be suitable targets for studies of disorders of the peripheral nervous system (Schmidt, 1999). Experimental studies have also revealed that less purified myelin proteins PMP22 and P0 also have neuritogenic effects in rats (Gabriel et al., 1998). Some antigens such as Myelin basic protein (MBP) and Myelin associated glycoprotein (MAG), are shared by central and peripheral nervous systems which can induce inflammatory response. These antigens mainly affect the spinal cord but in rat’s cellular infiltrations have also been reported both in the sciatic nerve and spinal nerve roots (Abromson-Leeman et al., 1995; Weerth et al., 1999).

1.5.2. Clinical Presentation of EAN in rats

The early clinical presentation of EAN starts with weakness of the animal's tail and then progressively impairs motor function ascending from distal to proximal. Impaired walk and movement can be observed in the later phase of disease. Abrupt weight loss after immunization is a marker of the onset of the disease and weight loss correlates with the disease progress. Symptoms usually appear about 10-12 days after immunization (Luongo et al., 2008; Moalem-Taylor et al., 2007). Mortality of animals has been reported with severe progress of the disease. In the case of slow progression of the disease or non-mortality, a brief period of retention is observed, followed by gradual recovery (Arnason & Soliven, 1993).

1.5.3. Neuropathological Features of EAN

Histological studies of EAN lesions were reported with segmental demyelination and perivenular infiltration of cells in the peripheral nerves (Mäurer et al., 2002). Light microscopic observations from animal studies showed that during the initial development of EAN lesions seen after 12-16 days of immunization, perivenular infiltration of monocytes with less or no demyelination was observed. These infiltrates were attached to or within the walls of the blood vessels. After the third week of immunization, a complete demyelination of axons occurred followed by accumulation of macrophages with myelin debris.

Through electron microscopic analysis of EAN lesions, an early stage of EAN lesion appearance of myelinated axons remained normal (Ballin & Thomas, 1969; Lampert, 1969). Monocytes are usually found below and between endothelial cells. An extent of plasma protein was also leaked by the vessels which are traversed by these monocytes. The preliminary change in the structure of nodes of Ranvier leads to the separation of myelin from the axonal part and loss of the nodal process of Schwan cells. In normal myelin sheaths, Schwan cells exhibit an increased proportion of ribosomes and granular endoplasmic reticulum. At the initial phase, myelinated sheaths of such Schwann cells seem to be intact but occasionally it is breached by cytoplasmic processes of monocytes. These invading cytoplasmic processes from mononuclear cells project underneath the lamina and attack the mesaxon. After getting access into the space between the external most myelin and the Schwan cell outer tongue, which is filled with cytoplasm, the invading monocytes surround the myelin sheath. Dissolution of myelin sheath occurs after invasion of monocytes. After dissolution, phagocytes pass through the defective myelin and remove the remaining intact myelin fragments. Pairs, individual lamellae or thick strata of compact myelin are stripped off from the sheaths, this phenomenon is called macrophage mediated demyelination. Thus, in this process, the complete fragment of myelin sheath is detached from one node of Ranvier to the next (Lampert, 1969). From immunohistochemical studies of experimental autoimmune neuritis

(EAN), it was observed that macrophages and lymphocytes infiltrated the peripheral nerves culminating in nerve demyelination. Immunohistochemical staining of EAN lesions showed that macrophages were the predominant cell population and significantly outnumbered T cells (Mathias Mäurer et al., 2002).

1.5.4. Immunological Mechanism of EAN

The precise mechanism consisting of immunological and cellular steps involved in the disease course development of EAN is not yet elucidated. In general, it is postulated that following immunization with autoantigens, T cells and macrophages play a pivotal role in demyelination of the peripheral nerves (Gold et al., 1999).

1.5.4.1. Role of T cells in EAN

Observations from EAN lesion studies affirmed the important role of T cells in mediating the immune response in the pathogenesis of Guillain-Barre syndrome (Arnason & Soliven, 1993). After active immunization, the injected autoreactive antigen is presented to the "naïve" T cells by antigen presenting cells such as macrophages and dendritic cells, culminating in the activation of CD4+ T cells. T-cells mostly express the CD4+ phenotype before the onset of symptoms, whereas the CD8+ phenotype is expressed throughout the disease course of EAN, but their role is not well defined (Mathias Mäurer et al., 2002). To activate the T cells by antigen presentation, two types of signals are mandatory. One is an antigen dependent signal which is given by an immunogenic peptide and is presented in the context of molecules of MHC on antigen presenting cells. The other type of signal is antigen independent which is mediated by different costimulatory molecules expressed both on the T cells and antigen presenting cells such as, VCAM-1, ICAM-1 and B7 (Gold et al., 1999). After activation, T-cells circulate in the bloodstream, attach to the vascular endothelium in the peripheral nervous system and cross the BNB, recruiting more T cells, B cells and macrophages to amplify the immune response by releasing cytokines and chemokines (Hartung et al., 1996). Activation of T cells is a hallmark for the pathogenesis of EAN and GBS. A high titer of circulating T cells possessing activation markers has been observed in GBS patients (Taylor & Hughes, 1989). After activated T cells leave the circulation and enter the peripheral nervous system, they are presented to the non-neuronal cells, such as Schwann cells, and endoneurial antigen presenting cells (resident macrophages) with a suitable epitope in the context of MHC-II, which turns into the proliferation of T cells and secretion of cytokines (Gold et al., 1999).

T cells differentiate into two types: Th1 and Th2, which secrete different cytokines. In the acute phase of EAN, Th1 mediated response is predominant which is characterized by high expressions of proinflammatory cytokines such as IL-1β, TNF-α and - γ. However, during the recovery phase,

Th2 response is predominant, as indicated by high expressions of anti-inflammatory cytokines such as IL-10 and tissue growth factor (TGF-b1) (Zhang et al., 2013). This immune mediated response is consistent with the Th1/Th2 paradigm which suggests that Th1 cells promote the disease, whereas Th2 cells provide a countermeasure to reduce the Th1 response (Lambracht-Washington & Wolfe, 2011).

1.5.4.2. Adhesion and Transportation of T cells and Macrophages

To induce an inflammatory response in the sciatic nerve milieu, activated T cells have to cross the blood nerve barrier (BNB) and enter into the PNS. A complex process of adhesion and migration involving adhesion molecules (AMs), matrix metalloproteinases and several chemokines are involved in the transportation of activated T cells across the BNB (Kieseier et al., 2004). During an inflammatory response, proinflammatory cytokines such as TNF-α, IL-1β, IL-2, IL-4, and IL-6, released by Schwann cells, mast cells and resident macrophages, induce expression of adhesion molecules on endothelial cells which forms the blood-nerve barrier (Ho et al., 1998).

Three types of adhesion molecule families are involved in the migration of leukocytes across the endothelium. Selectins, integrins, and proteins which are members of the Ig superfamily. Selectins roll the leukocytes along the endothelium. Sialic acid-containing carbohydrates serve as ligands for selectins. Rolling of these leukocytes is followed by strong adhesion with endothelial cells. On strong adhesion, the presence of a suitable chemoattractant such as macrophage inflammatory protein (MIP-1), facilitates the monocytes to cross the endothelial barrier (Ho et al., 1998). Presence and up regulation of adhesion molecules on the ligands of monocytes and endothelium during the peak disease condition marks the important role of AMs in propagating inflammation in EAN (Gold et al., 1999).

In an acute phase of EAN, upregulation of adhesion molecules such as vascular cell adhesion molecule (VCAM-1) and intracellular adhesion molecule (ICAM-1) on the lesion adjacent to blood vessels is directly associated with disease propensity and inflammatory monocytes infiltration (Enders et al., 1998; Stoll et al., 1993). This was further supported when attenuation in the severity of EAN was observed with the treatment of EAN with ICAM-1 mAbs (Archelos et al., 1994; Enders et al., 1998). Complement receptor 3 is an adhesion molecule, expressed by macrophages and involved in the development of EAN, which interacts with ICAM-1 to recruit macrophages into PNS (Chen et al., 2015).

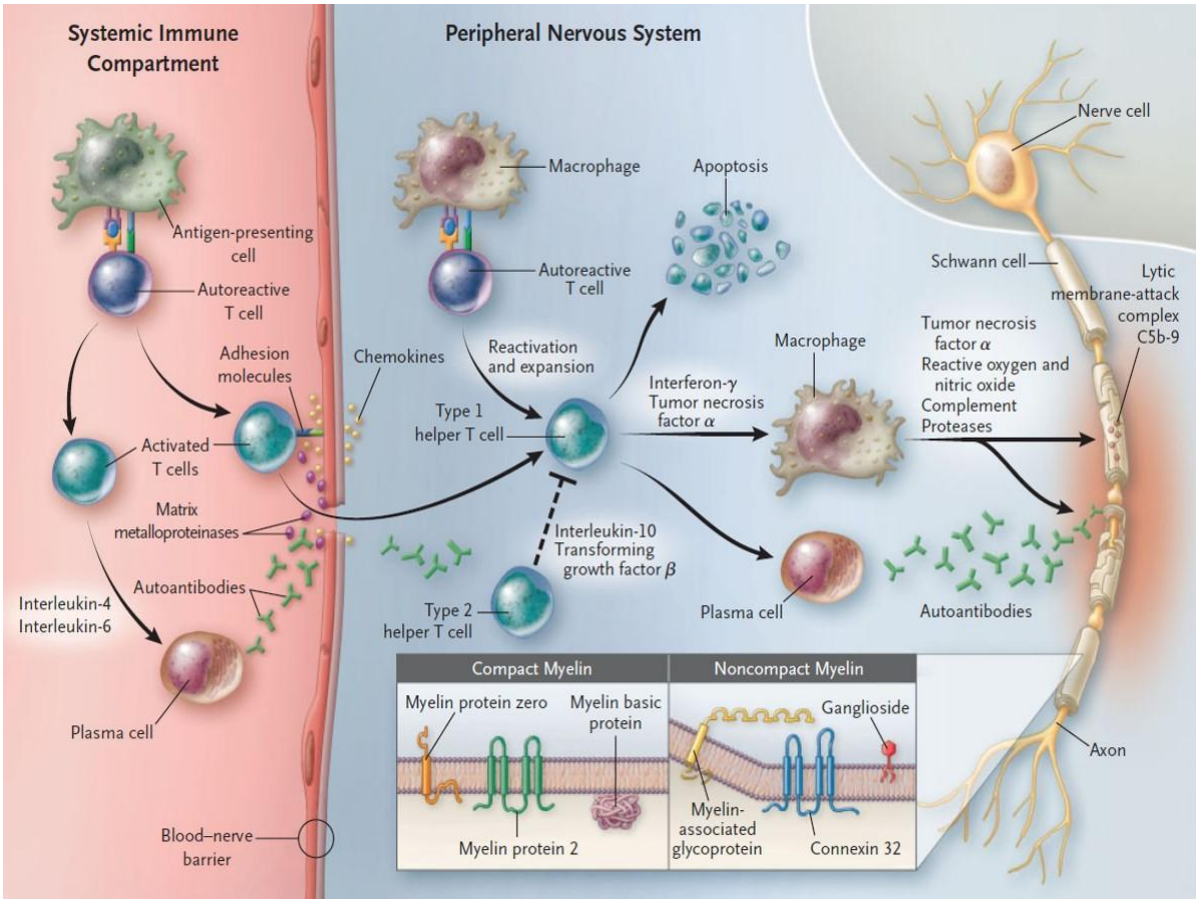

Figure 1. Simplified scheme depicting the hypothetical sequence of major immune mechanisms in EAN (Köller et al., 2005).

1.5.4.3. Role of Macrophages in EAN

Macrophages are considered to be involved in all phases of EAN such as, early phase of immune surveillance, mechanism of antigen presentation, initiation of immune cascade by activation of immune cells throughout the disease span, antigen specific demyelination, axonal destruction, non-specific secondary tissue damage, debris removal and regeneration (Kiefer et al., 2001; Müller et al., 2006).

In an immune response, antigen presenting macrophages express and upregulate the MHC-I and MHC-II class antigens (Nyati et al., 2011). In the early phase of EAN, blood nerve barrier permeability and trafficking of circulating monocytes across the blood nerve barrier are crucial. Macrophages play an important role in this process by modulating the release of chemokines, cytokines, matrix metalloproteinases (MMP), Nitric oxide (NO), and adhesion molecules (Zhang et al., 2013).

Macrophages can be classified into two types, classically activated (proinflammatory) macrophages M1 and alternatively activated (anti-inflammatory) macrophages M2. These M1/M2 types mirror the Th (Th1/Th2) polarization (Mantovani et al., 2004; Martinez et al., 2008). Antigen presenting macrophages play an important role in the promotion of Th1 polarization (Shen et al., 2018). Once polarized, the Th1 cells cause the activation of macrophages (M1).

Activated M1 macrophages can upregulate the expression of MHC-II, inflammatory cytokines, adhesion molecules and reactive oxygen intermediates (ROI), culminating in inflammation, breakage of BNB and demyelination. For the activated macrophage phenotype M1, CD68 is considered as a typical marker (Han et al., 2016; Zhang et al., 2013). CD68 is a lysosomal membrane protein, mostly found on activated microglia and macrophages (Zhang et al., 2008). Upregulation of CD68 has been observed in EAN during the disease course (Han et al., 2016).

In the initial phase of EAN, monocytes roll along the endothelium with the help of adhesion molecules like selectins (Tedder et al., 1995). After adhesion with endothelial cells, chemotactic signals pave the way for monocytes into nerve milieu. Amidst many chemokines, some are very important in the context of gradual development of EAN (Luster, 1998). In EAN, high mRNA expression of macrophage inflammatory proteins MIP1a and MIP1b from the early to the peak phase, indicates their important role in the recruitment of macrophages (Kieseier et al., 2000). To breach into the endothelium and basal lamina, proteases like matrix metalloproteinases (MMP) are required. In EAN models, high mRNA expressions of MMPs were observed together with the infiltrating monocytes, indicating their pivotal role in the recruitment of macrophages and the penetration of BNB (Kiefer et al., 2001; Kieseier et al., 1999).

Activated macrophages M1 can induce nerve demyelination in EAN by secreting many proinflammatory cytokines such as TNF-α, IL-6 and IL-12 (Shen et al., 2018; Zhang et al., 2013). Macrophages can induce axonal degeneration and demyelination by releasing reactive oxygen species such as Nitric oxide (NO). IFN-γ and TNF-α stimulate the production of NO by inducible Nitric oxide synthase in the macrophages, which is associated with peripheral nerve demyelination (Kiefer et al., 2001; Shen et al., 2018). Besides phagocytic attack by activated macrophages, another hypothesis regarding nerve demyelination is also relevant. It is suggested that antibodies bind to the macrophages through the Fc receptor and direct these macrophages towards the antigen binding sites on the myelin of axons and initiate antibody mediated cytotoxicity. Furthermore, antibodies might also induce the activation of the complement pathway which culminates into the formation of the complement complex resulting in antibody mediated cellular toxicity. Therefore, antibodies might be involved in the opsonization of antigenic sites and promote their phagocytosis by macrophages (Mathias Mäurer et al., 2002).

In addition to blood derived macrophages invading the peripheral nerve, there exists a population of resident macrophages which reside in the endoneurium of the sciatic nerve. In case of nerve injury, these resident endoneurial macrophages can swiftly react by upregulating MHC-II molecules and phagocytosing the myelin prior to infiltration by homogeneous macrophages (Mueller et al., 2003).

In comparison to M1 macrophages, M2 macrophages may exhibit a neuroprotective effect in pathogenesis of EAN (Shen et al., 2018). M2 macrophages may induce axonal remyelination and regeneration by increasing apoptosis of T cells (Kiefer et al., 2001). CD163 is considered to be expressed in M2 macrophages (Mantovani et al., 2004; Shen et al., 2018). They are also involved in promoting the secretion of anti-inflammatory cytokines i.e., TGF-beta and IL-10 (McWhorter et al., 2015). Arginase and activin A are abundantly expressed by M2 macrophages, which promotes arginase-1, resulting in the downregulation of iNOS, leading to the reduction of secretion of NO. This promotes the regeneration of axons (Mokarram et al., 2012).

1.5.4.4. Role of Cytokines in EAN

Cytokines play varying roles during different phases of EAN. For instance, there is a proportional relation between the release of proinflammatory cytokines such as IL-1β, IL-2, IL-17, IFN- γ, TNF-α and TNF-β and their disease promoting role in the clinical progression of EAN. While the elevation of tissue growth factor TGF- β and IL-10 is related to the recovery phase of EAN (Zhang et al., 2013). Some of the cytokines that play an important role in the development and progress of EAN are described in this section.

IFN- γ, produced by Natural Killer cells, classically activated macrophages (M1) and CD4+ Th1 cells, plays an important role during Th1 mediated innate immune response. It activates the macrophages, endothelial cells, Schwann cells and T cells, eliciting its proinflammatory function. It is also involved in the upregulation of MHC-II expression in Schwann cells and macrophages. Serum analysis from the acute phase of GBS reported an increase in levels of IFN- γ. The clinical condition of GBS patients was ameliorated with the administration of antibodies that targeted IFN- γ (Zhang et al., 2013).

TNF-α plays a vital role in the development and progression of EAN. In the peripheral nerves, elevated mRNA expression of TNF-α has been reported during the peak phase of clinical EAN. Administration of TNF-α into the sciatic nerves of rats induced endoneurial inflammatory response resulting in axonal destruction and demyelination. Furthermore, intravenous administration of TNF-α significantly aggravated the EAN. In GBS patients' serum, elevated TNF-α levels have been associated with disease propensity. Immune modifying therapy reduced the TNF-α levels in GBS patients' serum, which is in agreement with the clinical recovery of GBS (Zhang et al., 2013).

IL-1β serves a key role as a proinflammatory cytokine. It is involved in the activation of Schwan cells to secrete the IL-6 (Bolin et al., 1995). Upon microbial or inflammatory stimulation, mononuclear cells promptly synthesize IL-1β. Lymphocyte function-associated antigen 1 (LFA-1), an adhesion molecule, and IL-1β play a costimulatory role in the activation of T cells. In

cooperation with TNF-α, IL-1β is a strong promoter of adhesion molecules and triggers the protease release. Autoimmune response in EAN is suggested to be instigated by IL-1β (Zhu et al., 1997).

IL-6 is one of the important cytokines which plays a role in the induction of an immune response. IL-6 is produced by numerous cell types, such as T cells, monocytes, and Schwann cells. IL-6, together with other inflammatory cytokines such as TNF-α, IFN- γ and IL1, is affiliated with a group of endogenous cytokines which are secreted by the host during an inflammatory response. IL-6 is also considered to be involved in BNB disruption. During the early onset of EAN, increased levels of IL6 have been observed. It was reported that IL-6 levels were upregulated during peak EAN, whereas during the recovery phase they were downregulated (Zhu et al., 1998). IL-10 is involved in reducing proinflammatory cytokine production as well as inhibiting the antigen presenting function of cells. It also induces humoral immune response and helps in the inhibition of proliferation of T cells. During the recovery phase of EAN and GBS, it has been reported that the mRNA expressions of IL-10 and TGF-β are elevated. Moreover, IL-10 is crucially involved in the production of Tregs. The inflammatory responses in EAN were improved when treated with recombinant IL-10 (Zhang et al., 2013).

1.5.5. Recovery Phase

After the peak phase of disease is achieved, animals start to recover. Apoptosis of autoreactive T-cells is an important mechanism in the termination of inflammatory response in the peripheral nervous system. In experimental autoimmune neuritis, apoptosis of T cells in the peripheral nerves occurs early, peaking at the time of elevated T cell infiltration (Gold et al., 1999; Kiefer et al., 2001). It is believed that macrophages might induce apoptosis by releasing pro-apoptotic cytokines like NO and reactive oxygen intermediates (Weishaupt et al., 2000; Wu et al., 1995; Zettl et al., 1997). Moreover, macrophages release anti-inflammatory cytokines like TGF-β and IL-10. IL-10 has shown disease alleviating property when administered before and during the onset of EAN (Bai et al., 1997). Macrophages are vastly involved in the repair process of peripheral nerves by promoting proliferation of Schwann cells, remyelination and axonal regeneration once the inflammatory process is halted (Kiefer et al., 2001).

1.5.6. Treatment studies of EAN

Various therapeutic approaches have been carried out to abrogate the immune attack and reduce the severity of the disease course of the EAN. These therapeutic approaches are generally effective in the management of EAN, even though their mechanism of action is not completely known. It is commonly suggested that the therapeutic drugs or agents used in these approaches might be involved in inducing a cytokine balance shift from Th1 response to Th2 response

(Fujioka, 2018). Some of the therapies used and their subsequent effects on the disease course of EAN are mentioned in the following table (Table 3.).

Table 3. Treatments and their effects on EAN

Treatment	**Effects**	**References**
Steroid	Suppressed paralysis and electro-physiological findings. Relapse not significant	(Stevens et al., 1990)
Pentoxifylline	Improved EAN, TNF-α inhibitors	(Constantinescu et al., 1996)
Matrix metalloproteinase inhibitors (BB-1101)	Improved EAN, TNF-α inhibition	(Redford et al., 1997)
Thalidomide	suppressed T cell response	(Zhu et al., 1997)
Antidepressants i. Imipramine ii. Clomipramine	Improved EAN through T-/B-cell response	(Zhu et al., 1998)
Rolipram	Improved EAN, TNF-α inhibitors	(Zou et al., 2000)
Leflunomide	Prevented paraparesis	(Korn et al., 2001)
Cyclooxygenase-2 inhibitors i. Celecoxib ii. Meloxicam	Reduced histopathological damage of the sciatic nerve	(Miyamoto et al., 2002)
Atorvastatin	Improved EAN, Th1 to Th2 shift was observed	(Kiyozuka, 2005)
Immunoglobulins	Improved EAN (Reduced histological score)	(Lin et al., 2007)
Lovastatin	Improved EAN, Th1 to Th2 shift was observed	(Sarkey et al., 2007)
Crotapotin	Reduction in the mononuclear cells infiltrating the sciatic nerve	(Castro et al., 2007)
Valproic acid	Suppressed the expression of IL-1β, IL-6	(Zhang et al., 2008)
Minocycline	Reduction in the mononuclear cells infiltrating the sciatic nerve IL-1β inhibition	(Zhang et al., 2009)
Sildenafil	Accelerated the recovery of EAN	(Kudeken, 2009)
Quinpramine	Suppressed the monocyte infiltration	(Hörste et al., 2011)
Angiotensin II receptor blocker (Irbesartan)	Chemokine receptor -2 inhibition may be involved	(Kiazono et al., 2014)

Natural herbal medicines (Curcumin)	Reduced the mRNA expression of IL-1β	(Han et al., 2014)
Immunoglobulin	Improved the Clinical symptoms of EAN by suppressing the MIP-1α	(Kajii et al., 2014)
Dimethyl fumarate	Improved EAN by altering the balance of M1/ M2 macrophages	(Han et al., 2016)
Fingolimod	Reduced the Levels of circulating T cells	(Ambrosius et al., 2017)
Human Immunoglobulin	Reduced the levels of activated macrophages and T cells	(Pitarokoili et al., 2017)
Cilostazol	Reduced maximum paralysis	(Hagiwara et al., 2018)

2. Aim of the Study

Although many conventional therapies have been proposed for the treatment of Experimental Autoimmune Neuritis (EAN) as shown in Table 3., with the exception of IVIG, so far none of them have been established as a clinical application in the treatment of GBS patients. Here, it was assumed that a therapy which is based on nanoparticles could be an intriguing alternative approach to treat EAN. As mentioned earlier, Getts et al. reported that negatively charged PLGA nanoparticles without bearing an active pharmacological drug, have ameliorated the disease progression of EAE, a multiple sclerosis disease model (Getts et al., 2014). Keeping in view their reports, it was hypothesized that the administration of negatively charged PLGA nanoparticles without any active pharmacological drug attached to them could also exhibit their immune modifying effect in the disease course of Experimental Autoimmune Neuritis (EAN). In the presented study, the main concern was to determine the therapeutic efficacy of drug free negatively charged PLGA nanoparticles (NPs) on the disease course of EAN as well as their impact on the infiltration of proinflammatory monocytes into the peripheral nervous system. Moreover, it was envisaged that if there is any effect of change in the size, dose and surfactant modifications of NPs on the disease course.

3. Materials and Methods

3.1. Preparation and Administration of NPs

NPs were prepared by the conventional oil-water emulsion solvent evaporation technique. A quantity of 100mg PLGA was first dissolved in 5 mL of ethyl acetate, forming the organic phase. This organic solution was then poured into 10 mL of an aqueous surfactant solution, containing either polyvinyl alcohol (PVA) or sodium cholate. A primary coarse emulsion was then further homogenised using ultrasonic cell disruptor (Banoelin sonopuls, Berlin, Germany) for 2 min on an ice bath, followed by solvent evaporation under reduced pressure using a Büchi Rotavapor RE 120 (Büchi, Flawil, Switzerland). The preparation conditions were adjusted to produce NPs with monomodal size distributions and mean diameters of around 130 and 500 nm by changing the concentration of surfactant. This was achieved by using 1% (*w*/*v*) or 0.2% (*w*/*v*) of PVA to obtain NPs with a nominal diameter of 130 and 500 nm, respectively, while sodium cholate was used at concentration of 0.1% *w/v* in the aqueous phase. For the preparation of PCL-PVA nanoparticles, PCL was dissolved in 2ml of ethyl acetate forming the organic phase. This organic solution was then poured into 12 ml of an aqueous PVA solution (1% w/v) to form a coarse emulsion, which was then further homogenized using ultrasonic cell disruptor (Banoelin sonopuls, Berlin, Germany), followed by solvent evaporation using a Büchi Rotavapor RE 120 (Büchi, Flawil, Switzerland). Unbound surfactant was removed from the supernatant by a dialysis step (membrane cut-off: 100 kDa), formulations were then freeze dried without cryoprotectant, and redispersed in isotonic phosphate buffered saline (pH7.4) prior to injection.

After immunization with P2-peptide, NPs, surfactant and polymer-modified nanoparticles were re-suspended in Phosphate Buffer Solution (PBS) to a final concentration of 6.2mg/ml and administered to animals into the tail vein root. The administered dose (9 mg/kg) was calculated by using an equation of body surface area (Reagan-Shaw et al., 2008). Before euthanization of animals, the last three doses of NPs were given with a fluorescent dye attached FITC (fluorescein isothiocyanate) labelled NPs. To differentiate rats of each group, their tails were marked with permanent colouring markers. Following table shows the polymer, surfactant, size and zeta potential values of each nanoparticle type.

Table 4. Types of polymers and surfactant used in NPs preparation

NPs	Polymer	Surfactant	Size (nm)	Polydispersity Index	Zeta Potential (mV)
NP-PVA500	Poly (lactic-co-glycolic acid) (PLGA)	Polyvinyl alcohol (PVA)	497.5 ±12.2	0.05 ±0.01	−33 ± 1
NP-PVA130	Poly (lactic-co-glycolic acid) (PLGA)	Polyvinyl alcohol (PVA)	130 ± 10	0.071 ± 0.08	-44± 1
NP-Chol130	Poly (lactic-co-glycolic acid) (PLGA)	Na-Cholate	131.8 ± 2.5	0.06 ± 0.05	-40 ± 5
NP-PCL130	Polycaprolactone (PCL)	Polyvinyl alcohol (PVA)	130.5 ± 2.6	0.05 ± 0.07	-0.5±10

3.1.1. Determination of the Particle Size and Zeta Potential

The prepared NPs were analysed for their particle size and size distribution in terms of the average volume diameters and polydispersity index (PI) by photon correlation spectroscopy using particle size analyzer (Brookhaven Instruments Corporation, Holtsville, NY, USA) at a fixed angle of 90° at 25 °C. The nanoparticle suspension was diluted with distilled water before particle size analysis. Samples were diluted with a solution containing sodium chloride to adjust the conductivity to 50 μS/cm for zeta potential measurement. All samples were analyzed in triplicates at 25 °C and the error was calculated as standard deviation (S.D).

3.2. Animals and Ethics

All experimental procedures followed the guidelines of the German Animal Protection Law and were approved by the local authorities (Landesamt für Natur, Umwelt und Verbraucherschutz NRW; 84-02.04. 2014.A413). Animal husbandry and clinical score assessment experiments took place in the S1 (Sicherheitsstufe 1, §§ 4-7 GenTSV) animal facility of the university hospital in Bonn (Haus für experimentelle Therapy, HET).

Experiments were carried out using female Lewis rats, 6-8 weeks old. The animals were purchased from Charles River Laboratories (Sulzfeld, Germany). A maximum of four rats were housed in plastic cages. Cages were kept in the room under controlled illumination (light-dark cycle: 12:12 h) and environmental conditions (temperature: 22 ± 2 °C; humidity: 55 ± 5 %). Water (ad libitum) and food pellets were freely available for all rats. Animals were housed for at least four days before the start of the experiments.

3.3. Antigen

Immunogenic P2 peptide (amino acids 53-78) (RTESPFKNTEISFKLGQEFEETTADN) (Institute of Medical Immunology, Charité, Berlin, Germany) dissolved in sterile 1X phosphate-buffered saline (PBS) to a concentration of 2 mg/ml was used for P2-peptide immunization.

3.4. Immunization with P2-Peptide

P2-peptide (amino acids 53-78) emulsified with an equal volume of CFA (Complete Freund's adjuvant) (Sigma Aldrich, Germany) containing inactivated Mycobacterium tuberculosis particles in mineral oil was used to enhance the immunogenic effect of P2-peptide immunization. The resulting emulsion was tested by placing one drop of emulsion on the surface of water at room temperature. The drop of emulsion was not allowed to disperse. If it dispersed on the surface of water, then it would not be stable and hence not suitable for injection. P2 administration into hind paws and tail root were performed under the anaesthesia of Isoflurane 3% in 95% oxygen. All efforts were made to minimize the number of animals used and minimize their suffering. In the first two experimental studies, 100µg of P2-peptide emulsified with CFA containing 1mg/ml of inactivated mycobacterium tuberculosis particles was injected into each hind paw of the rats. In the following studies 100µg of P2-peptide emulsified with CFA containing 3mg/ml mycobacterium tuberculosis particles was injected into each hind paw of the rats and 200ug was injected into the tail root under the anaesthesia.

3.5. Clinical Score Assessment

Animals were weighed and scored for disease severity daily from the day of immunization till the end of the experiment. Disease progress and propensity was assessed clinically employing a scale ranging from zero to 10 originally described by (Enders et al., 1998): 0 normal; 1 hanging tail-tip; 2 tail paralysis; 3 absent righting/ inability to sit up; 4 gait ataxia abnormal position; 5 mild paraparesis; 6 moderate paraparesis; 7 severe paraplegias; 8 tetraparesis/ complete paralysis of all extremities; 9 moribund; 10 death. The accumulative score is the sum of the observed clinical scores of each animal at the end of the experiment.

3.6. Histology

3.6.1. Tissue Processing for Histology

The tissues for histological assessment, like routine histology and immunohistochemistry, were collected from each group of animals (P2- group, NP-group, and control). Immediately after, euthanasia sciatic nerves were collected from animals and were fixed overnight in PBS buffered 4% paraformaldehyde at 4 °C and were later washed with 1XPBS. For H&E (Haematoxylin and eosin) and immunohistochemistry on cryosections, tissues were embedded with Tissue Tek® (Sakura Finetek, Staufen, Germany) and snapped frozen in liquid nitrogen. Sections (10µm) were

prepared for H&E (Haematoxylin and eosin) and immunohistochemical analysis by using Leica microtome CM3050 S (Leica Biosystems, Germany).

3.6.2. Routine Histology and Immunohistochemistry

Frozen nerve sections were stained with H&E (Haematoxylin and eosin) for routine histological assessments. For immunohistochemistry, cryosections were first fixed with ice-chilled methanol/acetone. Endogenous peroxide was inhibited by 0.5% H2O2 in Methanol (Merck, Darmstadt) for 10 minutes. Sections were incubated with 10% bovine serum albumin to block nonspecific binding of immunoglobulins for 30 minutes at room temperature followed by overnight incubation with primary antibodies (1/100) at 4°C. Antibodies binding to tissue sections were visualized with secondary biotinylated antibodies (donkey anti-mouse; 1/200). Sections were treated with a horseradish peroxidase-conjugated Streptavidin complex (Vector Laboratories) (1/200) for 45 minutes. Signals were visualized by NovaRED colouring reagent (Axxora, Lörach, Germany) according to the manufacturer's instructions. A list of primary antibodies used with specifications and dilution is presented in Table 4. Conventional and immunohistochemical-stained sections were examined under a bright field and fluorescent microscope, E-800 Nikon eclipse (Nikon, Dusseldorf, Germany). Bright-field images were acquired using a 15.2 SPOTFLEX camera. The acquired fluorescence signals were merged using SPOT advanced 4.5 software (Diagnostic Instruments, Sterling, MI).

Table 5. List of Primary antibodies for histological examination of sciatic nerves

Antibody	**Specificity**	**Dilution**
ED-1 (CD68) (BioRad)	Activated Macrophages (Müller et al., 2006)	1:100
CD43 (W3/13) (BioRad)	T cells (Zhang et al., 2009)	1:100
OX-6 (BioRad)	MHC-II positive cells (Müller et al., 2006)	1:100

3.7. Flow Cytometric Analysis of Splenic Tissue

To determine the percentage of colocalization of nanoparticles into the cells, characterization of the immune cell population and the paradigm shift of macrophages, fluorescence-activated cell sorting (FACS) was used. At the end of the early onset treatment experiment (day 17 post immunization) with both the sizes of NPs (NP-PVA500, NP-PVA130), rats were anesthetized, and blood was drawn intracardially which was collected into tubes containing EDTA (Ethylenediaminetetraacetic acid). EDTA tubes containing blood samples were centrifuged at 500g at 4^0C and the supernatant was discarded. Then the samples were resuspended into 1ml of 1X PBS buffer solution (Roche Diagnostics, Mannheim, Germany) and transferred to FACS tubes. Approximately 2ml of RBC lysis buffer (BD Bioscience, San Jose, USA) with ratio of 1:10

(dist. Water) was added and incubated at room temperature for 10 minutes. Then the FACS buffer was added, and samples were subjected to centrifugation at 800g for 10 minutes at 4^0C. 100µl of sample was collected and blocked with CD16/CD32 (Fc block; BD Bioscience) antibody. Staining antibodies were added with a ratio of 1:100. Samples were incubated with fluorochrome-conjugated antibodies to detect CD45 (OX-1, Pecy5) and CD11b (OX-42, PeCy7) (BD Bioscience). NPs were conjugated with FITC dye and therefore, they were separated in FITC channel. After staining, antibody bound samples were detected using a BD FACSCanto II (BD Bioscience), and the gathered data was analysed using the flow cytometry software FlowJo 10 (TreeStar, San Carlos, CA).

In the flow cytometric analysis of splenocytes, animals were euthanized under anaesthesia (3% isoflurane, 95% oxygen) and spleens were removed carefully and placed in an ice-chilled petri dish containing 1XHBSS (Hank's Balanced Salt Solution; Gibco Life Technologies, Darmstadt, Germany). Spleen tissue was cut into pieces and homogenized using a needle (0.6x 25) and a syringe (5 ml) before passing it through a 70µm cell strainer (BD Bioscience, Heidelberg, Germany). The RBC lysis buffer was added into room temperature incubated splenocytes and then washed with PBS at 500g for 10 minutes at 4º C. Supernatant was discarded, and 100 µl of the sample was collected from each sample tube and blocked with a 1:100 ratio of CD16/CD32 (Fc block; BD Bioscience) antibody. Staining antibodies were added with a ratio of 1:50. Samples were incubated with fluorochrome-conjugated antibodies to detect CD45 (OX-1, Pecy5), CD11b (OX-42, PeCy7).

To determine the colocalization of nanoparticles with surfactant and polymer modification, at the end of early onset treatment (day 17 post immunization) with 130 nm NPs with different surfactant and polymer, flow cytometric analysis of blood and splenocytes was performed by following the above-mentioned protocol. Supernatant was discarded, and 100 µl of the sample was collected from each sample tube and blocked with a 1:100 ratio of CD16/CD32 (Fc block; BD Bioscience) antibody. Staining antibodies were added with a ratio of 1:50. Samples were incubated with fluorochrome-conjugated antibodies to detect CD45 (OX-1, Pecy5), CD11b (OX-42, PeCy7). (BD Bioscience), CD68 (ED1, PE) (eBioscience) CD163 (ED2, PE) (Bio-Rad AbD Serotec GmbH, Puchheim, Germany). NPs were conjugated with FITC dye, and therefore, they were separated in the FITC channel. After staining, antibody-bound samples were detected using a BD FACS Canto II (BD Bioscience), and gathered data was analysed using the flow cytometry software FlowJo 10 (TreeStar, San Carlos, CA).

Table 6. List of antibodies used in FACS analysis.

Antibody	**Dilution**
CD16/CD32 (Fc block; BD Bioscience)	1:100
CD45 (OX-1, Pecy5 (BD Bioscience)	1:50
CD11b (OX-42, PeCy7) (BD Bioscience)	1:50
CD68 (ED1, PE) (eBioscience)	1:50
CD163 (ED2, PE) (Bio-Rad AbD Serotec)	1:50

3.8. Determination of Inflammatory Markers and Cytokines by Real Time-PCR

Sciatic nerves from all animal groups (Control, P2, NPs) were collected and snapped frozen in liquid nitrogen. Total RNA was isolated from the whole sciatic nerve using Trizol (Sigma-Aldrich) reagent method. Total RNA (1µg) was reverse transcribed into cDNA by using SuperscriptTM III reverse transcriptase (Invitrogen, Germany). Quantitative PCR assays were carried out by using SYBRgreen. The composition of reaction mixture contained 1.5µl of cDNA, 1µl of each primer, 7.5µl Distilled H_2O, 10µl of 2X SYBR Green PCR SsoAdvanced Universal SYBR Green Supermix (Applied Biosystems, Darmstadt, Germany) in a total volume of 20µl. For Rt-PCR assay a pre incubation period of 2 minutes at 95 °C was chosen and 39 PCR cycles (5 minutes at 95 °C, and 30 minutes at 60 °C) were performed at CFX connect Real-Time PCR detection system (Applied Biosystems, Darmstadt, Germany). In each cycle, the SYBR Green fluorescence signal was measured. Samples were analysed simultaneously for GAPDH mRNA as housekeeping internal control. The mRNA levels for each target were normalized to mRNA levels of GAPDH and expressed relative to that of control animals. Each sample was assayed in duplicate. Data was determined as the mRNA fold of change ± SEM. Primer sequences of targets were as follows.

Table 7. List of qRT-PCR assays

Target	Primer pair	Sequence
GAPDH (Bio-RAD)	5′-GCATCTTCTTGTGCAGTGCC-3′ 5′-GATGGTGATGGGTTTCCCGT-3′	Forward Reverse
CD68 (Bio-RAD)	5′-CTTGGTGGCCTACAGAGTGG-3′ 5′-ACCCGGAGACGACAATCAAC-3′	
IL-1β (Bio-RAD)	5′-GCTCTCCACCTCAATGGACA-3′ 5′-GATTCTTCCCCTTGAGGCCC-3′	
TNF-α (Bio-RAD)	5′-TTCCTTACGGAACCCCCTCT-3′ 5′-CCCGTAGGGCGATTACAGTC-3′	
CD163 (Bio-RAD)	5′-CTGCGGGCACAAAGAAGATG-3′ 5′-TGAATGACCTGTGCCATGCT-3′	
IFN-γ (Bio-RAD)	5′-TCGAGGTGAACAACCCACAG-3′ 5′-CTACCCCAGAATCAGCACCG-3′	
IL-17 (Bio-RAD)	5′-GTGAAGGCAGCGGTACTCAT-3′ 5′-ATGTGGTGGTCCAACTTCCC-3′	

3.9. Experimental Study Outline

In the presented work, five in vivo experimental studies with different treatment goals were performed. At first, the therapeutic efficacy of 9 mg/kg (PVA500) NPs in the before onset and the early onset treatment of EAN was determined. Then in the third experiment, two different sizes (PVA500 nm, PVA130 nm) of NPs (9mg/kg) were used to determine their efficacy in the early onset treatment of EAN. While in the fourth experiment, three different doses (3mg/kg, 9mg/kg, 27mg/kg) of (PVA130) NPs were given to treat the animals in the before onset treatment of EAN. Then in the fifth experiment, NPs bearing different surfactants and another type of polymer-based nanoparticles (130 nm) in the treatment of EAN were used. In each experiment animals were divided into three main groups, one was control group which did not receive any treatment, the other was NP treatment in which P2-peptide immunized animals were treated with immune modifying NPs, while the last was P2-peptide group, in which animals only received P2-peptide immunization and did not receive any particle treatment. All the rats were monitored carefully for any unwanted effect till the end of the experiment. The study design of each experiment is explained in detail below.

I- Before-Onset Treatment with NP-PVA500

In this in vivo experimental study, the therapeutic efficacy of 9 mg/kg of PVA500 NPs before the onset of experimental autoimmune neuritis was determined. Rats were immunized with P2-peptide and monitored from the day of immunization till the end of the experiment. In before

onset treatment, NP-PVA500 were administered intravenously three days prior to the first symptom.

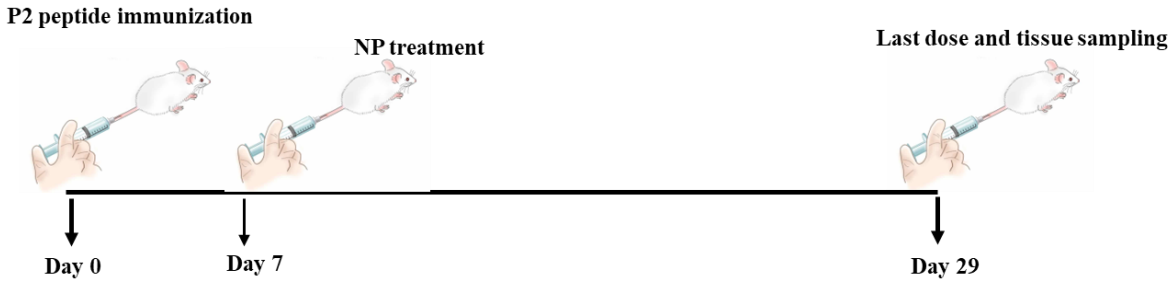

Figure 2. Study I: Before-Onset Treatment with NP-PVA500

Table 8. Experimental study groups in before onset treatment with NP-PVA500

Animal Group	Treatment	Number of animals
Control	-	3
P2-peptide	P2-peptide	13
NP-PVA500	P2-peptide-NP-PVA500	13

II- Early-Onset Treatment with NP-PVA500

In this in vivo experiment, NP-PVA500 were used to determine the immune modulating effect on the disease course of EAN. Intravenous administration of 9 mg/kg of NPs commenced at around day 12 when the early symptoms of EAN appeared.

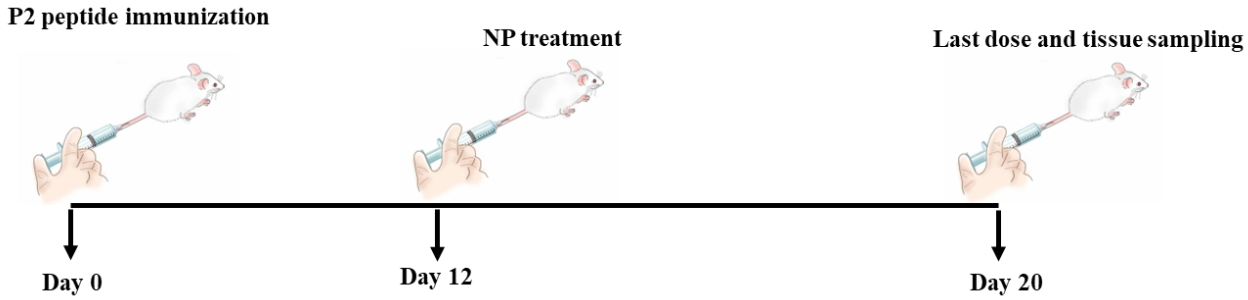

Figure 3. Study II: Early-Onset Treatment with NP-PVA500

Table 9. Experimental study groups in early onset treatment with NP-PVA500

Animal Group	Treatment	Number of animals
Control	-	3
P2-peptide	P2-peptide	11
NP-PVA500	P2-peptide-NP-PVA500	11

III- Early-Onset Treatment with Different Sizes (NP-PVA500, NP-PVA130)

In this experiment, the impact of different sizes of negatively charged NPs bearing no active pharmacological agent was determined on the disease course of EAN. Intravenous dose 9 mg/kg of both types of particles was started as the symptoms appeared.

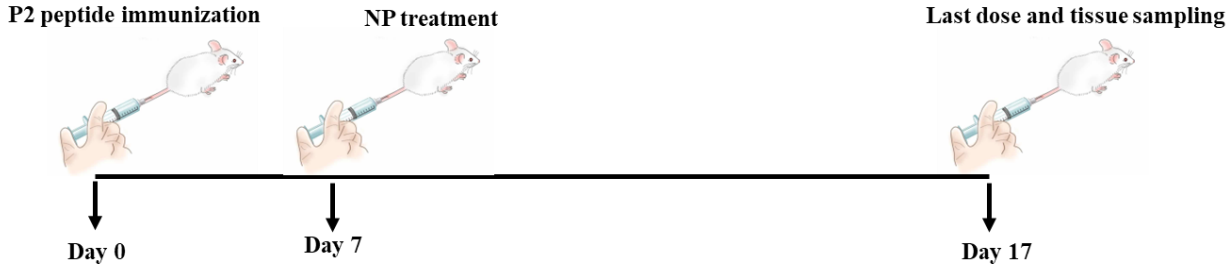

Figure 4. Study III: Early-Onset Treatment with Different Sizes of NPs

Table 10. Experimental study groups in determination of impact of different size of NPs on course of EAN

Animal Group	Treatment	Number of animals
Control	-	3
P2-peptide	P2-peptide	9
NP-PVA500	P2-peptide- NP-PVA500	9
NP-PVA130 nm	P2-peptide- NP-PVA130	9

IV- Dose dependent effect of NPs (NP-PVA130) on disease course of EAN

In this experiment, the dose dependent effect of negatively charged NP-PVA130 containing no active pharmacological ingredient was determined, before the onset of EAN. To determine the dose dependent effect and their efficacy on the disease course, three doses (3mg/kg, 9mg/kg, 27mg/kg) of NPs were used. All doses were administered intravenously before the disease symptoms appeared.

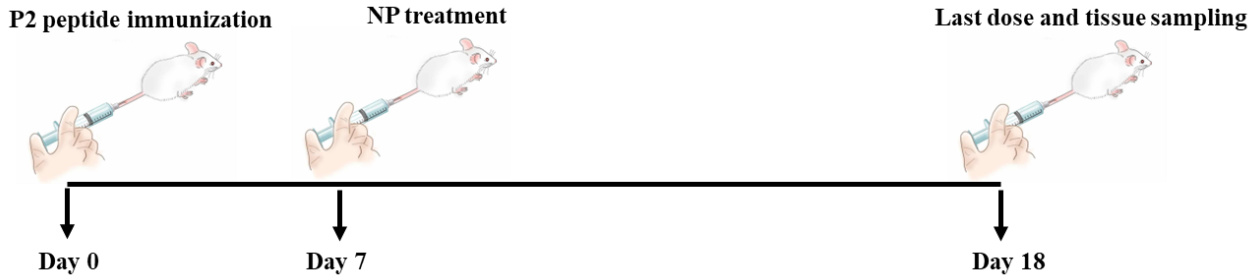

Figure 5. Study IV: Dose dependent effect of NPs on the clinical course of EAN

Table 11. Experimental study groups in determination of dose dependent effect of NPs

Animal Group	Treatment	Number of animals
Control	-	3
P2-peptide	P2-peptide	8
NP **(3mg/kg)**	P2-peptide- NP-PVA130	8
NP **(9mg/kg)**	P2-peptide- NP-PVA130	8
NP **(27mg/kg)**	P2-peptide- NP-PVA130	8

V- Surfactant modification effect on disease course of EAN

In this fifth experimental study, to determine the therapeutic efficacy of drug free NPs bearing different surfactants, another polymer-based nanoparticles Polycaprolactone (PCL) with Polyvinyl alcohol (PVA) surfactant (NP-PCL130) at the early onset of EAN were used. Herein, three different types of nanoparticles were used. One type was the previously used NPs bearing polyvinyl alcohol as surfactant, the second was NPs bearing sodium cholate as a surfactant, while the third particles were made up of Polycaprolactone polymer. An Intravenous dose of 9 mg/kg of each type of NPs was administered to the respective treatment group. However, for the FACS analysis of splenic tissues, the last three doses of NPs were given with fluorescent dye FITC labelled particles.

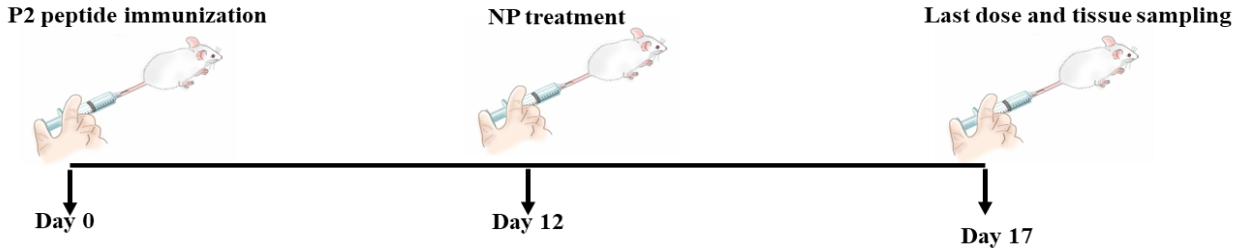

Figure 6. Study V: Surfactant modification effect on disease course of EAN

Table 12. Experimental study groups in determination of surfactant modification effect of NPs on disease course of EAN

Animal Group	Treatment	Number of animals
Control	-	3
P2-peptide	P2-peptide	5
NPs **-1 (NP-PCL130)**	P2-peptide-NP-PCL130	7
NPs **-2 (NP-Chol130)**	P2-peptide-NP-Chol130	7
NPs **-3 (NP-PVA130)**	P2-peptide-NP-PVA130	7

3.10. List of Materials Used

In this section, a comprehensive list of all the materials used in the course of this study is presented below.

Table 13. List of Chemicals

List of Chemicals	**Manufacturer**
PLGA (Resomer RG503H)	Evonik AG (Germany)
PVA (Mowiol 4-88),	Sigma-Aldrich, Germany
Sodium cholate	Sigma-Aldrich, Germany
Polycaprolactone	Sigma-Aldrich, Germany
Ethyl acetate	Sigma-Aldrich, Germany
NaCl	AppliChem GmbH, Germany
KCL	AppliChem GmbH, Germany
Na2HPO4	AppliChem GmbH, Germany
KH2PO4	AppliChem GmbH, Germany
HCL	AppliChem GmbH, Germany
NaOH	AppliChem GmbH, Germany
Paraformaldehyde	Sigma Aldrich, Germany
Complete Freund's adjuvant	Sigma Aldrich, Germany
Mycobacterium tuberculosis particles	Difco Laboratories GmbH, Germany
Bovine serum albumin	Boehringer Ingelheim, Germany
Trizol	Ambion by life technologies. Carlsbad CA, USA
Methanol	AppliChem GmbH, Germany
Ethanol	AppliChem GmbH, Germany
Isoflurane	Piramal Critical Care Deutschland GmbH
Eosin	Sigma Aldrich, Germany
Hematoxylin	Sigma Aldrich, Germany
H_2O_2	Carl Roth, Germany
DPX mountant medium	Sigma Aldrich, Germany
Tissue Tek®	Sakura Finetek, Staufen, Germany

Table 14. List of Solutions

I - 4% Paraformaldehyde, pH 7,4

For 1 Litre of 4% paraformaldehyde, pH 7,4
1 L 1XPBS at 40-50°C
5g NaOH
40 g paraformaldehyde
pH was adjusted to 7,4 with HCl and kept it at 4°C.

II- 1X Phosphate Buffer Solution

For 1 litre of 1X PBS
8.0 g NaCl
0.2 g KCL
1.44 g Na_2HPO_4
0.24 g KH_2PO_4
Distilled water
Adjusted pH to 7.4 and kept at room temperature**.**

Table 15. List of Reagents and kits

Reagents	**Manufacturer**
1X HBSS (Hank's Balanced Salt Solution	Gibco Life Technologies, Darmstadt, Germany
RBC lysis Buffer	eBioscience, San Diego, CA, USA
2X SYBR Green PCR Master Mix	Applied Biosystems, Darmstadt, Germany
SuperscriptTM III reverse transcriptase	Invitrogen, Germany
Horseradish peroxidase-conjugated Streptavidin complex	Vector Laboratories, Burlingame, CA, USA

Table 16. List of Equipment

Equipment	**Manufacturer**
CFX connect Real-Time PCR detection system	Applied Biosystems, Darmstadt, Germany
FACS Canto II	BD Bioscience, Germany
Bright field and fluorescent microscope, E-800 Nikon eclipse	Nikon, Dusseldorf, Germany
15.2 SPOTFLEX camera SPOT advanced 4.5 software	Diagnostic Instruments, Sterling, MI
Leica Microtome Leica CM3050 S	Leica Biosystems, Germany
Ultrasonic cell disruptor	(Banoelin sonopuls, Berlin, Germany)
Particle size analyzer	(Brookhaven Instruments Corporation, Holtsville, NY, USA)
Büchi Rotavapor RE 120	(Büchi, Flawil, Switzerland)
Heraeus MULTIFUGE 1S-R (centrifuge)	Applied Biosystems, Darmstadt, Germany

Table 17. List of antibodies

Antibodies	**Analysis**	**Catalog Number**	**Manufacture**
CD16/CD32	FACS	550271	BD Bioscience
Anti-Rat CD45 (OX-1)	FACS	559135	BD Bioscience
Anti-rat CD11b (OX-42)	FACS	562222	BD Bioscience
Anti-Rat MHC-II (OX-6)	FACS	MA5-17432	eBioscience
Anti-Rat CD68 (ED1)	FACS	MA5-16653	eBioscience, Germany
Anti-Rat CD163 (ED2)	FACS	MCA342PE	Bio-RadAbD Serotec
Anti-Rat ED-1 (CD68)	Histology	MCA341R	Bio-Rad, Germany
Anti-Rat CD43	Histology	MCA54R	Bio-Rad Germany
Anti-Rat OX-6	Histology	MCA2687R	(Bio-Rad, Germany

Table 18. List of RT-PCR Primers

RT-PCR Primers	**Unique Assay ID**	**Manufacture**
GAPDH	qRnoCID0057018	Bio-Rad, Germany
CD68	qRnoCED0005201	Bio-Rad, Germany
IL-1β	qRnoCID0004680	Bio-Rad, Germany
IFN- γ	qRnoCID0006848	Bio-Rad, Germany
IL-17	qRnoCED0004697	Bio-Rad, Germany
CD163	qRnoCID0008321	Bio-Rad, Germany
TNF-α	qRnoCED0009117	Bio-Rad, Germany

3.11. Statistical Analysis

For statistical analyses and generation of several graphs for this data, GraphPad Prism (GraphPad Software, San Diego, CA, USA) was used. For statistical analysis of clinical scoring data, a Mann-Whitney nonparametric *U*-test was used while for RT-PCR, a student's *t*-test (unpaired) was used. For the FACS data analysis, one-way ANOVA with a Bonferroni post-test and *t*-test (unpaired) was performed. Different levels of significance are given in the respective result sections, $p \leq 0.05$ (*), $p \leq 0.01$ (**) or $p \leq 0.005$ (***).

4. Results

4.1. Mild Disease Scenario

4.1.1. Before and Early Onset Treatment with NP-PVA500 improved the clinical course of EAN in rats

4.1.2. Before-Onset Treatment with NP-PVA500

In the recent past, the use of cargo free PLGA-NPs without any adjuvant or active pharmacological drug has established their worth by improving the clinical course of experimental autoimmune encephalitis (Getts et al., 2014). Considering the above notion this study was conducted using cargo free NPs without any drug to evaluate their therapeutic efficacy in the EAN disease model.

Of the 29 rats that were used, 3 were used as control, while 26 were immunized with P2-peptide emulsified with an equal volume of complete Freund's adjuvant containing Mycobacterium tuberculosis particles. 13 out of these 26 received only P2-peptide in their hind paws. Whereas the other 13 rats that received P2-peptide were also administered with a daily intravenous dose of 9 mg/kg of NP-PVA500 at the 7^{th} day of post immunization to evaluate the therapeutic efficacy of NPs.

All the animals were observed for a 29-day period. No mortality of any animal group was observed during the time period of the experiment. There was a significant difference in the mean clinical scores of P2-peptide and NP treatment (Figure 7. a).

Clinical symptoms of EAN appeared around the 9-10^{th} day of post-immunization. On the 10^{th} day, 30% of the P2-Peptide treated rats developed the initial disease symptoms, while 7 % of NPs treated animals were observed with similar symptoms. Though the disease severity was milder, the peak clinical score was 2.46 ± 0.14 in the P2 group and 1.30 ± 0.1*** in the NPs treated group ($p < 0.05$, Mann-Whitney test)**.** A statistically significant difference was observed in the accumulative scores of both the groups. The total score of the P2-peptide group was 24.19 ± 3.4 after 29 days of the experimental period, whereas the total score of NPs treated group was 4.84 ± 0.7***, which depicts the efficacy of particle treatment in lowering the propensity of EAN disease course (Figure 7. b). A summary of incidence, mortality, peak scores and the accumulative clinical scores of this experimental study are shown in Table 19. After achieving peak clinical score at around day 15-16, arrest or recovery phase of the disease followed. A clear attenuation of disease course has been observed with the before onset treatment of NP-PVA500.

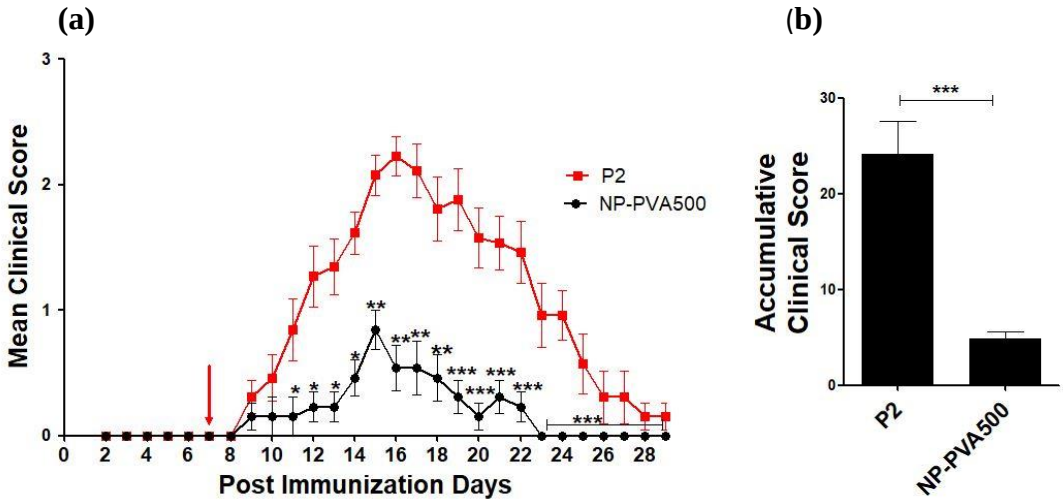

Figure 7. Before-Onset Treatment with NP-PVA500. **(a):** Mean clinical score (± S.E.M.) post immunization with P2-peptide and NPs. The P2-peptide (n=13) group was administered with P2-peptide only. The NP-PVA500 (n=13) group, in addition with P2-peptide, was administered with a daily intravenous dose of 9 mg/kg of NP-PVA500nm at the 7th day of post immunization. Arrow indicates the start of NPs treatment. Rats receiving NP treatment developed less severe disease symptoms, which was evidenced by lower clinical score. **(b):** Accumulative clinical scores of both groups have a statistically significant difference.

Animal group	Incidence	Mortality	Peak score	Accumulative clinical score
P2	13/13	0/0	2.46 ± 0.14	24.19 ± 3.40
NP-PVA500	13/13	0/0	1.30 ± 0.13***	4.84 ± 0.74***

Table 19. Peak and Accumulative clinical scores of Before Onset treatment with NP-PVA500. P ≤ 0.05 (*): significant, P ≤ 0.01 (**): very significant, P ≤ 0.005 (***): highly significant.

4.1.3. Before-Onset Treatment with NP-PVA500 reduced the inflammatory response in sciatic nerves

To correlate the clinical differences observed in P2-Peptide and NPs treatment of rats with histopathological findings, routine histology and immunohistochemistry were used to evaluate the inflammatory response in sciatic nerves of control, P2-peptide and NP treatment group. As expected, none of the control group animals exhibited any histopathological changes in routine histology and immunohistochemistry (Figure 8. a-d-g-j). However, extensive tissue destruction and accumulation of mononuclear cells in the perivascular region of sciatic nerves of P2-peptide group animals were observed (Figure 3. b), whereas a lesser extent of tissue destruction and less infiltration of monocytes were observed in the NP-PVA500 treatment (Figure 8. c).

To further characterize the infiltration of different types of inflammatory cells into the sciatic nerves, their immunohistochemistry was analysed. A high level of infiltration of activated macrophages (ED1) was observed in the perivascular region of the sciatic nerves of P2-peptide group animals (Figure 3. e). In contrast, a lesser population of activated macrophages were found in the sciatic nerves of the NPs treated animals (Figure 8. f). Furthermore, the sciatic nerves of P2-peptide group animals and NP-PVA500 treated animals were also examined for the distribution and accumulation of T-cells (CD43) and MHC-II (OX-6) positive cells. A substantial amount of CD43 and MHC-II positive cell population was observed in the sciatic nerves of the P2-peptide group. In contrast, a lesser population of these infiltrates was observed in the sciatic nerves of the NPs treated animals (Figure 8. h-i-k-l).

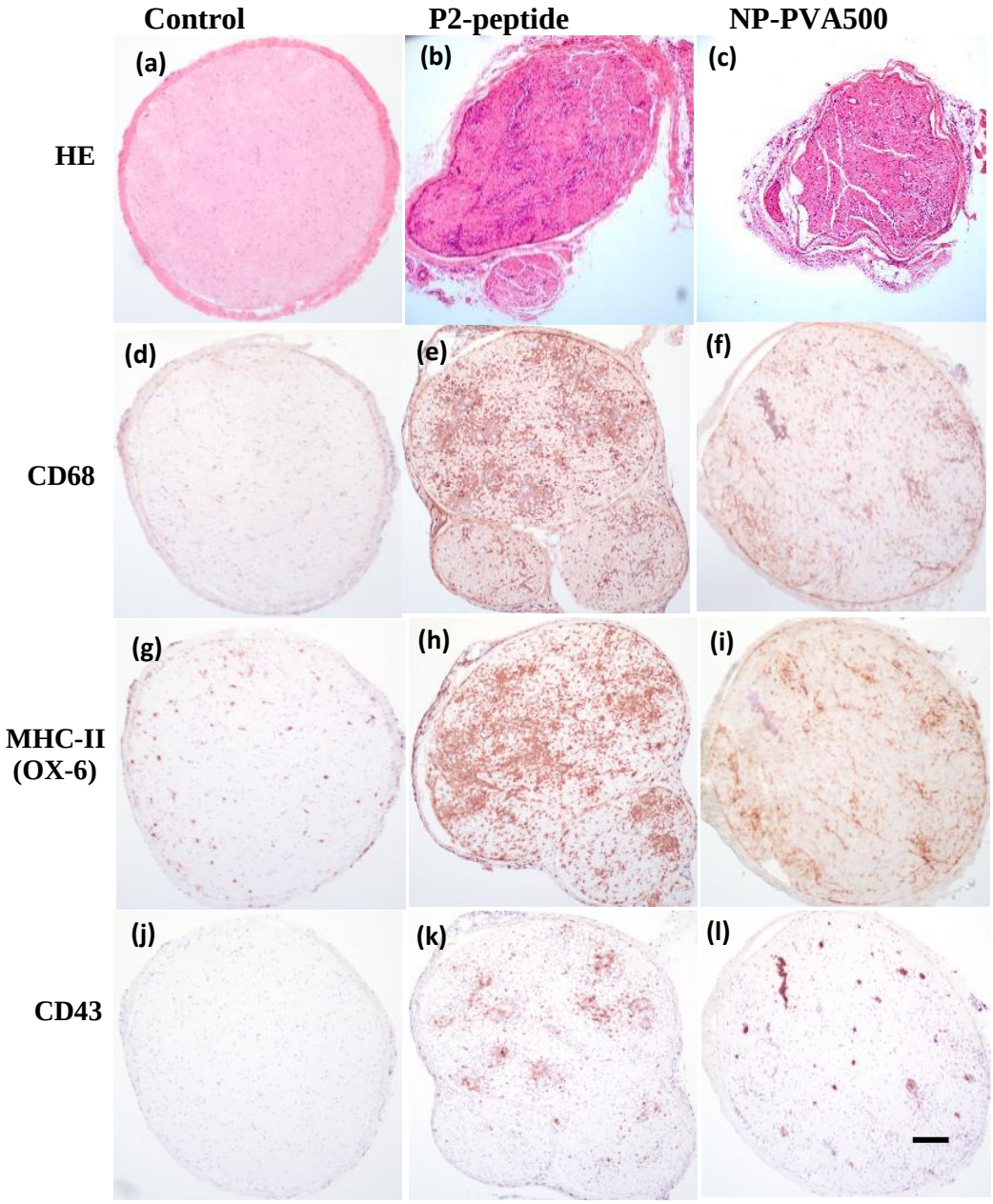

Figure 8. Histological changes in the sciatic nerves of control, P2-peptide, and NP-PVA500 treated animals and co-localization of infiltrates with routine H&E histology and immunohistochemistry. A high titer of activated macrophages (CD68) was observed in the P2-peptide group (**e**) in contrast to less proportion of macrophages found in the NP treatment group (**f**), while in the control animals no such response was observed (**d**). A considerable accumulation of T-cells (CD43+) was observed in P2 animals (**k**) at the end of the experimental phase, while a lesser population of T-cells was observed in the NP treatment group (**l**) at the same time. A clear difference in MHC-II (OX-6) positive cell population between the P2-peptide group and the particle treatment group was observed (**h**)(**i**). Magnification 10x. Scale bar represents 50µm.

4.1.4. Early-Onset Treatment with NP-PVA500 improved the clinical course of EAN in rats

In the Before Onset treatment experiment, it was observed that NP-PVA500 reduced the severity of EAN disease course. Therefore, this study was conducted to evaluate the therapeutic effectiveness of NP-PVA500 at the early onset of the disease course. Of the 25 female Lewis rats, 3 were used as control, whereas 22 were immunized with the inoculation of P2-peptide emulsified with an equal volume of complete Freund's adjuvant containing Mycobacterium tuberculosis particles. These rats were divided into two groups, as the disease symptoms appeared at around day 12. Of the 22 immunized rats, 11 rats received only P2-peptide in their hind paws. The other 11 rats received P2-peptide along with a daily intravenous dose of 9 mg/kg of NP-PVA500 at the early onset of EAN. All animals were observed for a 20-day period. No mortality in any of the animal groups was observed during the experimental period. Peak clinical score was achieved, and the arrest or recovery phase of the disease followed. (Figure 9. a).

Neurological symptoms of EAN appeared around 12^{th} day of post immunization. On the 14th day, approximately 55% of the animals treated with P2-peptide showed early disease symptoms, while 18% of the NP-PVA500 treated animals were observed with similar symptoms. The overall disease severity was milder in P2-peptide group achieving a maximal mean clinical score of 2.40 ± 0.13, whereas in the NP-PVA500 treated animals, the mean peak clinical score was 1.18 ± 0.12***. An early decline phase with NPs treatment was observed. This evidenced the therapeutic efficacy of early onset daily doses of intravenous cargo free NPs. Accumulative clinical scores of both the groups have a significant difference. The total score of P2-peptide group was 14.09 ± 1.0 after 20 days of the experimental period, whereas the total score of NP-PVA500 treated group was 4.90 ± 0.57*** (Figure 9. b). A brief overview of the incidence, mortality, peak scores and the accumulative clinical scores of this experimental study are shown in Table 20.

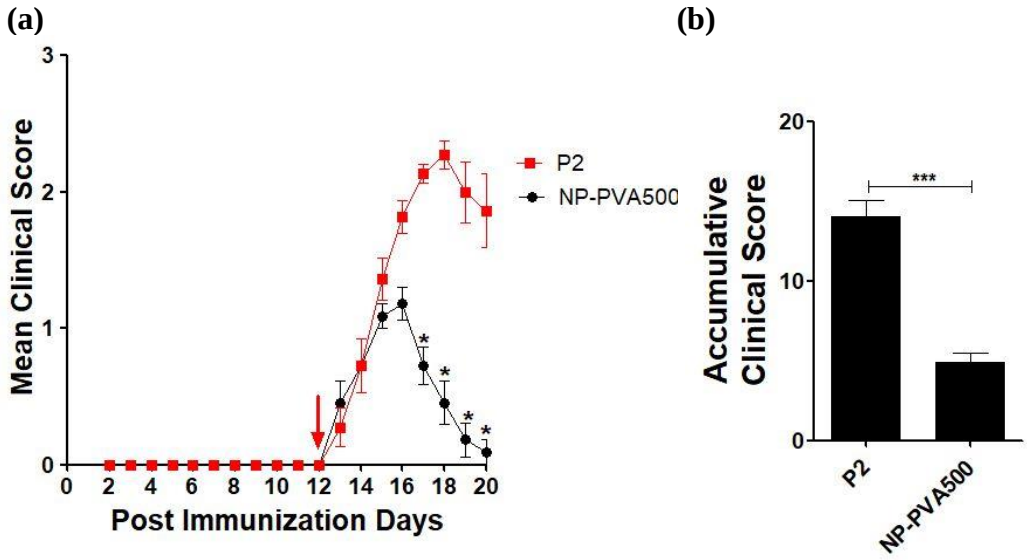

Figure 9. Early-Onset Treatment with NP-PVA500. **(a):** Mean clinical scores (± S.E.M.) of P2-peptide group and NP treated group. The animals began to develop clinical symptoms at around day 12 after immunization in both P2 (n=11) and NP-PVA500 (n=11) groups. The NP-PVA500 (n=11) group was administered with a daily intravenous dose of 9 mg/kg of NP-PVA500 at the onset of the disease. Arrow indicates the start of NPs treatment. Peak clinical score was achieved, and after a brief progression phase, a decline in the symptoms started. **(b):** Accumulative clinical scores of both the groups have a statistically significant difference.

Animal group	Incidence	Mortality	Peak score	Accumulative clinical score
P2	11/11	0/0	2.40 ± 0.13	14.09 ± 1.00
NP-PVA500	11/11	0/0	1.18 ± 0.12***	4.90 ± 0.57***

Table 20. Peak and Accumulative clinical scores of Early Onset treatment with NP-PVA500. $P \leq 0.05$ (*): significant, $P \leq 0.01$ (**): very significant, $P \leq 0.005$ (***): highly significant.

4.1.5. Early-Onset Treatment with NP-PVA500 reduced the inflammatory response in sciatic nerves

In the previous experiment of before onset treatment of EAN with NP-PVA500, an improvement in the clinical presentation of EAN was observed. Therefore, this in vivo experiment was carried out in which an intravenous dose of 9 mg/kg of NP-PVA500 was administered at the early onset of the disease and observed its therapeutic effect on the disease course. To establish a correlation

between the observed clinical scores of the P2-Peptide group and NPs treatment group, a routine histological examination of the sciatic nerves of both the groups was carried out. (Figure 10.). As the control group didn't receive any treatment, neither P2-Peptide nor any nanoparticles, the sciatic nerves of the control group didn't show any inflammatory lesions or histological changes in their nerve milieu (Figure 10. a-d). However, an enormous tissue destruction and accretion of the inflammatory monocytes in the perivascular region of the sciatic nerves of the P2-Peptide group animals was observed (Figure 10. b-e). A comparatively lesser magnitude of destruction of the nervous tissue and lesser accumulation of mononuclear cells across the perivascular region in the NP-PVA500 treated animals was observed (Figure 10. c-f), which depicts a clear therapeutic attribution of nanoparticle therapy in the treatment of EAN.

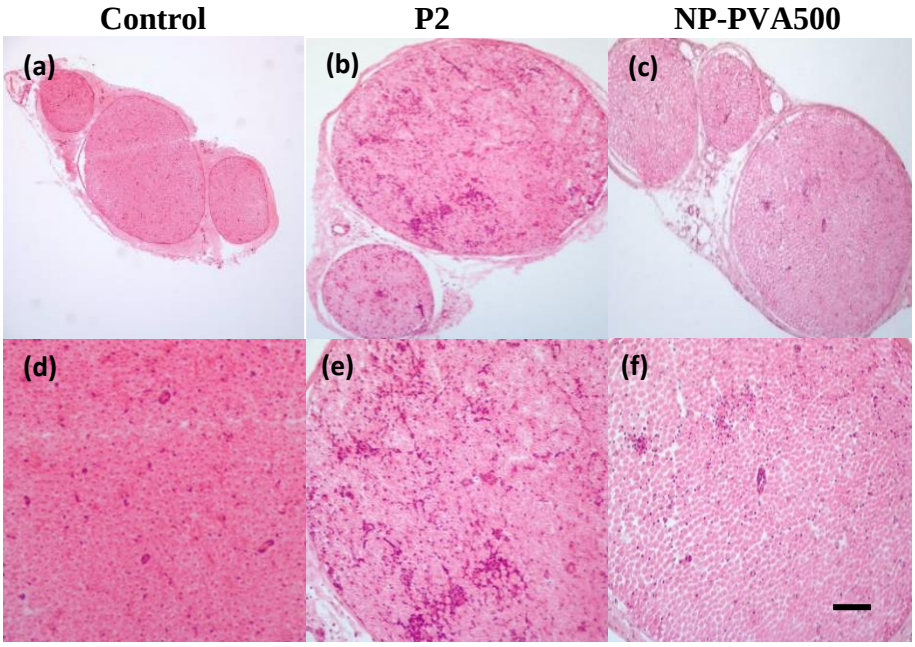

Figure 10. Histological and pathological changes in the sciatic nerves of control, P2-peptide, and NP-PVA500 treated animals. Co-localization infiltrates with routine H&E histology (a-f). Early onset treatment with 9 mg/kg dose of NP-PVA500 reduced the perivascular infiltration of mononuclear cells (c)(f). While a high titer of accumulation of infiltrating monocytes across the perivascular region of the sciatic nerves was observed in P2-Peptide treated rats (b)(e). The control group didn't exhibit any histological changes (a)(d). Magnification 10x(a-b-c), 20x(d-e-f). (n=8). Scale bar represents 50μm.

4.2 Sever Disease scenario

4.2.1. Early-Onset Treatment with Different Sizes (NP-PVA500, NP-PVA130)

Considering the initial therapeutic outcomes of the before and early onset treatment of EAN with NP-PVA500, it has been observed that the use of NP-PVA500 alleviated the symptoms of EAN both in the before and early onset treatment approaches. Keeping the therapeutic efficacy of NPs in mind, this study was conducted to determine the impact of size difference of NPs on the disease course of EAN.

Of the 30 female Lewis rats used in this experiment, 3 were used as control, whereas 27 were immunized with the inoculation of P2-peptide emulsified with an equal volume of complete Freund's adjuvant containing Mycobacterium tuberculosis particles. To validate the therapeutic effectiveness of cargo free NPs, particles of two different sizes, NP-PVA500 and NP-PVA130, were used to evaluate the effect of change in particle size on the clinical course of EAN. Rats were divided into three groups as the disease symptoms appeared at around day 7-8. Of the 27 immunized rats, 9 rats received only P2-peptide in their hind paws and tail roots. Out of the remaining 18 rats, 9 rats received a daily intravenous dose of 9 mg/kg of NP-PVA500, whereas the other 9 rats received a similar dose of NP-PVA130 at the early onset of disease symptoms. All the animals were observed for a 17-day period. No mortality in any of the animal groups was observed during the time period of the experiment. Peak clinical score was achieved, and the arrest or recovery phase of the disease followed. (Figure 11. a).

Early neurological symptoms of EAN appeared between 7-9 days of post immunization in the aforementioned animal groups. About 70 % of the P2-peptide group animals developed the initial symptoms of tail limb paralysis on the 10th day of post immunization. While approximately 30 % of the NP-PVA500 group animals exhibited similar symptoms. Whereas, 45% of the NP-PVA130 animal group showed similar symptoms of early neuritis. Peak clinical score in the P2-peptide group was 5.50 ± 0.33, whereas the peak clinical score of the NP-PVA500 treated group was 2.55 ± 0.38***, and the peak score of the NP-PVA130 treated group was 3.00 ± 0.11***. In the P2-peptide group, the peak clinical score was observed at around day 16, whereas in the NP-PVA500

and the NP-PVA130 groups, it was observed on day 14. A significant difference in the total or accumulative score of all the groups was also observed. The accumulative score of the whole experimental period in the P2 group was 33.78 ± 2.08, whereas the accumulative score of the NP-PVA500 group was 13.50 ± 2.09*** and the accumulative score of NP-PVA130 group was 15.89 ± 1.34*** (Figure 11. b)**.** An early recovery of the disease was observed as a result of treatment with NPs of both sizes. The clinical score at the last day of this experiment also had a significant difference among all the groups. At the end of the experiment, the clinical score of P2-peptide group was 4.50 ± 0.43 whereas the score of NP-PVA500 group was 2.05 ± 0.24 and the score of NP-PVA130 group was 2.05 ± 0.10 (Figure 11. c). Treatment with the different sized NPs reduced the clinical severity of the disease course of EAN.

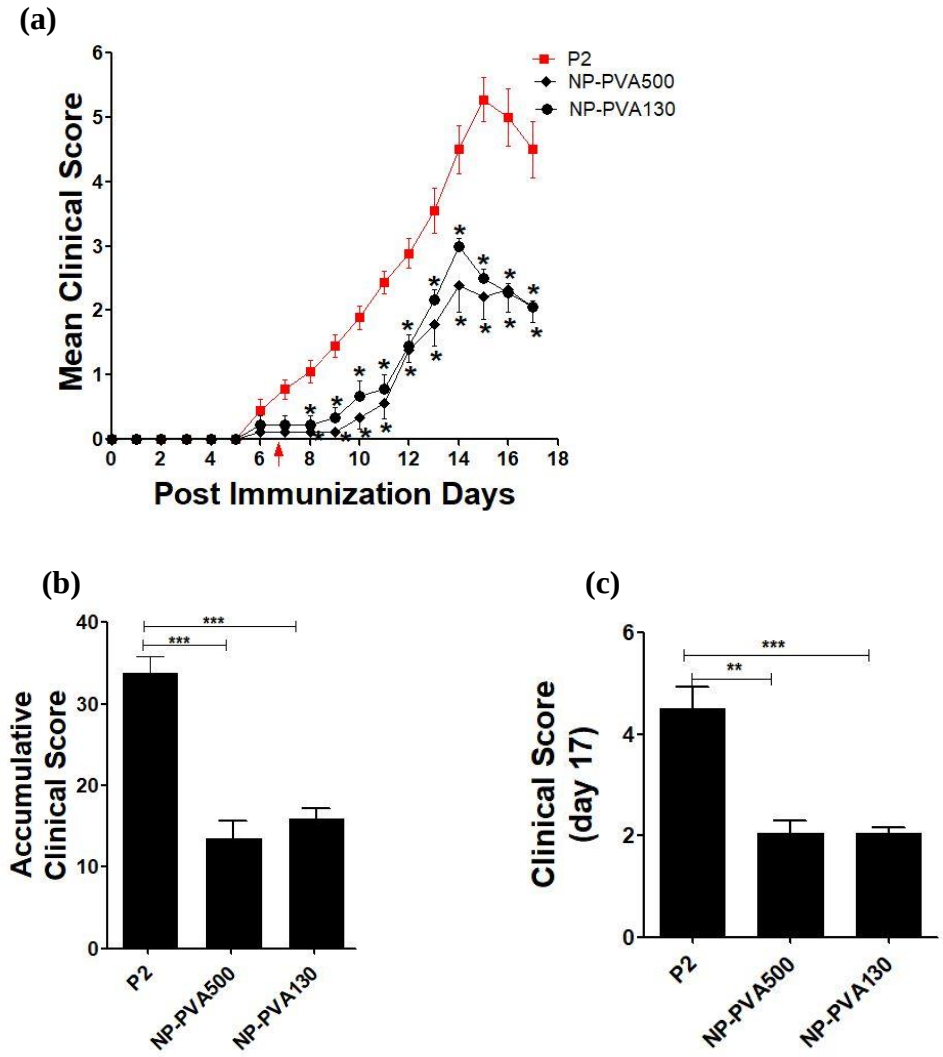

Figure 11. Early-Onset Treatment with Different Sizes of NPs. **(a):** Mean clinical scores (± S.E.M.) post immunization with P2-peptide and treatment with drug free NPs. The animals began to develop clinical symptoms at day 7-9 after immunization in each group P2 (n=9), NP-PVA500 (n=9), and NP-PVA130 (n=9). Arrow indicates the start of NPs treatment. An intravenous daily dose of 9 mg/kg of both sizes of NPs, NP-PVA500 and NP-PVA130 were administered to treatment group animals at the onset of the disease. **(b):** The accumulative clinical scores of both the nanoparticle treatment groups have a significant difference as compared to the P2-peptide group. **(c):** The clinical score at the end of this experiment also had a significant difference in the clinical scores among all the groups.

Experiment (17 days)	Incidence	Mortality	Peak score (Max)	Accumulative clinical Score	Clinical score at day 17
P2-Group	9/9	0	5.50 ± 0.33	33.78 ± 2.08	4.50 ± 0.43
NP-PVA500	9/9	0	2.55± 0.38***	13.50 ± 2.09***	2.05 ± 0.24**
NP-PVA130	9/9	0	3.00 ± 0.11***	15.89 ± 1.34***	2.05 ± 0.10***

Table 21. Clinical course of early onset treatment of EAN with different size of NPs. $P \leq 0.05$ (*): significant, $P \leq 0.01$ (**): very significant, $P \leq 0.005$ (***): highly significant.

4.2.2. Early-Onset Treatment with Different Sizes of NPs (NP-PVA500, NP-PVA130) reduced the inflammatory response in sciatic nerve

Since the use of NP-PVA500 ameliorated the clinical severity of neuritis symptoms in female rats, another in vivo experiment was performed in which two different sizes of NPs (NP-PVA500, NP-PVA130) were used. Intravenous doses of 9 mg/kg of both NP-PVA500 and NP-PVA130 reduced the severity of inflammatory response in their respective sciatic nerves. To establish a correlation between the observed clinical scores, a routine histological assay was conducted, for which tissues were collected at day 17 as the peak score was achieved (Figure 12.). P2-peptide only treated nerve tissue exhibited a clear accumulation of inflammatory monocytes across the perivascular loci of sciatic nerves, which depicts the severity of disease and correlates with the clinical scores observed (Figure 12. b-f). Comparative to the P2-peptide group, a low grade of infiltrates across the perivascular area of the sciatic nerve was observed with the treatment of NP-PVA500 (Figure 12. c-g). Treatment with NP-PVA130 also lowered the magnitude of the inflammatory response in the sciatic nerve milieu (Figure 12. d-h), which ascertained its role in the management of the clinical course of EAN. While the control animals showed no such response as they didn't receive any treatment (Figure 12. a-e).

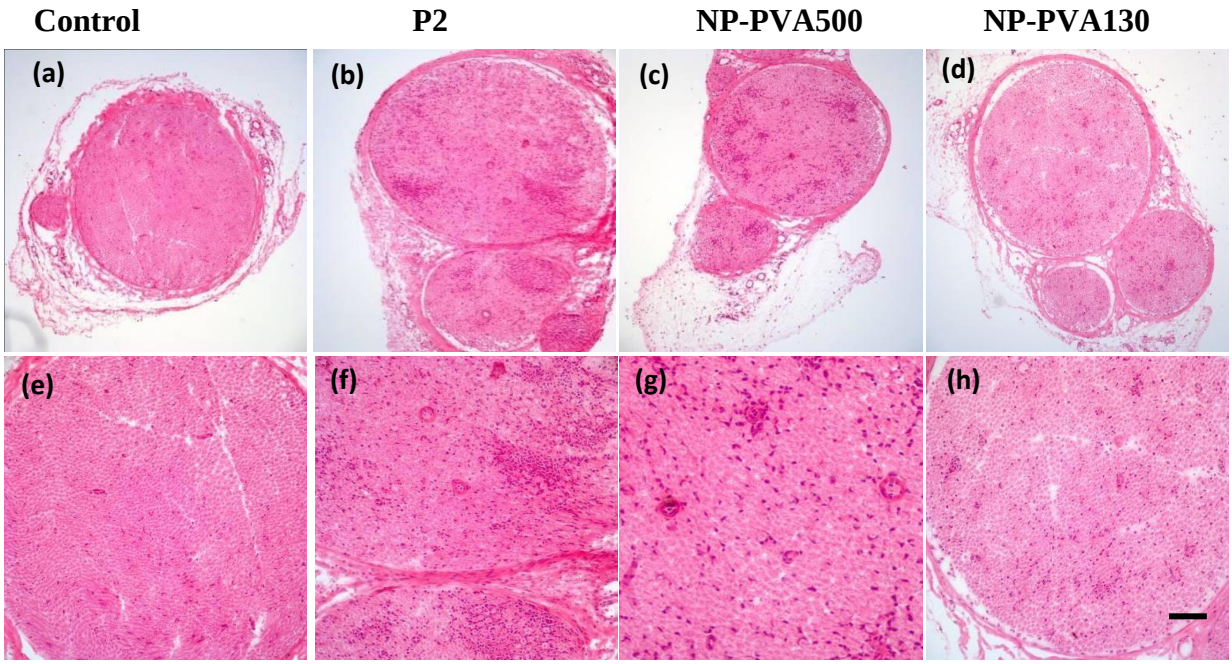

Figure 12. Early-Onset Treatment with Different Sizes of NPs (NP-PVA500, NP-PVA130) reduced the inflammatory response in the sciatic nerve. Histological and pathological changes in sciatic nerves of control, P2-peptide, and NPs treated animals (a-h). 9 mg/kg doses of both sizes of (NP-PVA500, NP-PVA130) reduced the trafficking of infiltrates into sciatic nerve milieu. Early onset treatment with NP-PVA500 diminished the inflammatory response in sciatic nerves of treated rats (c)(g). Treatment with NP-PVA130 also lowered the extent of inflammatory response in sciatic nerves of treated rats (d)(h). A clear inflammatory response and accumulation of infiltrates have been observed in sections of the P2-Peptide group (b)(f). While the control sections didn't show up with any inflammatory response (a)(e). Magnification 10x(a-b-c-d), 20x(e-f-g-h). (n=6). Scale bar represents 50μm.

4.2.3. Determination of the percentage of colocalization of NPs into the immune cells

To determine the uptake of NPs by monocytes and their accumulation in the spleen, FITC-labelled NPs were administered, and these particles were detected by FACS analysis in blood samples and splenic tissue. From this data, it was observed that NPs were successfully internalized by the circulating monocytes (CD45+CD11b+) and were diverted to the spleen where a higher percentage of these monocytes was observed (Figure 13 a). Whereas P2-peptide treated animals didn't receive the nanoparticle regimens, so as expected, they didn't show any particle signal in the P2-peptide group. Moreover, when the percentage of the extent of colocalization of both the sizes were compared i.e., NP-PVA500 (1.27 ± 0.31 n=6) and NP-PVA130 (1.15 ± 0.22 n=6) in the blood (Figure 13. b), no significant difference was observed. Whereas a higher percentage of NP-FITC+CD11b+ monocytes was observed in the spleens of both the sizes of negatively charged NPs i.e., NP-PVA500 (3.840 ± 0.938) and NP-PVA130 (5.047 ± 0.568) (Figure 13. c). Apart from the internalization of NPs into immune cells, a significantly lower percentage of CD11b+ monocytes was observed in the blood samples of NPs (PVA500, PVA130) treated animals as compared to P2-peptide group where a higher percentage of circulating CD11b+ monocytes was observed (Figure 13. d).

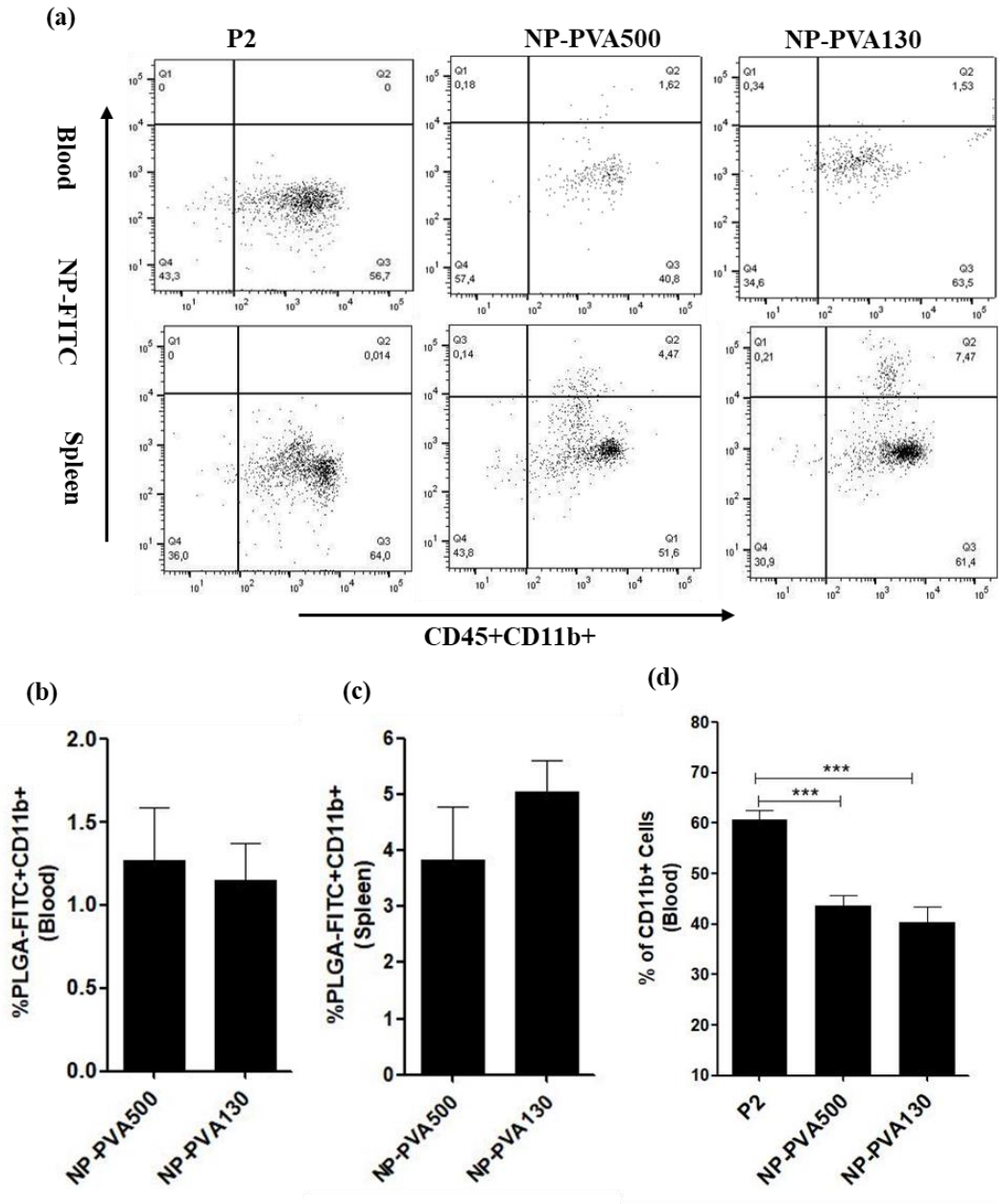

Figure 13. Dot plots of the flow cytometric representation of the percentage of the extent of NP-FITC+ monocytes. Blood and spleen mononuclear cells (MNCs) were isolated from the P2-peptide and different sized NPs (NP-PVA500, NP-PVA130) treatment groups at day 17 of post immunizations. The percentage (Q2) of NP-FITC+CD11b+ cells of each group was determined. The data of the 6 animals is presented in the figure above. Data of the percentage of the extent of NP-FITC+ monocytes of both in blood and spleen.

4.2.4. Dose dependent effect of NPs (NP-PVA130) on the clinical course of EAN

After the establishment of therapeutic efficacy of the 9 mg/kg dose of drug free NPs, an in vivo experimental study was conducted in which the impact of different doses before the onset of clinical symptoms of EAN was determined. Three doses of NPs were used, (3mg/kg, 9mg/kg and 27mg/kg). All doses were prepared with NP-PVA130 because of its established efficacy in the previous treatment experiment. Of the 35 female Lewis rats used in this experiment, 3 were used as a control, whereas 32 were immunized with the inoculation of P2-peptide emulsified with an equal volume of complete Freund's adjuvant containing Mycobacterium tuberculosis particles. Of the 32 female Lewis rats, 8 received only P2-peptide in hind paws and tail roots, while all other animals of each group (n=8) which received P2-peptide in the same manner were also administered with daily intravenous doses (3mg/kg, 9mg/kg, 27mg/kg) of NP-PVA130. All the rats were observed for 18 days. No mortality in any of the animal groups was observed during the experimental period. Peak clinical score was achieved, and arrest or recovery phase of the disease followed (Figure 14. a).

Treatment with different doses of NPs was started on day 7. Neurological symptoms of experimental autoimmune neuritis appeared between 9-10 days of post-immunization in the above-mentioned animal groups. About 62.5 % of P2-peptide group animals developed the initial symptoms of tail limb paralysis at the 13th day of post immunization. Whereas 37 % of 3mg/kg and 25 % of 9mg/kg group exhibited similar symptoms to that of P2-peptide group. 20 % of the 27mg/kg group exhibited the similar symptoms to that of the P2-peptide group.

The administration of different doses in treatment of experimental autoimmune neuritis exhibited their preventive effects on the disease course of EAN. A statistically significant difference in mean Peak clinical score was observed between P2-peptide and treatment groups. Peak score of P2-peptide group was 4.93 ± 0.58, whereas Peak clinical score of 3mg/kg was 2.18 ± 0.23**, 9mg/kg was 1.75 ± 0.163** and 27mg /kg was 1.25 ± 0.35**. A significant difference in the accumulative scores between the P2-peptide group and all the other nanoparticle treated groups was observed. Accumulative score of P2-peptide group was 23.88 ± 2.16, whereas the

accumulative score of the respective dose groups 3mg/kg was 10.69 ± 1.24**, 9mg/kg was 8.18 ± 0.85*** and 27mg /kg was 4.56 ± 1.53*** (Figure 14. b). The clinical score at the end of this experiment also had a significant difference among all the groups (Figure 14. c). Before onset treatment with different doses of NPs significantly delayed the onset of disease as compared to the P2-peptide group. At the end of the experiment, the clinical score of P2-peptide was 3.68 ± 0.53 while the score of respective dose groups, 3mg/kg was 1.56 ± 0.175**, 9mg/kg was 1.43 ± 0.11**, and 27mg /kg was 0.87 ± 0.36**. Result of this experimental study showed that a gradual increase in dose potency lowered the clinical course of experimental autoimmune neuritis significantly.

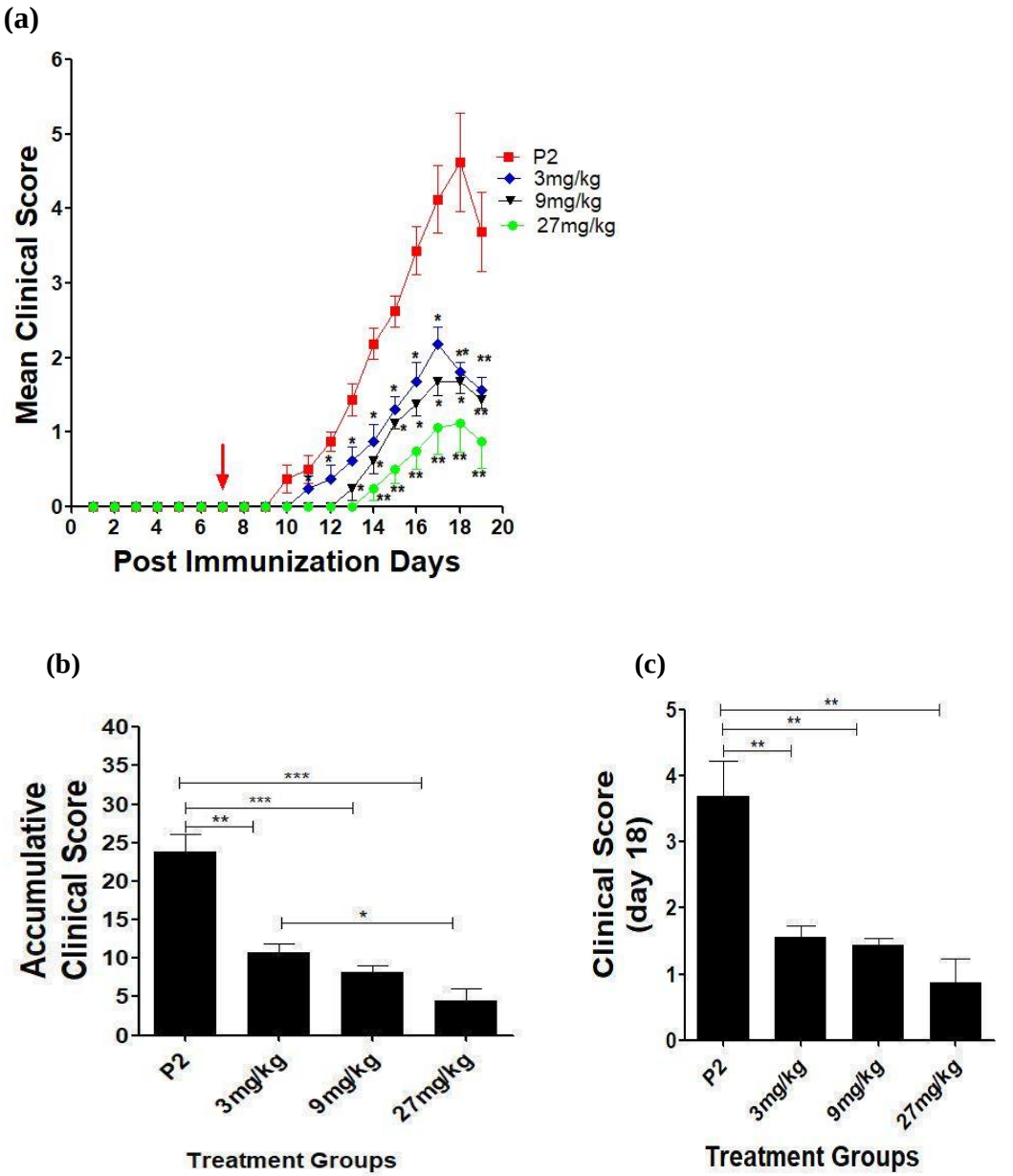

Figure 14. Dose dependent effect of NPs on the clinical course of EAN. (a): Mean clinical scores (± S.E.M.) post immunization with P2-peptide and treatment with different doses of NP-PVA130. Each treatment group was administered with a respective dose at the 7th day of post immunization. P2 (n=8), 3mg/kg (n=8), 9mg/kg (n=8), 27mg/kg (n=8). Arrow indicates the start of NPs treatment. (b): Accumulative clinical scores of treatment groups have a statistically significant difference with the P2-peptide group. (c): Clinical score at the end of experiment of the treatment groups had a statistically significant difference with the P-peptide group.

Animal Group	Incidence	Mortality	Accumulative clinical score	Peak Score	Clinical score at day 18
P2	8/8	0/0	23.88 ± 2.16	4.93 ± 0.58	3.68 ± 0.53
3mg/kg	8/8	0/0	10.69 ± 1.24**	2.18 ± 0.23**	1.56 ± 0.17**
9mg/kg	8/8	0/0	8.188 ± 0.85***	1.75 ± 0.16**	1.43 ± 0.11**
27mg/kg	8/8	0/0	4.56 ± 1.53***	1.25 ± 0.35**	0.87 ± 0.36**

Table 22. Clinical course of early onset treatment of EAN with different doses of NP-PVA130. P ≤ 0.05 (*): significant, P ≤ 0.01 (**): very significant, P ≤ 0.005 (***): highly significant.

4.2.4. Dose dependent effect of NPs (NP-PVA130) on infiltration of inflammatory cells in sciatic nerve

After attaining promising results from the use of 9 mg/kg of NP-PVA130 on the disease course of EAN, another in vivo experiment was conducted to determine the impact of different doses of NP-PVA130 before the onset of EAN. For this, three doses of NPs were used (3mg/kg, 9mg/kg, and 27mg/kg). To establish a correlation between observed clinical scores of all dose groups and P2-Peptide group, a routine histological assay (H&E) was conducted in which tissues were collected as the peak score was achieved. P2-peptide treated nerves showed an immense inflammatory response, as well as a higher accumulation of inflammatory monocytes across the perivascular region of the sciatic nerve (Figure 15. a, e). In comparison to the P2-peptide group, treatment with a minimal dose of 3mg/kg of NP-PVA130 reduced the inflammatory response to a lower extent (Figure 15. b, f). While a lesser grade of inflammatory response was observed with the treatment of 9mg/kg dose of NP-PVA130 (Figure 15. c, g). Moderate accumulation of inflammatory monocytes and less damage to perivascular part of sciatic nerves were observed with 27mg/kg dose of NP-PVA130 (Figure 15. d, h).

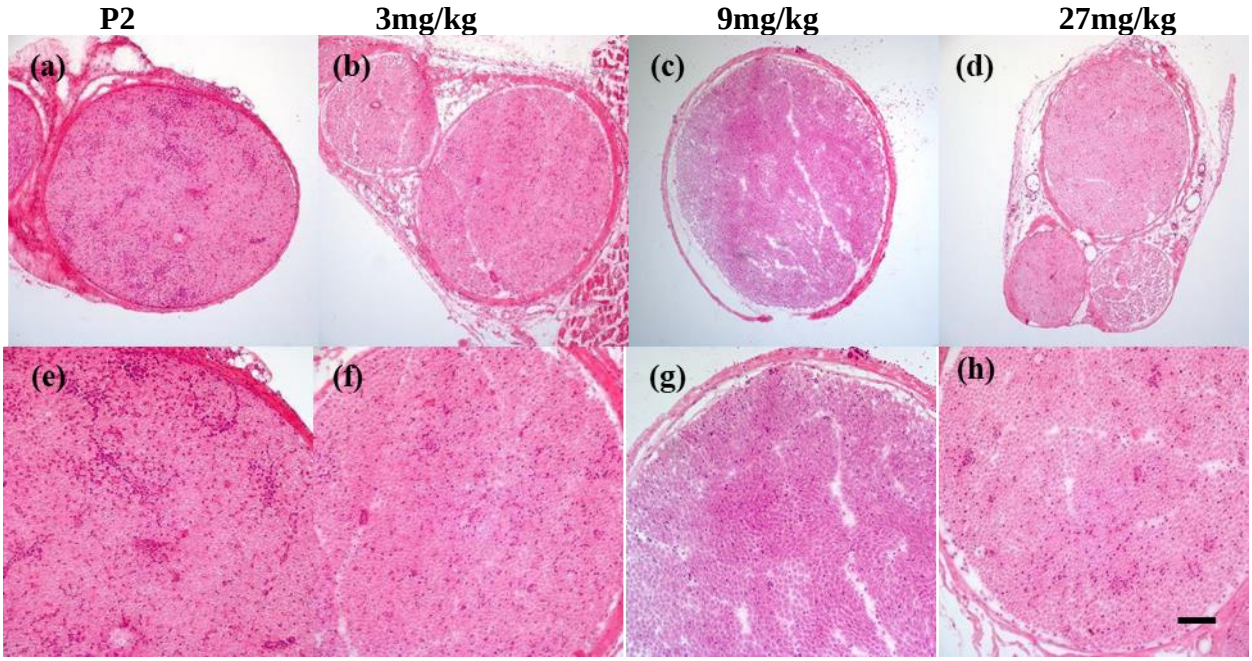

Figure 15. Dose dependent effect of NPs (NP-PVA130) on infiltration of inflammatory cells in sciatic nerve. Histological and pathological changes in sciatic nerves of P2-peptide and different doses of NP-PVA130 treated animals. Co-localization of infiltrates with routine H&E histology (a-h). Accumulation of inflammatory cells in the perivascular area of nerve tissue has been observed in the cross section of the P2-Peptide animal group (a)(e). 3mg/kg dose of NP-PVA130 treatment reduced the inflammatory response to a lower extent (b)(f). A lesser graded inflammatory response has been observed with 9mg/kg NP-PVA130 (c)(g). While the higher dose of 27mg/kg of NP-PVA130 halted the inflammatory response very effectively and a very less perivascular infiltration of monocytes was observed (d)(h). Magnification 10x(a-b-c-d), 20x(e-f-g-h). (n=6). Scale bar represents 50μm.

4.2.5. Early-Onset Treatment Effect with Surfactant and Polymer Modified NPs on EAN

In the previous experimental study, promising results on the clinical propensity of EAN by using three different doses of NP-PVA130 were observed. Since NPs bearing Polyvinyl alcohol (PVA) as surfactant yielded promising results by lessening the severity of disease course of EAN, an experimental study was proposed to evaluate the therapeutic efficacy of NPs bearing different surfactants as well as nanoparticles made from a different polymer.

Of the 29 female Lewis rats used in this experiment, 3 were used as a control, whereas 26 were immunized with the inoculation of P2-peptide emulsified with an equal volume of complete Freund's adjuvant containing Mycobacterium tuberculosis particles. Of the 26 animals, 5 received only P2-peptide in hind paws and tail root, while all other animals of each group (n=7) which received P2-peptide in the same manner were also administered with daily intravenous doses of 9 mg/kg of different types of nanoparticles at the early onset of EAN. Groups were divided on the basis of surfactant and the polymer used. All animals were observed for a 17-day period. No mortality in any of the animal groups was observed during the experimental period. Peak clinical score was achieved, and arrest or recovery phase of the disease followed (Figure 16. a).

Early symptoms of EAN appeared between 11-12 days of post immunization in the aforementioned animal groups. Treatment with different immune modifying nanoparticles was started at disease-onset. About 60% of the P2-peptide animal group developed the early symptoms of EAN such as tail paralysis on the 14th day of post immunization. Whereas, 42% of NP-PCL130 treated animals developed symptoms similar to those of P2-peptide treated animals, and a lesser extent of disease progression was observed in other treatment groups. Approximately 35% of NP-Chol130 and 30% of NP-PVA130 treated animals exhibited symptoms similar to those of P2-peptide treated animals.

An alternative approach to alleviate the disease severity by surfactant modification also yielded similar therapeutic results. A significant improvement in the clinical manifestation of EAN was observed in this experiment. A statistically significant difference in the peak clinical scores between P2-peptide and the other treatment groups, especially NP-PVA130, has been observed. Peak clinical score of P2-peptide was 4.40 ± 0.678, whereas the peak clinical score of NP-PCL130 was 2.50 ± 0.21*, NP-Chol130 was 2.14 ± 0.17* and NP-PVA130 was 1.92 ± 0.07**.

A significant difference in the accumulative scores between the P2-peptide group and all the other nanoparticle treated groups was observed. Accumulative score of P2-peptide animal group was 18.30 ± 1.48, whereas the accumulative score of NP-PCL130 was 12.29 ± 0.82*, NP-Chol130 was 9.71 ± 0.61**, and NP-PVA130 was 8.07 ± 0.81** (Figure 16. b). The clinical score at the

end of this experiment also showed a significant difference among all the groups. At the end of the experiment, the clinical score of P2-peptide group was 3.80 ± 0.75, while the score of NP-PCL130 was 2.21 ± 0.21*, NP-Chol130 was 2.14 ± 0.17* and NP-PVA130 was 1.78 ± 0.10* (Figure 16. c)

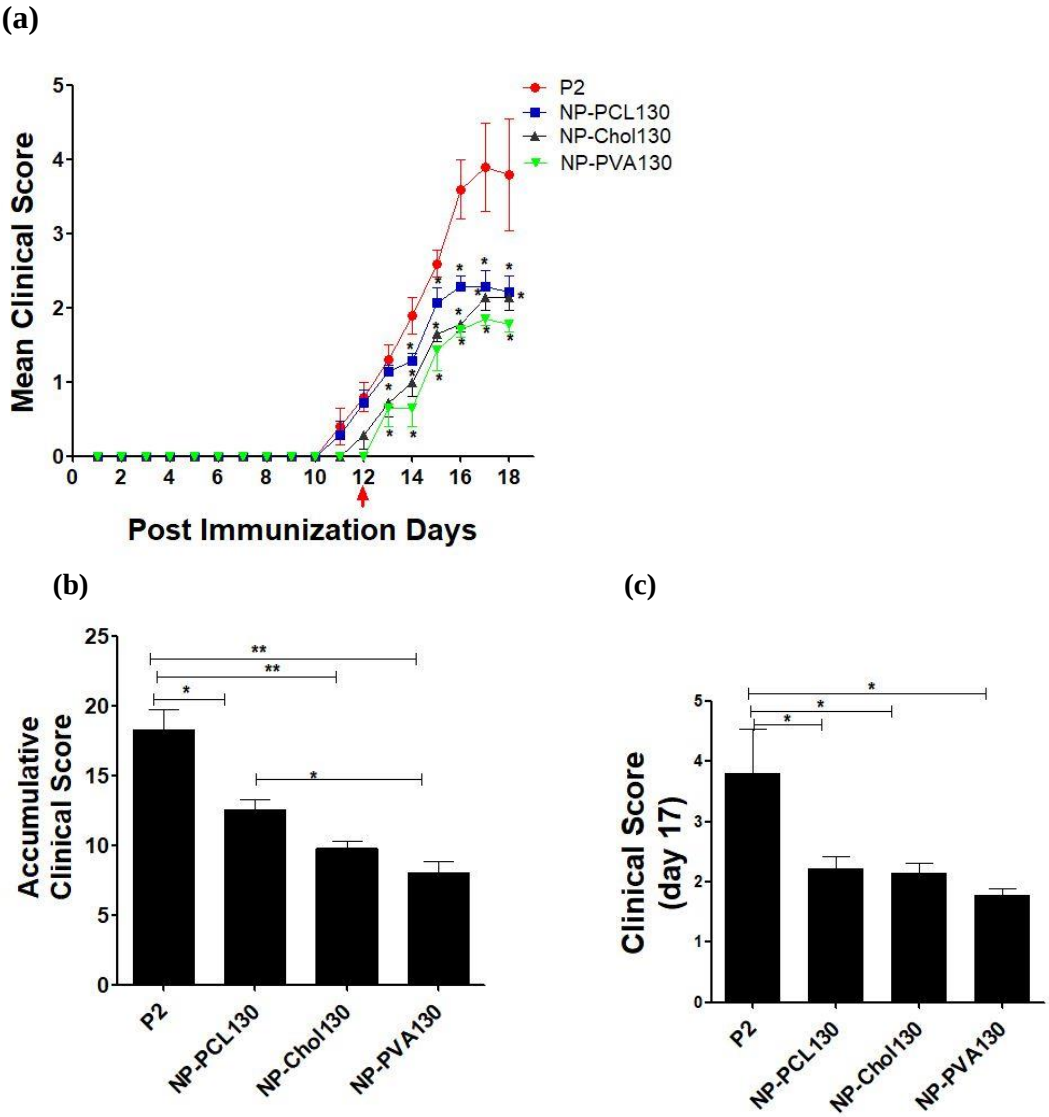

Figure 16. Early-Onset Treatment Effect with Surfactant and Polymer Modified NPs on EAN. (A): Mean clinical scores (± S.E.M.) post immunization with P2-peptide and treatment with surfactant modified NPs. Symptoms of experimental autoimmune neuritis (EAN) appeared

between 10-12 days of post immunization in each group P2 (n=5), NP-PCL130 (n=7), NP-Chol130 (n=7), NP-PVA130 (n=7). Arrow indicates the start of NPs treatment. Each group was administered with 9 mg/kg dose at the early onset of disease. (b): Accumulative clinical scores of treatment groups have a statistically significant difference with the P2 group. (c): Clinical outcome of the treatment groups has a statistically significant difference with the P2-peptide group.

Animal Group	Incidence	Mortality	Peak Score	Accumulative score	Clinical score at day 17
P2	5/5	0/0	4.40 ± 0.67	18.30 ± 1.48	3.80 ± 0.75
NP-PCL130	7/7	0/0	2.50 ± 0.21*	12.29 ± 0.82*	2.21 ± 0.21*
NP-Chol130	7/7	0/0	2.14 ± 0.17*	9.714 ± 0.61*	2.143 ± 0.17*
NP-PVA130	7/7	0/0	1.92 ± 0.07**	8.071 ± 0.81**	1.78 ± 0.10*

Table 23. Clinical course of Early Onset treatment of EAN with surfactant and polymer modified NPs. $P \leq 0.05$ (*): significant, $P \leq 0.01$ (**): very significant, $P \leq 0.005$ (***): highly significant.

4.2.6. Treatment with surfactant and polymer modified NPs reduced the inflammatory response in sciatic nerves

Since the immune modifying NPs bearing Polyvinyl alcohol (PVA) as surfactant yielded promising results by lessening the severity of disease course of EAN. So, an experimental study was proposed to evaluate the therapeutic efficacy of NPs bearing different surfactants as well as nanoparticles made from a different polymer. To corroborate the observed clinical scores of all treatment groups and P2-Peptide group, a routine histological examination (H&E) was carried out in which tissues were collected as the peak score was achieved. P2-peptide treated nerves exhibited an immense inflammatory response as well as the accumulation of inflammatory monocytes in the perivascular portion of the nerve section (Figure 17. a). Treatment with NP-PCL130 had a very mild or moderate effect on the disease course. A considerable hoard of infiltrates was also observed in the sections of NP-PCL130 treated animals (Figure 17. b). Compared to NP-PCL130 treatment, a lesser magnitude of inflammatory response was observed in the sciatic nerves of animals which were treated with NP-Chol130 surfactant (Figure 17.c). A

slightly considerable accumulation of monocytes was observed in the perivascular part of the sciatic nerve tissue, therefore treatment with this particle group improved the disease course of EAN to a significant level. Sections of animals treated with NP-PVA130 showed less tissue damage and less vascular infiltration of monocytes (Figure 17. d).

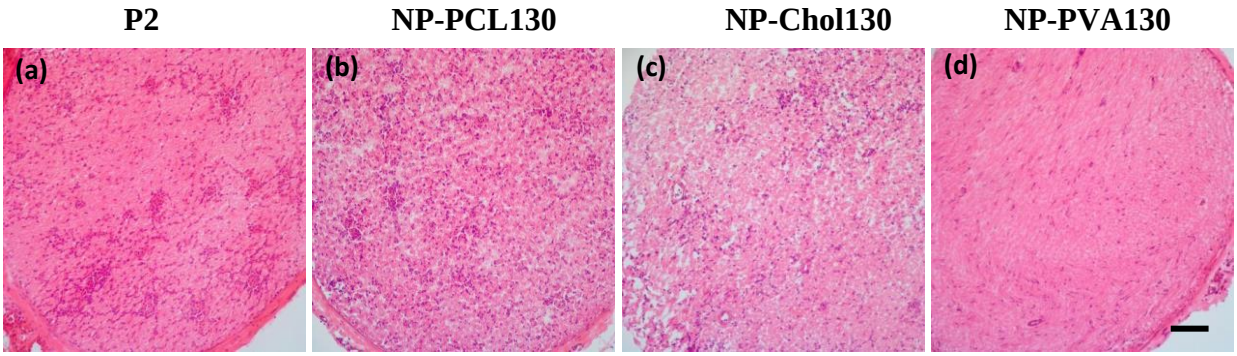

Figure 17. Treatment with surfactant and polymer modified NPs reduced the inflammatory response in sciatic nerves. Histological and pathological changes in sciatic nerves of P2-peptide and surfactant modified NPs treated animals (a-d). P2-Peptide treated nerves showed a marked inflammatory response and vascular localization of infiltrating monocytes (a). Mild or moderate improvement in the disease course with 9 mg/kg dose of NP-PCL130 was observed (b). Treatment with nanoparticles containing NP-Chol130 reduced vascular infiltration and improved the disease course of EAN (c). Whereas sections treated with NP-PVA130 nanoparticles showed less inflammatory response and less localization of infiltrates at the inflammatory loci (d). (n=3). Magnification 20x. Bar size 50µm.

4.3. Biodistribution of surfactant and polymer modified NPs in the blood and spleen

To determine the biodistribution of surfactant and polymer modified nanoparticles and their association with circulating monocytes (CD11b+) and splenic tissue, all the modified NPs were labelled with the fluorescent FITC dye. From flow cytometric data, a considerable fluorescence intensity in the blood samples was observed (Figure 18.). Whereas, a greater extent of fluorescence intensity was observed in the spleen as compared to the blood, which is in line with the findings that nanoparticles are internalized by circulating monocytes and diverted to the spleen. When the fluorescence intensity of each type of nanoparticle in the blood was compared i.e. NP-PCL130 = 3481 ± 451.7, NP-Chol130 = 3586 ± 600.2), and NP-PVA130 =4383 ± 743.3), no significant difference was observed (Figure 18. a). Similarly, even with a larger extent of

fluorescence signals in the spleen, no significant difference in the fluorescence intensity among the three particle groups, NP-PCL130 = 4391 ± 238.8, NP-Chol130 = 5296 ± 654.2, and NP-PVA130 =5563 ± 550.1 was observed (Figure 18. b).

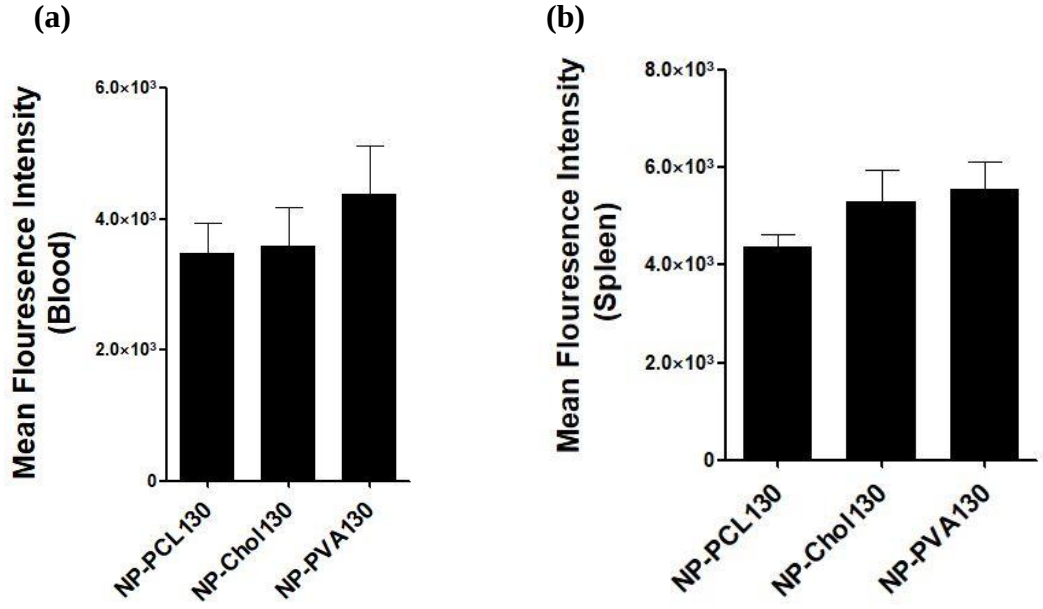

Figure 18. Biodistribution of NPs in blood and spleen

4.4. Impact of different polymer and surfactant modified NPs on the percentage expression of pro and anti-inflammatory macrophages

In this experiment, three different types of nanoparticles bearing different types of surfactants and a polymer were used, including the previously used NP-PVA130 to assess their immune modulation capability on the disease course of EAN. Flow cytometric analysis was used to determine and quantify the relative changes in the percentage distribution of specific immune cell populations (Figure. 14.). Spleens harvested at peak disease (day 17 post immunization) level were analysed for a paradigm shift in the monocyte proliferation. The infiltrating monocytes were gated and quantified, and the percentage expression of each particle group was determined and compared with the P2-peptide group. From the presented data, a considerable reduction in the pool of activated macrophages (CD11b+CD68+) in the spleens of nanoparticle treatment groups as compared to the P2-peptide group (12.32 ± 2.38 n=3) was observed (Figure 19. a). NP-

PVA130 lowered the expression of the activated macrophages to a significant level (5.53 ± 0.87 n=3). Whereas other types of surfactants and polymer modified nanoparticles such as NP-PCL130 (8.06 ± 0.23 n=3) and NP-Chol130 (8.40 ± 0.47 n=3) also reduced the expression levels of CD68+, but compared to negatively charged PLGA-PVA nanoparticles, it was not statistically significant. From this experimental data, a slight increase in the percentage of the expression of CD11b+CD163 cells in nanoparticle treatment groups as compared to the P2 peptide group (1.78 ± 0.354 n=3) was observed (Figure 19. b). Whereas the percentage expression of CD11b+CD163+ in NP-PCL130 treated animals was 2.18 ± 0.32 (n=3), NP-Chol130 was 2.17 ± 0.29 (n=3), and NP-PVA130 showed a percentage expression of 2.37 ± 0.44 (n=3). The dot plots of the flow cytometric analysis of CD11b+CD68+and CD11b+CD163+ splenocytes are shown below (Figures 20., 21.).

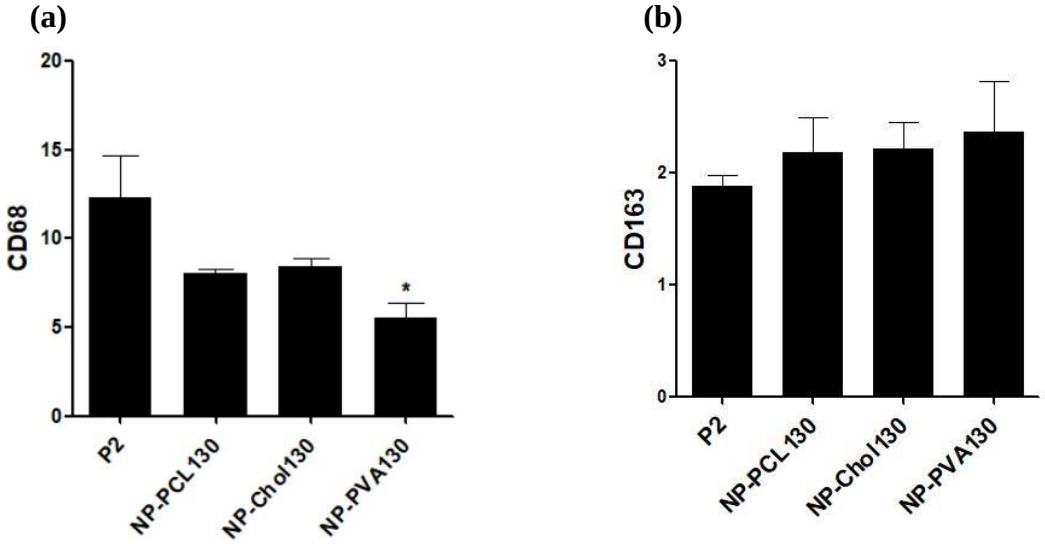

Figure 19. Impact of different polymer and surfactant modified NPs on the percentage expression of pro and anti-inflammatory macrophages. Spleen mononuclear cells (MNCs) were isolated from the P2-Peptide and different treatment groups of NPs at day 17 of post immunizations. With flow cytometry, gated splenic mononuclear cells were fluorescently labelled and quantified. Flow cytometry data represents the percentage expression of activated macrophages (a), (CD11b+CD68+) (b), CD11b+CD163 of three different nanoparticle types and P2-peptide treated group comprising of 3 female Lewis rats per group. For statistical analysis, one-way ANOVA with Bonferroni post-test was applied with a P-value <0.05***.

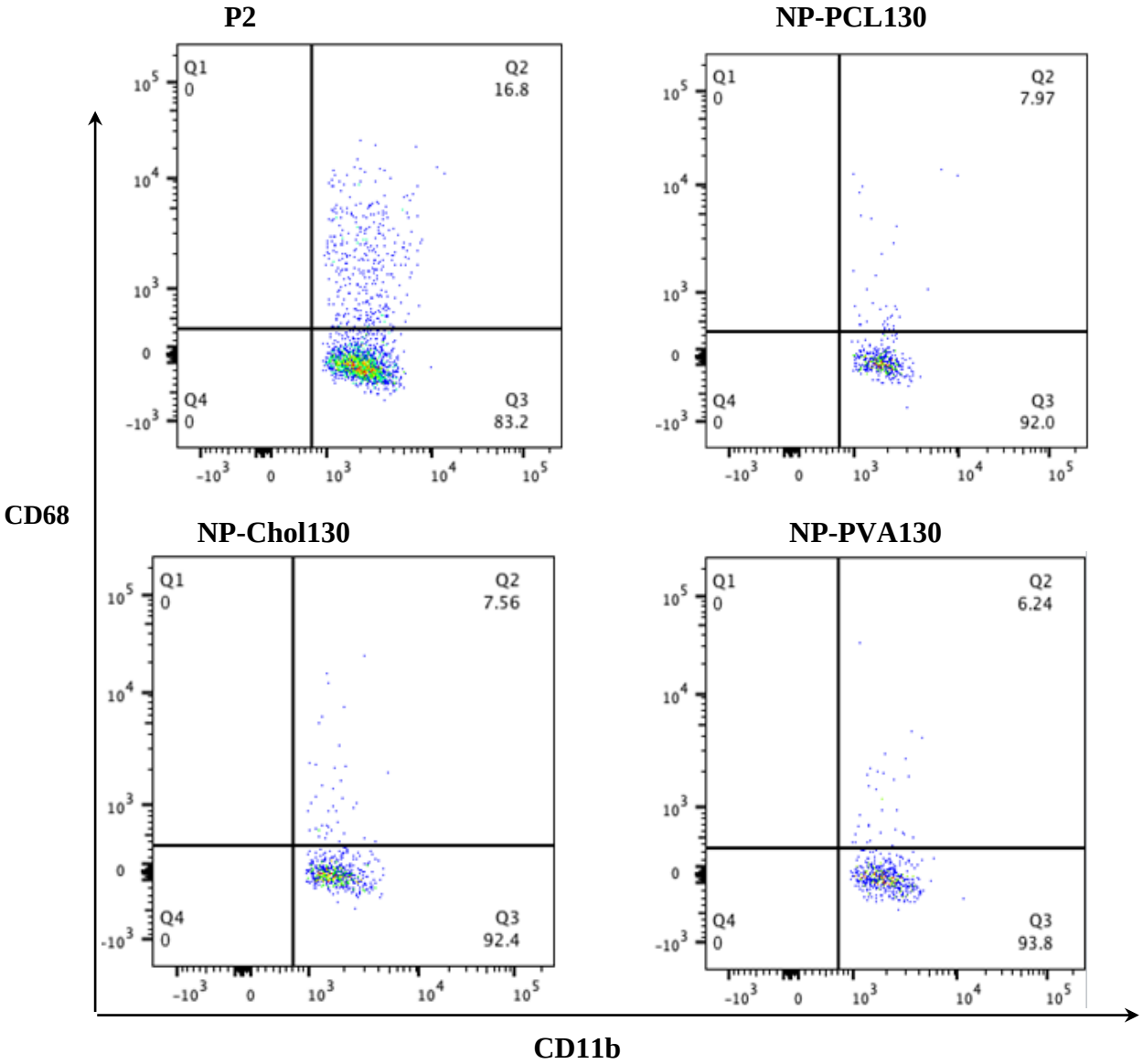

Figure 20. Dot plots of flow cytometric representation of activated macrophages CD68 percentages in CD11b population. Spleen mononuclear cells (MNCs) were isolated from the P2-Peptide and different treatment groups of NPs at day 17 of post immunizations. With flow cytometry, these monocytes were identified by gating against the side and forward scatter. The percentage (Q2) of activated macrophages (CD68) of each polymer type was determined and compared with the P2-peptide treatment group.

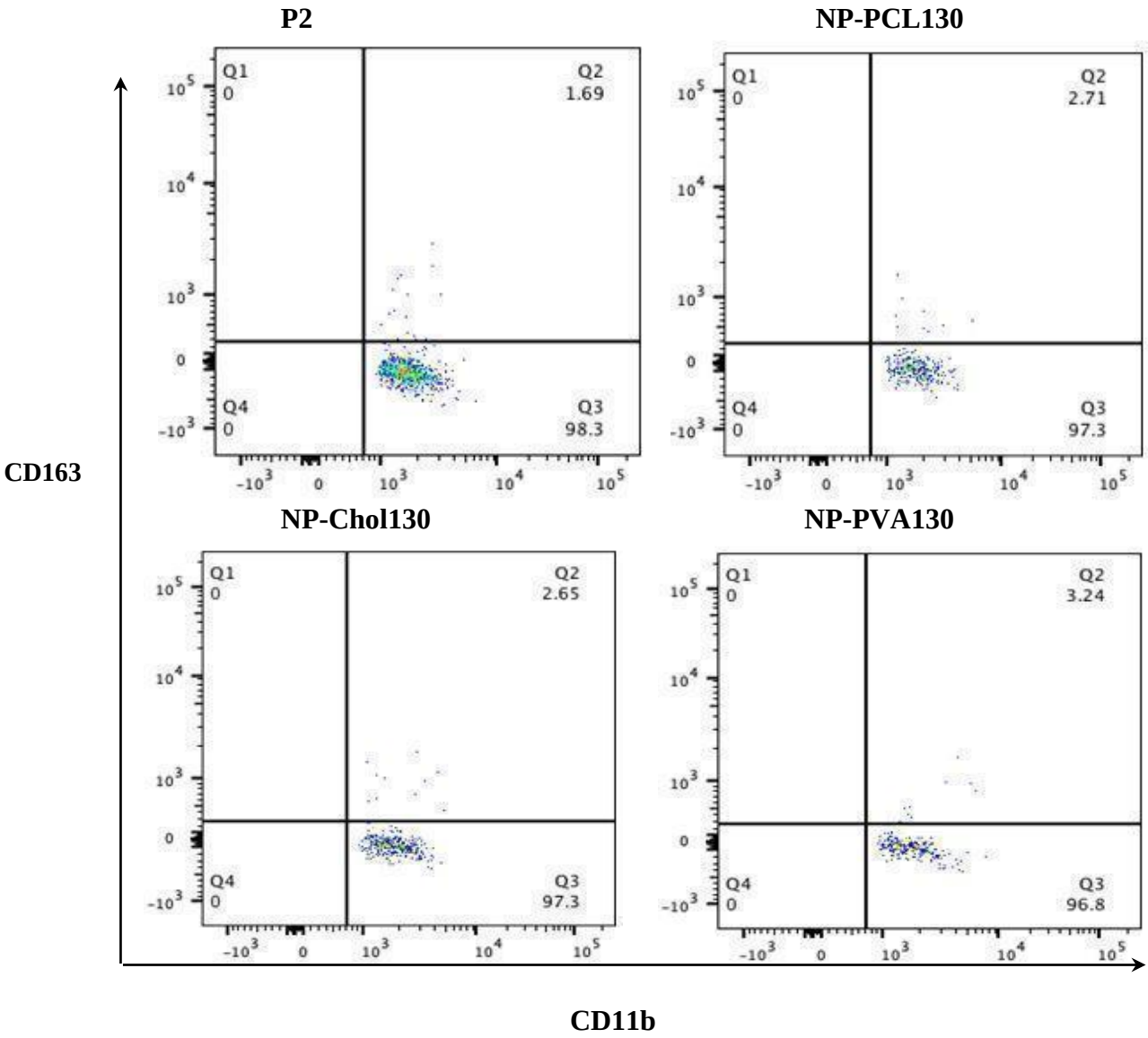

Figure 21. Dot plots of flow cytometric representation of CD163 percentages in CD11b population. Spleen mononuclear cells (MNCs) were isolated from the P2-Peptide and different treatment groups of NPs at day 17 of post immunizations. With flow cytometry, these monocytes were identified by gating against the side and forward scatter. The percentage (Q2) of CD11b+CD163 cells of each polymer type was determined and compared with the P2-peptide treatment group.

4.5. Treatment with NPs modulates the local immune response in EAN

To get further into the mechanistic insights of the use of drug free NPs at the early onset of EAN, to validate the therapeutic efficacy of NP-PVA130, and to correlate the results with histopathological changes and accumulation of inflammatory monocytes in the sciatic nerve, a quantitative a real-time PCR assay was conducted to compare the RNA expression levels of the selected pro and anti-inflammatory markers such as TNF-α,IL-1β, IFN-γ, IL-17, CD68, and CD163 in the sciatic nerves of NP-PVA130 (n=3) and P2-peptide treated rats (n=3). Expression levels (fold increases of mRNA expression) of each respective marker from both the particle treatment and P2-peptide group were normalized with the above-mentioned specific markers' expression levels in the control group (Figure: 22. a).

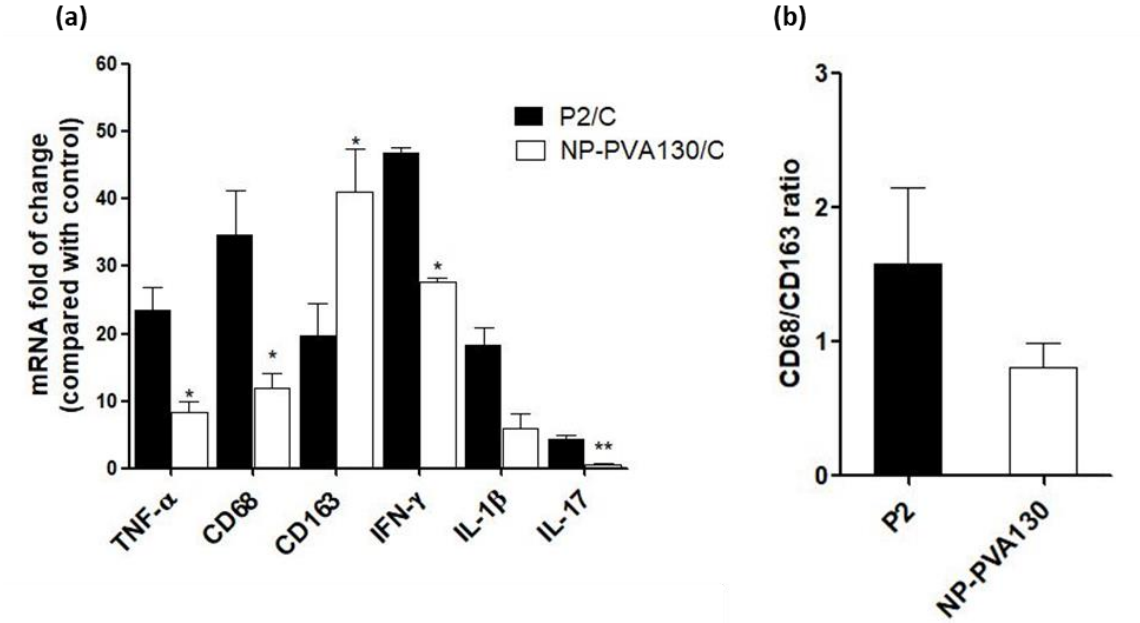

Figure 22. (a): Treatment with NP-PVA-130 attenuated the expression levels of pro-inflammatory markers and increased the expression levels of anti-inflammatory markers. **(b)** mRNA expression ratio of CD68/CD163. (n = 3), t-test (unpaired) * $p \leq 0.05$, ** $p \leq 0.01$.

The expression level of the proinflammatory cytokine TNF-α in the P2-peptide group was 23.54 ± 3.69 folds, whereas the expression level of TNF-α level in the NP-PVA130 treated animals was 8.30 ± 1.67 folds. Raised levels of activated macrophages (CD68) were observed in P2-peptide

treated animals (34.75 ± 6.58 folds), on the other side NP-PVA130 treatment lowered the levels of activated macrophages to a comparable range (11.91 ± 2.25 folds). Higher folds of expression of IL-1β were observed in P2-peptide treated animals (18.30 ± 0.77), as compared to the NP-PVA130 treated animals (5.83 ± 2.23). Similarly, higher folds of expression of IFN-γ were observed in the P2-peptide treatment group (46.8 ± 0.77), as compared to NPs treatment group (27.66 ± 0.59). Fold of expression of IL-17 was considerably higher in the P2-peptide group (4.25 ± 0.77) as compared to NPs treated group (0.53 ± 0.16). A considerably higher expression level of CD163 (41.07 ± 6.46 folds) was observed in the sciatic nerves of animals treated with NP-PVA130, whereas P2-peptide group animals showed a lesser expression of CD163 (19.74 ± 2.96 folds) in their sciatic nerves. As mentioned earlier, classically activated macrophages (M1) are intimately linked with the induction of proinflammatory response in EAN (Zhang et al., 2013). For the activated macrophage phenotype M1, CD68 is considered as a typical marker (Han et al., 2016). M2 macrophages, in comparison to M1 macrophages, may exhibit a neuroprotective effect in the pathogenesis of EAN (Shen et al., 2018). CD163 is considered to be expressed in M2 macrophages (Mantovani et al., 2004; Shen et al., 2018). From the above-mentioned results, an increased mRNA expression of CD68+ macrophages was observed in the P2-peptide group as compared to the NP-PVA130 treated group. On the other hand, raised mRNA expressions of CD163 were observed in the NPs treated group. The mRNA expression ratio of CD68 versus CD163 in the P2-peptide treated animals and the NP-PVA130 treated animals was calculated and compared (Figure 22. b). From this comparison, a higher ratio of mRNA expression of CD68/CD163 in the sciatic nerves of the P2-peptide group animals, whereas a considerably less mRNA expression ratio of CD68/CD163 was observed in the sciatic nerves of the NPs group animals. Furthermore, CD68/CD163 ratio comparison showed a higher expression of M1 phenotype macrophages in the P2-peptide group, whereas a less expression of M1 macrophages was observed in NP-PVA130 treatment group (Figure 22. b).

5. Discussion

Guillain-Barré syndrome is an autoimmune inflammatory disorder that causes inflammation and demyelination of the peripheral nervous system. Although the underlying immunopathogenesis that causes peripheral nerve damage is not yet completely elucidated, it is known that macrophage and T cell infiltration is linked with a monophasic demyelination of peripheral nerves (Che et al., 2016). It is considered as one of the most commonly occurring paralytic autoimmune diseases that accounts for a large number of deaths and morbidity (van den Berg et al., 2014).

Experimental autoimmune neuritis is an animal model which resembles many clinical, immunological, histological as well as electrophysiological aspects of Guillain-Barre syndrome. Therefore, due to aforementioned aspects of EAN, this disease model has been widely used to study the demyelinating diseases of the peripheral nervous system (Kieseier et al., 2004). Much like GBS, experimental autoimmune neuritis (EAN) also involves the infiltration of macrophages and T cells into the peripheral nervous system, breaching of the blood nerve barrier resulting in inflammatory demyelination of the peripheral nerves (Shen et al., 2018).

The critical role of macrophages in the pathogenesis of GBS and EAN has been reported in many studies. Macrophages have been classified into two major categories based on their phenotype namely M1 (proinflammatory) and M2 (anti-inflammatory). During the early stage of GBS, M1 macrophages promote cellular toxicity and increase the proinflammatory cytokines resulting in the demyelination of nerves. Whereas, in the later stage of GBS, M2 macrophages are associated with the recovery of disease by promoting the secretion of anti-inflammatory cytokines (Shen et al., 2018).

Therapeutic options to treat GBS are limited. The first effective treatment in GBS patients was plasma exchange. Its therapeutic effectiveness was more profound when administered within the first two weeks of disease onset in patients with impaired walk. In comparison to plasma exchange, IVIG treatment administered within the first two weeks of disease onset was found to be as efficacious as plasma exchange. The use of steroidal drugs such methylprednisolone or prednisolone did not significantly improve the recovery in GBS patients (Yuki & Hartung, 2012).

Despite the effectiveness of these treatment options, the course of GBS is long and complicated. The clinical outcome of these treatments in many of the patients is not optimal, 2-10% may die, whereas 20% remain unable to walk even after 6 months of treatment (Verboon et al., 2017). Therefore, more effective as well as less invasive and less costly therapeutic approaches are required to improve the treatment of GBS patients.

Nanoparticles with immune-modifying properties are emerging as a potential therapeutic option in immune mediated diseases. Strategies are developing which target the innate inflammatory cells in the blood, specifically inflammatory monocytes, with the aim to reduce their trafficking to the inflammatory site (Saito et al., 2019). Recent experimental studies which used nanoparticles to modulate the immune-mediated disorders, attained a lot of attention when PLGA (Poly-lactic co-glycolic acid) based nanoparticles carrying no active pharmacological agent were used to abrogate the severity of disease course in various immune disease models such as inflammatory bowel disease, experimental autoimmune encephalomyelitis (EAE), West-Nile virus encephalitis, spinal cord injury models and sodium thioglycolate-induced peritoneal inflammation. These studies revealed that activated inflammatory monocytes and their innate ability to engulf the invading materials make them a favourable candidate for the nanoparticle-based treatment approach. PLGA based targeted drug delivery approach was extensively used to treat several inflammatory diseases such as inflammatory bowel disease, experimental autoimmune encephalitis, and arthritis (Danhier et al., 2012; Getts et al., 2014; Lamprecht et al., 2001; Meissner & Lamprecht, 2008).

Experimental studies on the EAE model by Getts et al. revealed that the charge on the nanoparticle surface plays an important role and induces the amelioration of disease. In their studies, they used positive, neutral, and negatively charged nanoparticles in the treatment of EAE in the mice model. From their results, particles with negative surface charge reduced the severity of the disease, and improved survival statistics of animals treated with negatively charged particles were observed as compared to other treatment groups (Getts et al., 2014). Based on

above notions of uses of drug free PLGA nanoparticles, it was hypothesized that these negatively charged NPs might have the potential to treat the EAN as well.

At first, an in vivo study was conducted to examine the therapeutic potential of NP-PVA500 when applied before the onset of the EAN disease symptoms. Assessing the neurological development of EAN through a clinical score, a clear attenuation of the disease course was observed. Keeping in view the protocol of the before onset treatment, intravenous administration of NP-PVA500 was started three days prior to commencement of first EAN symptoms. Initial EAN symptoms appeared at day 10 of post immunization. 30% of P2-peptide group animals exhibited the early symptoms of EAN, whereas only 7% of NP-PVA500 treated animals showed similar symptoms at around day 10. Though the disease severity was milder, a significant difference ($p<0.05$) in the peak clinical score and accumulative clinical score was observed with the NP-PVA500 treatment group as compared to the P2-peptide group. The clinical score then decreased and returned to almost zero on day 22 of NP-PVA500 treated animals, whereas in the P2-peptide group a similar score was observed at day 29.

Intravenous immunoglobulin (IVIG) therapy is extensively used in the treatment of GBS patients (Yuki and Hartung, 2012). Although the exact underlying mechanism of action of IVIGs is not yet elucidated, it is believed that the treatment with IVIG has advantages over the available treatments. In before onset treatment with IVIG, intravenous administration of 1g/kg at day 0 and 7 significantly suppressed the neurological symptoms of EAN (Kajii et al., 2014). Similarly, with IVIG treatment, the overall clinical score almost returned to zero at around day 25. This shows that treatment with NP-PVA500 induces a comparatively faster recovery effect on the disease course as compared to their IVIG treatment. These comparable effects yielded by NP-PVA500 on the disease course argues that the use of NP-PVA500 in EAN treatment is not inferior to a treatment approach (IVIG), which is established in GBS as well.

In addition to the attenuated clinical course, treatment with NP-PVA500 reduced the endoneurial accumulation of inflammatory monocytes when compared to the P2-peptide group. Histological data of before onset treatment study showed that treatment of NP-PVA500 suppressed the

infiltration of T cells, macrophages (CD68+) and reduced the levels of MHC-II into the sciatic nerve.

The aforementioned before onset treatment with IVIG in rats also exerted a restrictive effect on infiltration of inflammatory cells into the sciatic nerves and reduced the histological damage (Kajii et al., 2014). In particular, a reduced infiltration of macrophages into the sciatic nerves was also observed with their IVIG treatment. A similar restrictive effect on infiltration of inflammatory cells into the sciatica nerves of NP-PVA500 treated animals was observed. Although a modest disease severity was observed in this P2 group as compared to P2 treatment group of Kajii et., al, less disease severity was noted with 9mg/kg NP-PVA500 treatment group as compared to their 1mg/kg IVIG treated group. Methodological differences may account for any minor differences in the clinical outcomes. Firstly, clinical scoring method is different in this study as compared to their clinical grading scale. Secondly, they administered only two infusions of 1mg/kg of IVIGs whereas in this study a daily dose of 9 mg/kg of NP-PVA500 was administered till the end of the experiment.

The endoneurial accumulation of T cells and macrophages is essential for the development of EAN (Mäurer & Gold, 2002). It can be suggested that the reduction of the accumulation of inflammatory cells into the sciatic nerves of the NP-PVA500 treated animals might be due to the ‘mopping effect’ mechanism of the negatively charged NPs, where adsorption of NPs to circulating monocytes can reduced their presence at inflammatory loci which is ultimately linked with amelioration of disease.

During EAN, MHC-II antigens are highly upregulated on macrophages. So, a possible hypothesis is that lowering the expression of MHC-II with NP-PVA500 treatment in the EAN disease model can ameliorate its severity. From histological data, a lesser extent of MHC-II (OX-6) levels in NP treated animals than in P2 treated animals was observed. Overall, this study uniquely demonstrated that NPs (NP-PVA500) were able to modulate the disease course and affirmed their potential therapeutic efficacy in the management of EAN.

The first experimental study provided the insight that NP-PVA500 are able to attenuate the disease course of EAN when given before the onset of EAN symptoms. To examine the effects of NPs in a setting which resembles more with the clinical situation of patients diagnosed with GBS, a second experiment was conducted in which rats were given NP-PVA500 after the onset of first EAN symptoms. Early onset treatment with drug NP-PVA500 again attenuated the clinical course of EAN and halted the infiltration of inflammatory cells. NP-PVA500 treatment was started as the initial EAN symptoms appeared at around day 12. 55% of P2-peptide group animals exhibited the early symptoms of EAN, whereas only 18% of NP-PVA500 treated animals showed similar symptoms at around day 14. The overall disease severity was milder, a significant difference ($p<0.05$) in the peak clinical score and accumulative clinical score was observed with the NP-PVA500 treatment group as compared to the P2-peptide group. An early decline phase was observed with NPs treatment. The clinical score then decreased and returned to almost zero on day 20 of NP-PVA500 treated animals, whereas the P2-peptide group still exhibited the milder symptoms of EAN. Previous studies have shown that early onset treatment with daily intravenous dose of drug free negatively charged 500nm PLGA-NPs are able to attenuate the clinical course of a variety of experimental autoimmune diseases including experimental autoimmune encephalomyelitis (Getts et al., 2014). Above mentioned results demonstrate that the early onset therapy with nanoparticles is applicable in EAN as well.

In an EAN treatment study, Lin et al., reported that administration of two doses of IVIG at early onset of disease symptoms proved effective in inhibiting further development and progression of EAN disease course (Lin et al., 2007). Interestingly, results from this early onset treatment with NP-PVA500 correlated with their report. However, some methodological differences may account such as, they administered two doses of 100mg/100g/ body weight of rats of IVIG for two consecutive days whereas in this study administered dose was 9mg/kg dose from the commencement of early symptoms till the end of experiment. Also, their clinical scoring grades differed. An early recovery phase was observed in NP treatment as compared to their treatment regimen, which could be an encouraging factor to translate these NPs from bench to clinical

settings, as well as to other experimental treatment models. Restriction in inflammatory monocyte trafficking towards the perivascular area was also observed in their study. Despite having these differences in therapeutic nature and duration of treatment, NP-PVA500 also showed a similar restriction in inflammatory monocyte trafficking towards the inflammatory loci, thus preventing excessive nerve demyelination. In comparison to the therapeutic approaches examined in the EAN model, such as IVIG, the therapeutic effect of NP-PVA500 was equally profound. Altogether, early onset treatment with NP-PVA500 demonstrated their therapeutic efficacy in the management of EAN.

Considering the curative potential of NP-PVA500, two different sizes of NPs (NP-PVA500, NP-PVA130) were used to evaluate therapeutic efficacy on the disease course of EAN. The advantage of smaller size (130 nm) NPs is the ease in their sterile filtration. In sterile filtration, pathogens are physically removed from thermally and chemically sensitive liquid preparations using 0.2 μm (200 nm) membrane filters. This method is extensively applicable because it does not adversely affect the physical properties of nanoparticles. It has been reported that 98-100% PLGA nanoparticles with a diameter range of 103-163 nm passed through 0.2 μm membrane filters without having any change in their physical properties such as particle size or distribution. Similarly, Polycaprolactone (PCL) nanoparticles with size below 200 nm were effectively sterilized by 0.2μm membrane filters without any change in their morphology, concentration, or size (Vetten et al., 2014). Early onset treatment with both sizes of NPs (NP-PVA500, NP-PVA130) reduced the clinical course of EAN. Treatment at the early onset with both sizes of NPs also reduced the perivascular infiltration into the sciatic nerve and less histological damage was observed. From these findings, it was observed that the use of different sized nanoparticles does not show a significant difference in the immune modulating effect of NPs. An early recovery of the disease was observed as a result of treatment with NPs of both sizes. Taking this into consideration, it can be speculated that the immune modulating effect of NPs may not primarily depend on their size but the surface charge. Taking into account the therapeutic efficacy of NP-PVA130 on EAN course and their smaller size, which is favourable for sterile filtration, this study

provides first proof of concept and proposes the use of NP-PVA130 as a novel and alternative therapeutic approach that can be translated to other NP based experimental treatment models.

In another in vivo study, dose dependent effect of NPs before the onset of EAN was determined. Considering the ease of sterile filtration process of smaller sized NPs, NP-PVA130 were used to determine their dose dependent therapeutic efficacy on the disease course of EAN. Three different doses (3mg/kg, 9mg/kg, 27mg/kg of rat body weight) of NP-PVA130 were used. From this experimental data, it was observed that the higher dose (27mg/kg) reduced the clinical severity of EAN very significantly and overall particle treatment with different doses also reduced the clinical severity of EAN, which was evident by the reduction in clinical scores and less histological tissue damage. About 62.5% of P2-peptide group animals developed the initial symptoms of EAN at the 13th day of post immunization. Whereas, 37% of 3mg/kg and 25% of 9mg/kg group animals exhibited similar symptoms to that of P2-peptide group. 20% of the 27mg/kg group animals exhibited similar symptoms to that of the P2-peptide group. A statistically significant difference in mean peak clinical score, accumulative score and clinical outcome was observed with NP-PVA130 treatment as compared to the P2-peptide treatment. A significant delay in the disease onset was observed with all the NPs treatments as compared to the P2-peptide treatment group. A dose dependent restrictive effect on infiltration of inflammatory cells was also observed in this before onset treatment with NP-PVA130.

At day 18, a significant suppression in the clinical score in all three treatment groups was observed as compared to the P2-peptide group. However, no significant difference was observed in the clinical outcome among all three dose regimens. From this observation of clinical outcome, it can be argued that previously used dose of 9mg/kg of NP-PVA130 might be as therapeutically efficient as the higher dose. To translate this into a potential human equivalent dose, the body surface equation was used as described by Reagan-Shaw et al. By using this equation, a dose of 1.4 mg/kg or approximately 87 mg per 60-kg patient was calculated. However, to use the drug-free NPs in clinical settings, one could lower or increase the dose of NPs as proposed above.

Moreover, an independent dose dependent study needs to be conducted to determine the optimal dose of NPs in the treatment of GBS patients.

The extent of internalization of nanoparticles into the immune cells in the blood and spleen was determined in this animal model. Findings from this study suggested that NPs were successfully internalized by circulating monocytes (CD45+CD11b+) and were diverted to the spleen where a higher percentage of these monocytes was observed. Apart from the internalization of NPs into immune cells, a significant reduction of CD11b+ monocytes was observed in the blood samples of NPs (NP-PVA500, NP-PVA130) treated animals as compared to the P2- peptide group. These findings are consistent with the observation described by Getts et al. regarding the use of drug free negatively charged PLGA-NPs in the treatment of EAE. A lesser percentage of circulating monocytes in the blood samples of NPs (NP-PVA500, NP-PVA130) treated animals was observed.

Upon intravenous administration, NPs immediately interact with immune cells and plasma proteins (opsonin). Immune cells can uptake NPs through various endocytic pathways and adsorption of plasma proteins to the surface of NPs can facilitate this process (Dobrovolskaia et al., 2008). For the selective adsorption of a particular protein the electrostatic interaction between protein and adsorbent can be changed by changing the surface charge of particles. It is known that negatively charged nanoparticles bind with positive sites on the surface of macrophages, recognized by macrophage receptors (Honary & Zahir, 2013) followed by internalization by monocytes-derived macrophages predominantly through dynamin and clathrin mediated endocytic pathways (de Almeida et al., 2021). Electrostatic interactions between negatively charged nanoparticles and positive sites on macrophages have been considered to be essential for the internalization of particles (Dobrovolskaia et al., 2008; Getts et al., 2014). However, non-opsonic receptors such as scavenger receptors, which are capable of interacting directly with the NP surface moieties, are also expressed on monocytes (de Almeida et al., 2021). Studies have reported that anionic NPs can also be internalized through a non-opsonic receptor present on monocytes i.e., MARCO (macrophage receptor with collagenous structure) receptor and modulate

the inflammatory response. It is important to consider that NPs are adsorbed and internalized but are not restricted to caveolae-clathrin mediated endocytosis, micropinocytosis and phagocytosis (Saito et al., 2019). From the results of this study, it can be concluded that negatively charged NPs might have selectively targeted the positive receptor site on the surface of circulating monocytes and diverting them to the spleen, resulting in reduction of inflammatory response in PNS which is evident by a low clinical score as well.

Other experimental therapies aiming at depleting monocytes from the bloodstream were described in the past. A liposomal preparation containing dichloromethylene diphosphonate (Cl2MDP) has been found to be effective in the selective elimination of macrophages from blood circulation, liver and the spleen. This selective elimination of macrophages mediated by liposomal preparation containing Cl2MDP prevented the development of EAN. Moreover, intravenous injection of Cl2MDP-liposomes at the early onset resulted in less infiltration of CD68+ cells (Jung et al., 1993). Consistent with their observations, this study also showed that early onset treatment with both the NPs significantly mitigated the severity of EAN. Moreover, elimination of monocytes from the bloodstream has also been observed with NPs treatment. Hence, it is reasonable to say that NPs (NP-PVA500, NP-PVA130) might also have selectively targeted the monocytes in the circulation and exhibited a similar monocyte depletion mechanism due to which an improvement in EAN course has been observed.

In another in vivo experimental study, the impact of modification of surfactants on the surface of NPs as well as the impact of a different polymer-based nanoparticle treatment on the disease course of EAN was determined. This surfactant modification approach to alleviate the disease severity yielded encouraging therapeutic results. A significant improvement in the clinical manifestation of EAN was observed with the treatment of surfactant and polymer modified nanoparticles. From this study it was observed that previously used NP-PVA130 significantly reduced the clinical severity and perivascular accumulation of inflammatory cells as compared to the other types of nanoparticles used. Moreover, a significant difference has also been observed in

the accumulative clinical scores of NP-PVA130 treated animals as compared to NP-PCL130 treated animals.

PLGA is a frequently used biodegradable polymer which is used to formulate the particles (Getts et al., 2014; Kumari et al., 2010). Another type of polymeric nanoparticles made up of Polycaprolactone (PCL) polymer were used. PCL polymer is preferred because of its biocompatible and biodegradable nature, being easily degraded by bacteria and fungi. It is also approved by FDA and EMA (Guarino et al., 2017). Owing to the numerous options of surfactants that can be used to design nanoparticles which can potentially change the treatment outcome, the surface properties of nanoparticles are of prime importance (Wachsmann et al., 2013).

From this data only a minor effect was observed by the change of particle size and charge. In opposition to that, other experimental studies on the EAE model revealed that the charge on the nanoparticle surface plays an important role and induces the amelioration of disease. In their studies, they used positive, neutral, and negatively charged drug free PLGA-NPs (500 nm) in the treatment of EAE in the mice model. From their results, particles with a negative surface charge reduced the severity of the disease and improved the survival rate of animals as compared to other particle treatment groups (Getts et al., 2014). This is moreover in line with reported efficacy of negatively charged NPs in other proinflammatory models such as inflammatory bowel disease, West-Nile virus encephalitis, spinal cord injury models and sodium thioglycollate-induced peritoneal inflammation (Getts et al., 2014; Saito et al., 2019). The reasons for these differences can be manifold, however particle surface charges that typically characterized by a standardized method (like measurements of the zeta potential) reflect in-vivo conditions only partially. Accordingly, effects immunomodulation or biodistribution related to corona formation on the particle surface may modify the behaviour in-vivo, while this depends on a large diversity of factors such as charge, hydrophilicity, material of particle matrix or even the preparation method. However, this requires further exploration. Accordingly, from this study one can only claim a general benefit for the EAN treatment by using cargo-free PLGA-based NPs while the impact of particle properties is minor.

This study showed a low disease severity as well as less perivascular infiltration of monocytes into the sciatic nerves of the surfactant and polymer modified NPs treated animals as compared to P2-peptide group animals. This reduced migration of the inflammatory cells motivated to identify the biodistribution of surfactant and polymer modified nanoparticles in the blood and spleen. From this data, a low fluorescence intensity in the blood and a comparably higher intensity in the spleen was observed, which supports hypothesis that these nanoparticles are internalized by circulating monocytes and no longer directed towards inflammatory loci, resulting in an overall disease modifying response. Recently, Saito et al observed a similar pattern of biodistribution of drug free PLGA-NPs in treatment of EAE mice model where a higher intensity of fluorescence signals was observed in the spleen than in the CNS (Saito et al., 2019). However, this study partially agrees with their results since they observed the particle distribution in the CNS and spleen, as compared to this study in which the similar pattern was observed in blood and spleen. The potential mechanism believed to be involved in the clearance of circulating monocytes is opsonization. However, previous studies have demonstrated that the uptake of negatively charged nanoparticles can be carried out in an opsonin independent fashion (Getts et al., 2014). One can speculate that a similar mechanism could be at play in the clearance of negatively charged nanoparticles from the circulation and their diversion to the spleen.

Flow cytometric analysis was used to determine and quantify the relative changes in the percentage distribution of specific immune cell populations. Spleens harvested at peak disease level (day 17 post immunization) were analysed for a paradigm shift in the monocyte proliferation. From this data, it was observed that splenic macrophages of NPs treated group were slightly polarized towards the M2 phenotype (CD163) as compared to the P2-peptide group. A considerably less population of inflammatory macrophages M1 (CD68) was observed in the NPs treated spleens as compared to P2-peptide group.

NP-PVA130 showed a considerable reduction in M1 macrophages in the spleen as compared to the P2 peptide group. In comparison, the other types of particle treatments (NP-PCL130, NP-Chol130) also showed a similar effect. Interestingly, this observation is in accordance with the

RT-PCR data from the sciatic nerves of NP-PVA130 treated animals, where less expression of inflammatory macrophages M1 (CD68) was observed as compared to those in the sciatic nerves of P2-peptide group. Moreover, a slight shift towards the M2 macrophages was observed in the splenic macrophages. This is also in agreement with the RT-PCR data where a higher expression of M2 (CD163) macrophages in NP-PVA130 was observed as compared to the P2-peptide group. In a previous EAN treatment study, a similar splenic macrophage polarization effect has been observed at the peak of disease where the early onset treatment with dimethyl fumarate (DMF) showed that splenic macrophages were more polarized towards the M2 type (Han et al., 2016). Moreover, a relatively less severe disease manifestation was also observed with NP-PVA130, and NP-Chol130 treatment as compared to the NP-PCL130. Similarly, less expression of M1 splenic macrophages was also observed with NP-PVA130 and NP-Chol130 as compared to NP-PCL130. However, no significant differences were observed between the respective NPs treatment groups. From this data, it is reasonable to speculate that all three types of nanoparticles exhibited their immune modifying ability by interfering with the polarization state of the splenic macrophages.

This therapeutic approach is the first of its kind in which PLGA based NPs were used in the treatment of the EAN model. Therefore, to validate the therapeutic efficacy of early onset treatment with NP-PVA130, as well as to correlate the results with histopathological changes and accumulation of inflammatory monocytes in the sciatic nerve, a quantitative real-time PCR assay conducted. This assay was used to compare the RNA expression levels of the selected pro and anti-inflammatory markers such as TNF-α, IL-1β, IFN-γ, IL-17, CD68 and CD163 in the sciatic nerves of NP-PVA130 and P2-peptide treated rats. Expression levels (fold increases of mRNA expression) of each respective marker from both the particle treatment and P2-peptide group were normalized with the above-mentioned specific markers' expression levels in the control group.

As mentioned earlier, classically activated macrophages (M1) are intimately linked with the induction of proinflammatory response in EAN (Zhang et al., 2013). For the activated macrophage phenotype M1, CD68 is considered as a typical marker (Han et al., 2016). CD68 is a lysosomal membrane protein, mostly found on activated microglia and macrophages

(Zhang et al., 2008). Upregulation of CD68 has been observed in EAN during the disease course (Han et al., 2016). M2 macrophages, in comparison to M1 macrophages, may exhibit a neuroprotective effect in the pathogenesis of EAN (Shen et al., 2018). CD163 is considered to be expressed in M2 macrophages (Mantovani et al., 2004; Shen et al., 2018).

The macrophages are activated from their resting stage to M1 state by microbial enentities and proinflammatory cytokines such as, tumor necrosis factor-α (TNF-α), interferon-γ (IFN-γ), and interleukin-1β (IL-1β) (Shen et al., 2018). This polarization of M1 macrophages activates different signaling pathways such as Janus Kinase/Signal Transducer and Activator of Transcription (JAK/STAT), myeloid differentiation factor 88 (MyD88) and nuclear transcription factor-κB (NF-κB). This results in the production of proinflammatory entities such as TNF-α, interleukin-1 (IL-1), inducible nitric oxide synthase (iNOS), IL-4 and IL-6. Whereas the polarization of M2 macrophages is induced by immune complexes by activation of signaling pathways such as phosphatidylinositide 3-kinases (PI3K) and Signal Transducer and Activator of Transcription (STAT6), which results in the upregulation of tumor growth factor-β (TGF-β), peroxisome proliferator-activated receptors (PPAR- δ/γ) and anti-inflammatory cytokines (IL-10) (Shen et al., 2018).

During the progression of the EAN disease course, the balance of M1/M2 is crucial. Some researchers are of the opinion that switching M1 to M2 can be beneficial in the disease outcome (Zhang et al., 2009). Early onset treatment with NP-PVA130 reduced the expression of M1 or activated macrophages (CD68) in the sciatic nerves of the particle treated animals. Also, an increase in the expression of M2 marker (CD163) was observed which affirms the immune modulatory effect of NP-PVA130. Moreover, it was observed that early onset treatment with NP-PVA130 switched the M1/M2 balance more towards the M2 as shown from the expression ratio of CD68/CD163. From this study, one can argue that early onset treatment with NP-PVA130 might have suppressed the M1 signalling pathways and upregulated the M2 pathways, due to which an increased expression ratio of M2 marker was observed. However, further studies need to be carried out to explore the insights of the mechanisms involved.

Cytokines play varying roles during different phases of EAN. For instance, there is a proportional relation between the release of proinflammatory cytokines such as IL-1β, IL-17, IFN- γ and TNF-α and their disease promoting role in the clinical progression of EAN (Zhang et al., 2013). IFN-γ, produced by Natural Killer cells, classically activated macrophages (M1) and CD4+ Th1 cells, plays an important role during Th1 mediated innate immune response. It activates the macrophages, endothelial cells, and T cells, eliciting its proinflammatory function. Serum analysis from the acute phase of GBS reported an increase in levels of IFN- γ. The clinical conditions of GBS patients were ameliorated with the administration of antibodies that targeted IFN- γ (Zhang et al., 2013). Consistent with the therapeutic treatment of EAN model with Chrysin (naturally occurring immunomodulatory flavonoid), NP-PVA130 also lowered the expression levels of IFN-γ in the sciatic nerves of the treated animals (Xiao et al., 2014).

TNF-α plays a vital role in the development and progression of EAN. In the peripheral nerves, elevated mRNA expression of TNF-α has been reported during the peak phase of clinical EAN. Administration of TNF-α into the sciatic nerves of rats induced endoneurial inflammatory response resulting in axonal destruction and demyelination. Furthermore, intravenous administration of TNF-α significantly aggravated the EAN. In GBS patients' serum, elevated TNF-α levels have been associated with disease propensity. Immune modifying therapy reduced the TNF-α levels in GBS patients' serum, which is in agreement with the clinical recovery of GBS (Zhang et al., 2013). It has been reported that early onset treatment with DMF and Minocycline of EAN model lowered the expression level of TNF-alpha in the sciatic nerves of treated animals (Han et al., 2016; Zhang et al., 2009). Consistent with these reports, NP-PVA130 treatment also lowered the expression of TNF-α.

IL-1β serves a key role as a proinflammatory cytokine. It is involved in the activation of Schwan cells to secrete the IL-6 (Bolin et al., 1995). Upon microbial or inflammatory stimulation, mononuclear cells promptly synthesize IL-1β. Lymphocyte function-associated antigen 1 (LFA-1), an adhesion molecule, and IL-1β play a costimulatory role in the activation of T cells. In cooperation with TNF-α, IL-1β is a strong promoter of adhesion molecules and triggers the

protease release. Autoimmune response in EAN is suggested to be instigated by IL-1β (Zhu, et al., 1998). Several EAN treatment studies have reported that early onset treatment lowered the expression of IL-1β, for instance, therapeutic treatment with minocycline, and chrysin lowered the expression levels of IL-1β in the peripheral nerves. (Xiao et al., 2014; Zhang et al., 2009). Interestingly, despite having a difference in therapeutic nature of treatment, NP-PVA130 reduced the IL1-β expression in the sciatic nerves of the treated animals as compared to P2-peptide group animals. This establishes the immune-modulatory role of NP-PVA130 treatment.

IL-17 mediates the chemotaxis of monocytes to the inflammatory loci, supports the activation of T cells by enhancing the induction of co-stimulatory molecule (e.g., ICAM-1), and increases the production of nitric oxide and IL-6 to aggravate the local inflammatory response (Yi et al., 2011). During the acute stage of GBS, an elevated level of plasma IL-17 has been reported. Whereas IVIG treatment lowers the IL-17 concentrations (Li et al., 2012). IL-17A has been observed to decrease with the ameliorated clinical severity of EAN when atorvastatin, a lipid-lowering drug with anti-inflammatory properties is administered (Zhang et al., 2013). IL-17 levels have been found to decrease with the improved clinical prognosis of EAN when treated with Atorvastatin (a lipid lowering drug). In a previous EAN treatment study, therapeutic treatment with Curcumin (a natural antioxidant) lowered the expression of IL-17 in the peripheral nerves (Han et al., 2014).

Interestingly, a similar result was also observed in which early onset NP-PVA130 treatment lowered the expression of IL-17 in the sciatic nerves of NP treated animals as compared to the P2-peptide group animals.

It can be speculated that the immune modifying ability of NPs which interferes with the pathological mechanism of EAN might be due to the inhibition of inflammatory cytokines. Furthermore, it is quite reasonable to propose that the speculative mopping effect, exerted by the drug free NPs which inhibit the inflammatory monocytes from reaching the inflammatory loci, might be the reason behind the lower activation of M1 macrophages, resulting in lowering of proinflammatory cytokine profile. Keeping this in consideration, it can be suggested that drug

free PLGA-NPs may also be harnessed in the treatment of other inflammatory disorders where the lowering of inflammatory cytokines profile is aimed.

In sum, the emerging use of drug free NPs as immune modulatory agents has been validated in various immune models. Potential mechanism is believed to be that these NPs exert their immune modifying role by interacting with mononuclear phagocyte system and influence their function in inflammatory response. (Casey et al., 2019; Getts et al., 2014; Jeong et al., 2017; Saito et al., 2019; Sharma et al., 2022). This intriguing approach opened a new spectrum of NP based therapies with a uniqueness of not having an active pharmacological agent in formulation and considering NP alone as therapeutic agents. This study in particular complements the immune modifying role of drug free NPs on the disease course of EAN model. Besides reduction in clinical severity of EAN, a shift towards M2 in the balance of M1/M2 macrophage expression has been observed with NPs treatment. This provides an interesting insight to future studies focusing on treatment of various inflammatory models in which proliferation of macrophages are targeted.

Summary and Conclusion

Experimental autoimmune neuritis (EAN) animal model mimics the human Guillain-Barre syndrome (GBS), an autoimmune disease of demyelination and inflammation of peripheral nerves. Despite advancement in clinical management and provision of palliative treatment to GBS patients, they cannot alleviate the severity of disease. Trafficking of circulating inflammatory monocytes across the peripheral nervous system is crucial for the development of EAN. In recent studies, infusion of cargo free nanoparticles (NPs), derived from biodegradable poly (lactic-co-glycolic) acid (PLGA) mitigated the severity of clinical symptoms of inflammatory disease models by reducing the migration of inflammatory monocytes at the inflammatory site.

The aim of this study was to determine the therapeutic efficacy of PLGA based NPs on the disease course of EAN. Five in-vivo experimental studies were conducted to evaluate the therapeutic efficacy of NPs. 6-8 weeks old female Lewis rats were immunized with P2-peptide emulsified with complete Freunde's adjuvant to induce EAN. Clinical assessment of the animals was done by scoring. Preventive dose of 9 mg/kg of NP-PVA500 was administered daily into the tail vein before the onset of symptoms. NP treatment significantly reduced the trafficking of inflammatory monocytes at inflammatory loci and promoted tissue repair. Suppressed levels of activated macrophages (CD68+ cells), T cells (CD43) and MHC-II cells were observed in the sciatic nerves of the nanoparticle treated rats.

Early onset treatment with a similar dose of NP-PVA500 nm also reduced the clinical severity of EAN and the perivascular infiltration of monocytes into the particle treated sciatic nerves of rats. Therapeutic treatment with two different sized NPs (NP-PVA500, NP-PVA130) also mitigated the severity of disease and reduced the perivascular migration of inflammatory cells. NP infusions diverted the circulating monocytes towards the spleen thereby abrogating the inflammatory response. Therapeutic treatment with NP-PVA130 at the early onset of EAN also modulated the local immune response in the peripheral nerves of NPs treated animals by reducing the expression of proinflammatory markers (CD68, IL-1β, TNF-α) and elevated the expression levels of anti-

inflammatory markers (CD163). A shift towards M2 in the balance of M1/M2 macrophage expression has been observed with nanoparticle treatment.

A clear dose-dependent attenuation in the severity of EAN disease was observed when treated with NP-PVA130. A higher dose of NPs reduced the clinical severity of EAN significantly which also correlated with reduced histological nerve damage. Surfactant and polymer modified NPs reduced the clinical severity of EAN. Results from this study suggested that NPs can be tuned that they can efficiently modulate the circulating monocytes, which is critical to halt the initial inflammatory response. Interestingly, these PLGA based nanoparticles do not need an active pharmaceutical drug.

This study highlighted the importance of cargo-free NPs towards a safe, specific and cost-effective treatment approach to modulate the inflammatory monocytes mediated pathology in various inflammatory disorders and also provided a first hint in view of a potential modulatory role on M1/M2 balance. Further advancement in the domain of nano immunology requires more studies focused on structure–activity relationship (SAR). A clear understanding of mechanism of NPs mediated immunomodulation and identification of key aspects (composition, dose, roue of administration and physicochemical properties) triggering the therapeutic effects can open a new arena for formulation scientists in choosing appropriate NPs based therapies.

Publication

A part of this thesis has been published,

Elahi E, Ali ME, Zimmermann J, Getts DR, Müller M, Lamprecht A. Immune Modifying Effect of Drug Free Biodegradable Nanoparticles on Disease Course of Experimental Autoimmune Neuritis. Pharmaceutics. 2022; 14(11):2410. https://doi.org/10.3390/pharmaceutics14112410.

Acknowledgment

I would like to express my sincere thanks to my supervisor Prof. Dr. Marcus Müller for giving me the opportunity to work on this interesting research topic and his continuous support. I am grateful for his motivation and the constructive discussions throughout my work. I am also grateful to Prof. Dr. Alf Lamprecht for being my co-supervisor and providing me the opportunity to present and discuss my progress reports in his group. I am very grateful to him for his nice and constructive comments which led to significant improvements in my thesis draft and publication.

I am also highly indebted to PD Dr. Christian Tränkle and and PD Dr. Osman El-Maarri Dr. for their willingness to review my thesis and being the part of examination committee.

My sincere thanks are extended to Dr. Ehab Ali for his excellent support and guidance in preparation steps of Nanoparticles and Dr. Julian Zimmerman for his suggestions and mentorship for flow cytometry experiments. I want to thank my colleagues, Louisa Nitsch, Simon Petzinna, Muhammad and a very good friend Marco Hessler for all the fun time we spent together. I am also highly indebted to Frau Sandra Papel from student international office of university of Bonn for her cooperation and generous guidance towards my DAAD-Uni Bonn scholarship applications.

I am deeply grateful to my friends Atif Shahzad, Syed Saoud Zaidi, Rizwan Hayat, Sabeeh ul Hassan, Muhammad Ahmar Jamil and Saad Abdullah for their encouragement and support. Furthermore, I also thank Mr. Muhmmad Shahbaz, Dr. Shahid Atiq, Dr. Imran Ahmad, Dr. Jamshed Arslan and Dr. Ghulam Safdar for their motivation and guidance.

I specially thank my father-in-law, my teacher and my mentor Sir Chaudhary Noor Muhammad for his support, visionary guidance and prayers. I also cordially thank Mahrukh Ehsan for her patience and solely taking care of Irha Fatima during this period. Her continuous encouragement and motivation helped me a lot.

Finally, my biggest thanks to my parents and my siblings (Rimsha and Usman) for the great support, encouragement and love that I received from them. I accomplished my goals, because you were always there for me when I needed you. THANK YOU!!

List of Abbreviations

µg	microgram
µl	microlitre
µm	micrometre
AM	Adhesion molecule
BNB	Blood nerve barrier
CFA	Complete Freund's adjuvant
Cl2MDP	Dichloromethylene diphosphonate
CNS	Central nervous system
CRISPR	Clustered Regularly Interspaced Short Palindromic Repeat
DMF	Dimethyl fumarate
DNA	Deoxyribonucleic acid
e.g.,	Latin: exempli gratia (for the sake of an example)
EAE	Experimental autoimmune encephalomyelitis
EAN	Experimental autoimmune neuritis
EDTA	Ethylenediaminetetraacetic acid
EMA	European Medicine Agency
FDA	Food and Drug Administration
FITC	Fluorescein isothiocyanate
g	Gram
GBS	Guillain-Barré Syndrome
H&E	Haematoxylin and eosin
HBSS	Hank's Balanced Salt Solution
iNOS	inducible nitric oxide synthase
ICAM	Induction of co-stimulatory molecule
IFN-γ	Interferon gamma
IL-10	Interleukin-10
IL-12	Interleukin-12
IL-17	Interleukin-17
IL-1β	Interleukin-1 beta
IL-6	Interleukin-6
IVIG	Intravenous immunoglobulin
JAK/STAT	Janus Kinase/Signal Transducer and Activator of Transcription
Kg	kilograms
LFA-1	Lymphocyte function-associated antigen-1
MAG	Myelin associated glycoprotein

MARCO	Macrophage receptor with collagenous structure
MBP	Myelin basic protein
mg	milligram
MHC	Major histocompatibility complex
MIP	Macrophage inflammatory protein
ml	Millilitre
MMP	Matrix metalloproteinases
MNCs	Mononuclear cells
mRNA	messenger ribonucleic acid
mV	millivolt
MyD88	Myeloid differentiation factor 88
Na.Chol	Sodium cholate
NF-κB	Nuclear transcription factor-κB
nm	Nanometre
NO	Nitric oxide
NP	Nanoparticles
PBS	Phosphate Buffer Solution
PCL	Polycaprolactone
PI	Polydispersity index
PLGA	Poly (lactic-co-glycolic acid)
PMP	Purified myelin proteins
PNS	Peripheral nervous system
PVA	polyvinyl alcohol
RBC	Red blood cells
ROI	Reactive oxygen intermediates
RT-PCR	Reverse transcription polymerase chain reaction
S.D.	Standard deviation
SEM	Standard error of mean
TNF-α	Tumour necrosis factor-alpha
TGF- β	Tumour growth factor-beta
VCAM	Vascular cell adhesion molecule
WNV	West Nile virus

List of Figures

List of Tables

References

Abromson-Leeman, S., Bronson, R., & Dorf, M. E. (1995). Experimental autoimmune peripheral neuritis induced in BALB/c mice by myelin basic protein specific T cell clones. *J Exp Med*, *182*(2), 587–592.

Ambrosius, B., Pitarokoili, K., Schrewe, L., Pedreiturria, X., Motte, J., & Gold, R. (n.d.). Fingolimod attenuates experimental autoimmune neuritis and contributes to Schwann cell mediated axonal protection. *J Neuroinflammation*, *14*, 92.

Ambrosius, B., Pitarokoili, K., Schrewe, L., Pedreiturria, X., Motte, J., & Gold, R. (2017). Fingolimod attenuates experimental autoimmune neuritis and contributes to Schwann cell mediated axonal protection. *J Neuroinflammation*, *14*, 92.

Archelos, J. J., Mäurer, M., & Jung, S. (1994). Inhibition of experimental autoimmune neuritis by an antibody to the lymphocyte function-associated antigen-1. *Lab Invest*, *70*(5), 667–675.

Arnason, B. G. W., & Soliven, B. (1993). 80. Acute inflammatory demyelinating polyradiculoneuropathy. In P. J. Dyck (Ed.), *Peripheral neuropathy* (3rd edn, pp. 1437–1497).

Bai, X. F., Zhu, J., Zhang, G. X., Kaponides, G., Höjeberg, B., Meide, P. H., & Link, H. (1997). IL-10 suppresses experimental autoimmune neuritis and down-regulates TH1-type immune responses. *Clin Immunol Immunopathol*, *83*(2), 117–126.

Bala, I., Hariharan, S., & Kumar, M. N. (2004). PLGA nanoparticles in drug delivery: the state of the art. *Crit Rev Ther Drug Carrier Syst*, *21*, 387–422.

Ballin, R. H., & Thomas, P. K. (1969). Electron microscope observations on demyelination and remyelination in experimental allergic neuritis. *I. Demyelination." J Neurol Sci*, *8*(1), 1–18.

Bolin, L. M., Verity, A. N., Silver, J. E., Shooter, E. M., & Abrams, J. S. (1995). Interleukin-6 production by Schwann cells and induction in sciatic nerve injury. *J Neurochem*, *64*(2), 850–858.

Botelho, D., Leo, B. F., Massa, C., Sarkar, S., Tetley, T., Chung, K. F., Chen, S., Ryan, M. P., Porter, A., Atochina-Vasserman, E. N., Zhang, J., Schwander, S., & Gow, A. J. (2018). Exposure to Silver Nanospheres Leads to Altered Respiratory Mechanics and Delayed Immune Response in an in Vivo Murine Model. *Frontiers in Pharmacology*, *9*, 213. https://doi.org/10.3389/fphar.2018.00213

Brunner, R., Jensen-Jarolim, E., & Pali-Scholl, I. (2010). The ABC of clinical and experimental adjuvants—a brief overview. *Immunol. Lett*, *128*, 29–35.

Casey, L. M., Kakade, S., Decker, J. T., Rose, J. A., Deans, K., Shea, L. D., & Pearson, R. M. (2019). Cargo-less nanoparticles program innate immune cell responses to toll-like receptor activation. *Biomaterials*, *218*, 119333. https://doi.org/https://doi.org/10.1016/j.biomaterials.2019.119333

Castro, F. R., Farias, A. S., & Proença, P. L. (2007). The effect of treatment with crotapotin on the evolution of experimental autoimmune neuritis induced in Lewis rats. *Toxicon*, *49*(3), 299–305.

Che, Y., Qiu, J., Jin, T., Yin, F., Li, M., & Jiang, Y. (2016). Circulating memory T follicular helper subsets, Tfh2 and Tfh17, participate in the pathogenesis of Guillain-Barré syndrome. *Scientific Reports*, *6*, 20963. https://doi.org/10.1038/srep20963

Cheaburu-Yilmaz, C. N., Karasulu, H. Y., & Yilmaz, O. (2019). Chapter 13 - Nanoscaled Dispersed Systems Used in Drug-Delivery Applications. In C. Vasile (Ed.), *Polymeric Nanomaterials in Nanotherapeutics* (pp. 437–468). Elsevier. https://doi.org/https://doi.org/10.1016/B978-0-12-813932-5.00013-3

Chen, P., Piao, X., & Bonaldo, P. (2015). Role of macrophages in Wallerian degeneration and axonal regeneration after peripheral nerve injury. *Acta Neuropathol*, *v;130(5):605-18*.

Constantinescu, C. S., Hilliard, B., Lavi, E., Ventura, E., Venkatesh, V., & Rostami, A. (1996). Suppression of experimental autoimmune neuritis by phosphodiesterase inhibitor pentoxifylline. *J Neurol Sci*, *143*, 14–18.

Crucho, C. I. C., & Barros, M. T. (2017). Polymeric nanoparticles: A study on the preparation variables and characterization methods. *Materials Science and Engineering: C*, *80*, 771–784. https://doi.org/https://doi.org/10.1016/j.msec.2017.06.004

Danhier, F., Ansorena, E., Silva, J. M., Coco, R., le Breton, A., & Préat, V. (2012). PLGA-based nanoparticles: An overview of biomedical applications. *Journal of Controlled Release*, *161*(2), 505–522. https://doi.org/10.1016/j.jconrel.2012.01.043

de Almeida, M., Susnik, E., Drasler, B., Taladriz-Blanco, P., Petri-Fink, A., & Rothen-Rutishauser, B. (2021). Understanding nanoparticle endocytosis to improve targeting strategies in nanomedicine. *Chem. Soc. Rev.*, *50*(9), 5397–5434. https://doi.org/10.1039/D0CS01127D

Dobrovolskaia, M. A., Aggarwal, P., Hall, J. B., & McNeil, S. E. (2008). Preclinical studies to understand nanoparticle interaction with the immune system and its potential effects on nanoparticle biodistribution. *Molecular Pharmaceutics*, *5*(4), 487–495. https://doi.org/10.1021/mp800032f

Dobrovolskaia, M. A., & McNeil, S. E. (2007). Immunological properties of engineered nanomaterials. *Nature Nanotechnology*, *2*(8), 469–478. https://doi.org/10.1038/nnano.2007.223

Enders, U., Lobb, R., Pepinsky, R. B., Hartung, H. P., Toyka, K. v, & Gold, R. (1998). The role of the very late antigen-4 and its counterligand vascular cell adhesion molecule-1 in the pathogenesis of experimental autoimmune neuritis of the Lewis rat. *Brain*, *121*(Pt 7), 1257–1266.

Fessi, H., Puisieux, F., Devissaguet, J. Ph., Ammoury, N., & Benita, S. (1989). Nanocapsule formation by interfacial polymer deposition following solvent displacement. *International Journal of Pharmaceutics*, *55*(1), R1–R4. https://doi.org/https://doi.org/10.1016/0378-5173(89)90281-0

Fleischer, C. C., & Payne, C. K. (2012). Nanoparticle Surface Charge Mediates the Cellular Receptors Used by Protein–Nanoparticle Complexes. *The Journal of Physical Chemistry B*, *116*, 8901–8907.

Fromen, C. A., Kelley, W. J., Fish, M. B., Adili, R., Noble, J., Hoenerhoff, M. J., Holinstat, M., & Eniola-Adefeso, O. (2017). Neutrophil–Particle Interactions in Blood Circulation Drive Particle Clearance and Alter Neutrophil Responses in Acute Inflammation. *ACS Nano*, *11*(11), 10797–10807. https://doi.org/10.1021/acsnano.7b03190

Fujioka, T. (2018). Experimental autoimmune neuritis. *Clinical and Experimental Neuroimmunology*, *9*(2), 84–92.

Gabriel, C. M., Hughes, R. A., Moore, S. E., Smith, K. J., & Walsh, F. S. (1998). Induction of experimental autoimmune neuritis with peripheral myelin protein-22. *Brain*, *121*(Pt 10), 1895–1902.

Getts, D. R., Shea, L. D., Miller, S. D., & King, N. J. C. (2015). Harnessing nanoparticles for immune Modulation. *Trends in Immunology*, *xx*, 1–9.

Getts, D. R., Terry, R. L., Getts, M. T., Deffrasnes, C., Müller, M., Vreden, C., Ashhurst, T. M., Chami, B., McCarthy, D., Wu, H., Ma, J., Martin, A., Shae, L. D., Witting, P., Kansas, G. S., Kühn, J., Hafezi, W., Campbell, I. L., Reilly, D., … King, N. J. (2014). Therapeutic inflammatory monocyte modulation using immune-modifying microparticles. *Sci Transl Med*, *15;6(219):*

Gold, R., Archelos, J. J., & Hartung, H. P. (1999). Mechanisms of immune regulation in the peripheral nervous system. *Brain Pathol*, *9*(2), 343–360.

Guarino, V., Gentile, G., Sorrentino, L., & Ambrosio, L. (2017). Polycaprolactone: Synthesis, Properties, and Applications. In *Encyclopedia of Polymer Science and Technology* (pp. 1–36). American Cancer Society. https://doi.org/https://doi.org/10.1002/0471440264.pst658

Guillain, G., Barré, J. A., & Strohl, A. (1916). Sur un syndrome de radiculonévrite avec hyperalbuminose du liquide céphalo-rachidien sans reaction cellulaire: remarques sur les caractères cliniques et graphiques des reflexes tendineux. *Bulletins et mémoires de la Société des Médecins des Hôpitaux de Paris*, *40*, 1462–1470.

Hagiwara, W., Konno, S., Kihara, H., Inoue, M., & Fujioka, T. (2018). Effect of phosphodiesterase-3 inhibition on experimental autoimmune neuritis. *Toho J Med*. https://doi.org/10.14994/tohojmed.2017-016.

Han, F., Luo, B., & Shi, R. (2014). Curcumin ameliorates rat experimental autoimmune neuritis. *J Neurosci Res*, *92*, 743–750.

Han, R., Xiao, J., Zhai, H., & Hao, J. (2016). Dimethyl fumarate attenuates experimental autoimmune neuritis through the nuclear factor erythroid-derived 2-related factor 2/hemoxygenase-1 pathway by altering the balance of M1/M2 macrophages. *J Neuroinflammation*, *13*(1).

Hans, M. L., & Lowman, A. M. (2002). Biodegradable nanoparticles for drug delivery and targeting. *Curr. Opin. Solid State Mater. Sci*, *6*, 319–327.

Hartung, H. P., Kieseier, B. C., & Kiefer, R. (2001). Progress in Guillain-Barré syndrome. *Curr Opin Neurol*, *14*(5), 597–604.

Hartung, H. P., Willison, H., Jung, S., Pette, M., Toyka, K. v, & Giegerich, G. (1996). Autoimmune responses in peripheral nerve. *Springer Semin Immunopathol*, *18*(1), 97–123.

Hillaireau, H., & Couvreur, P. (2009). Nanocarriers' entry into the cell: relevance to drug delivery. *Cell Mol Life Sci*, *66*, 2873–2896.

Ho, T. W., McKhann, G. M., & Griffin, J. W. (1998). Human autoimmune neuropathies. *Annu Rev Neurosci*, *21*, 187–226.

Honary, S., & Zahir, F. (2013). Effect of zeta potential on the properties of nano-drug delivery systems-a review (Part 2). *Tropical Journal of Pharmaceutical Research*, *12*(2), 265–273.

Hörste G, M., AK, M., JI, M., HC, L., S, L., P, G., HP, H., O, S., C, K., & BC, K. (2011). Quinpramine ameliorates rat experimental autoimmune neuritis and redistributes MHC class II molecules. *PLoS One*, *6*(6), 21223.

Hughes, R. A., & Cornblath, D. R. (2005). Guillain-Barré syndrome. *Lancet*, *366*(9497), 1653–1666.

Jeong, S. J., Cooper, J. G., Ifergan, I., McGuire, T. L., Xu, D., Hunter, Z., Sharma, S., McCarthy, D., Miller, S. D., & Kessler, J. A. (2017). Intravenous immune-modifying nanoparticles as a therapy for spinal cord injury in mice. *Neurobiology of Disease*, *108*, 73–82. https://doi.org/https://doi.org/10.1016/j.nbd.2017.08.006

Jung, S., Huitinga, I., Schmidt, B., Zielasek, J., Dijkstra, C. D., Toyka, K. v, & Hartung, H. P. (1993). Selective elimination of macrophages by dichlormethylene diphosphonate-containing liposomes suppresses experimental autoimmune neuritis. *Journal of the Neurological Sciences*, *119*(2), 195–202. https://doi.org/10.1016/0022-510X(93)90134-K

Kajii, M., Kobayashi, F., Kashihara, J., Yuuki, T., Kubo, Y., Nakae, T., Kamizono, A., Kuzumoto, Y., & Kusunoki, S. (2014). Intravenous immunoglobulin preparation attenuates neurological signs in rat experimental autoimmune neuritis with the suppression of macrophage inflammatory protein -1α expression. *J Neuroimmunol*, *15;266(1-2):43-8*.

Kiazono, H., Hagiwara, W., Inoue, M., Konno, S., & Fujioka, T. (2014). Irbesartan ameliorates experimental autoimmune neuritis in Lewis rats. *Neurol Ther*, *31*, 43–49.

Kiefer, R., Kieseier, B. C., Stoll, G., & Hartung, H. P. (2001). The role of macrophages in immune-mediated damage to the peripheral nervous system. *Prog Neurobiol*, *64*(2), 109–127.

Kieseier, B. C., Kiefer, R., Gold, R., Hemmer, B., Willison, H. J., & Hartung, H. P. (2004). Advances in understanding and treatment of immune-mediated disorders of the peripheral nervous system. *Muscle Nerve*, *30*(2), 131–156.

Kieseier, B. C., Krivacic, K., Jung, S., Pischel, H., Toyka, K. v, Ransohoff, R. M., & Hartung, H. P. (2000). Sequential expression of chemokines in experimental autoimmune neuritis. *J Neuroimmunol*, *110*(1–2), 121–129.

Kieseier, B. C., Seifert, T., Giovannoni, G., & Hartung, H. P. (1999). Matrix metalloproteinases in inflammatory demyelination: targets for treatment. *Neurology*, *53*(1), 20–25.

Kiyozuka, T. (2005). The effect of atorvastatin on experimental autoimmune neuritis (EAN) in rat. *J Med Soc Toho*, *52*, 438–444.

Köller, H., Schroeter, M., Kieseier, B. C., & Hartung, H.-P. (2005). Chronic inflammatory demyelinating polyneuropathy--update on pathogenesis, diagnostic criteria and therapy. *Current Opinion in Neurology*, *18*(3), 273–278. https://doi.org/10.1097/01.wco.0000169744.14288.d1

Korn, T., Toyka, K., Hartung, H. P., & Jung, S. (2001). Suppression of experimental autoimmune neuritis by leflunomide. *Brain*, *124*(Pt 9), 1791–1802.

Krishnamoorthy, K., & Mahalingam, M. (2015). Selection of a suitable method for the preparation of polymeric nanoparticles: multi-criteria decision making approach. *Advanced Pharmaceutical Bulletin*, *5*(1), 57—67. https://doi.org/10.5681/apb.2015.008

Kudeken, T. (2009). The effect of sildenafil on experimental autoimmune neuritis (EAN) in rat. *J Med Soc Toho*, *56*, 9–15.

Kumari, A., Yadav, S. K., & Yadav, S. C. (2010). Biodegradable polymeric nanoparticles based drug delivery systems, Colloids Surf. *B Biointerfaces*, *75*, 1–18.

Lambracht-Washington, D., & Wolfe, G. I. (2011). Cytokines in Guillain–Barre´ syndrome: a lesson in time. *Archives of Neurology*, *68*, 427–428.

Lampert, P. W. (1969). Mechanism of demyelination in experimental allergic neuritis. Electron microscopic studies. *Lab Invest*, *20*(2), 127–138.

Li, S., Yu, M., Li, H., Zhang, H., & Jiang, Y. (2012). IL-17 and IL-22 in cerebrospinal fluid and plasma are elevated in Guillain-Barré syndrome. *Mediators of Inflammation*, *2012*, 260473. https://doi.org/10.1155/2012/260473

Lin, H. H., Spies, J. M., Lu, J. L., & Pollard, J. D. (2007). Effective treatment of experimental autoimmune neuritis with human immunoglobulin. *Journal of the Neurological Sciences*, *256*(1–2), 61–67. https://doi.org/10.1016/j.jns.2007.02.017

Luongo, L., Sajic, M., Grist, J., Clark, A. K., Maione, S., & Malcangio, M. (2008). Spinal changes associated with mechanical hypersensitivity in a model of Guillain-Barre syndrome. *Neurosci Lett*, *437*, 98–102.

Luster, A. D. (1998). Chemokines–chemotactic cytokines that mediate inflammation. *N Engl J Med*, *338*(7), 436–445.

Mantovani, A., Sica, A., Sozzani, S., Allavena, P., Vecchi, A., & Locati, M. (2004). The chemokine system in diverse forms of macrophage activation and polarization. *Trends Immunol*, *Dec;25(12):677-86*.

Martinez, F. O., Sica, A., Mantovani, A., & Locati, M. (2008). Macrophage activation and polarization. *Front Biosci*, *13*, 453–461.

Mäurer, M., & Gold, R. (2002). Animal models of immune-mediated neuropathies. *Curr Opin Neurol*, *15*(5), 617–622.

Mäurer, M., Toyka, K. v, & Gold, R. (2002). Immune mechanisms in acquired demyelinating neuropathies: lessons from animal models. *Neuromuscular Disorders*, *12*(4), 405–414. https://doi.org/https://doi.org/10.1016/S0960-8966(01)00302-9

McWhorter, F. Y., Davis, C. T., & Liu, W. F. (2015). Physical and mechanical regulation of macrophage phenotype and function. *Cell Mol Life Sci*, *72*(7), 1303–1316.

Meissner, Y., & Lamprecht, A. (2008). Alternative drug delivery approaches for the therapy of inflammatory bowel disease. *J Pharm Sci*, *97*(8), 2878–2891.

Miyamoto, K., Oka, N., Kawasaki, T., Miyake, S., Yamamura, T., & Akiguchi, I. (2002). New cyclooxygenase-2 inhibitors for treatment of experimental autoimmune neuritis. *Muscle Nerve*, *25*(2), 280–282.

Moalem-Taylor, G., Allbutt, H. N., Iordanova, M. D., & Tracey, D. J. (2007). Pain hypersensitivity in rats with experimental autoimmune neuritis, an animal model of human inflammatory demyelinating neuropathy. *Brain Behav Immun*, *21*, 699–710.

Mokarram, N., Merchant, A., Mukhatyar, V., Patel, G., & Bellamkonda, R. v. (2012). Effect of modulating macrophage phenotype on peripheral nerve repair. *Biomaterials*, *33*(34), 8793–8801.

Mueller, M., Leonhard, C., & Wacker, K. (2003). Macrophage response to peripheral nerve injury: the quantitative contribution of resident and hematogenous macrophages. *Lab Invest*, *83*(2), 175–185.

Müller, M., Stenner, M., Wacker, K., Ringelstein, E. B., Hickey, W. F., & Kiefer, R. (2006). Contribution of resident endoneurial macrophages to the local cellular response in experimental autoimmune neuritis. *J Neuropathol Exp Neurol*, *65*(5), 499–507.

Nyati, K. K., Prasad, K. N., Rizwan, A., Verma, A., & Paliwal, V. K. (2011). TH1 and TH2 response to Campylobacter jejuni antigen in Guillain-Barre syndrome. *Arch Neurol*, *68*(4), 445–452.

Pitarokoili, K., Kohle, F., & Motte, J. (2017). Anti-inflammatory and immunomodulatory potential of human immunoglobulin applied intrathecally in Lewis rat experimental autoimmune neuritis. *J Neuroimmunol*, *309*, 58–67.

Rao, J. P., & Geckeler, K. E. (2011). Polymer nanoparticles: Preparation techniques and size-control parameters. *Progress in Polymer Science*, *36*(7), 887–913. https://doi.org/https://doi.org/10.1016/j.progpolymsci.2011.01.001

Reagan-Shaw, S., Nihal, M., & Ahmad, N. (2008). Dose translation from animal to human studies revisited. *FASEB Journal : Official Publication of the Federation of American Societies for Experimental Biology*, *22*(3), 659–661. https://doi.org/10.1096/fj.07-9574LSF

Redford, E. J., Smith, K. J., & Gregson, N. A. (1997). A combined inhibitor of matrix metalloproteinase activity and tumour necrosis factor-alpha processing attenuates experimental autoimmune neuritis. *Brain*, *120*(Pt 10), 1895–1905.

Saito, E., Kuo, R., & Pearson, R. M. (2019). Designing drug-free biodegradable nanoparticles to modulate inflammatory monocytes and neutrophils for ameliorating inflammation. *J Control Release*, *300*, 185–196.

Sarkey, J. P., Richards, M. P., & EB Jr, S. (2007). Lovastatin attenuates nerve injury in an animal model of Guillain-Barré syndrome. *J Neurochem*, *100*(5), 1265–1277.

Schmidt, S. (1999). Candidate autoantigens in multiple sclerosis. *Mult Scler*, *5*(3), 147–160.

Schwerer, B. (2002). Antibodies against gangliosides: a link between preceding infection and immunopathogenesis of Guillain-Barré syndrome. *Microbes Infect*, *4*(3), 373–384.

Sharma, P., Alakesh, A., & Jhunjhunwala, S. (2022). The consequences of particle uptake on immune cells. *Trends in Pharmacological Sciences*, *43*(4), 305–320. https://doi.org/https://doi.org/10.1016/j.tips.2022.01.009

Shen, D., Chu, F., & Lang, Y. (2018). Beneficial or Harmful Role of Macrophages in Guillain-Barré Syndrome and Experimental Autoimmune Neuritis. *Mediators Inflamm*, *2018*(4286364).

Slutter, B., Bal, S., Keijzer, C., Mallants, R., Hagenaars, N., Que, I., Kaijzel, E., Eden, W. V., Augustijns, P., Lowik, C., Bouwstra, J., Broere, F., & Jiskoot, W. (2010). Nasal vaccination with N-trimethyl chitosan and PLGA based nanoparticles: nanoparticle characteristics determine quality and strength of the antibody response in mice against the encapsulated antigen. *Vaccine*, *28*, 6282–6291.

Smith, D. M., Simon, J. K., & Baker, J. R. (2013). Applications of nanotechnology for immunology. *Nature Reviews Immunology*, *13*(8), 592–605. https://doi.org/10.1038/nri3488

Srikanth, M., & Kessler, J. A. (2012). Nanotechnology - Novel therapeutics for CNS disorders. *Nature Reviews Neurology*, *8*(6), 307–318. https://doi.org/10.1038/nrneurol.2012.76

Stevens, A., Schabet, M., Wietholter, H., & Schott, K. (1990). Prednisolone therapy of experimental allergic neuritis in Lewis rats does not induce relapsing or chronic disease. *J Neuroimmunol*, *28*, 141–151.

Stoll, G., Jander, S., & Jung, S. (1993). Macrophages and endothelial cells express intercellular adhesion molecule-1 in immune-mediated demyelination but not in Wallerian degeneration of the rat peripheral nervous system. *Lab Invest*, *68*(6), 637–644.

Taylor, W. A., & Hughes, R. A. (1989). T lymphocyte activation antigens in Guillain-Barré syndrome and chronic idiopathic demyelinating polyradiculoneuropathy. *J Neuroimmunol*, *24*(1–2), 33–39.

Tedder, T. F., Steeber, D. A., Chen, A., & Engel, P. (1995). The selectins: vascular adhesion molecules. *Faseb J*, *9*(10), 866–873.

Treuel, L., Jiang, X., & Nienhaus, G. U. (2013). New views on cellular uptake and trafficking of manufactured nanoparticles. *Journal of The Royal Society Interface*, *10*.

van den Berg, B., Walgaard, C., Drenthen, J., Fokke, C., Jacobs, B. C., & van Doorn, P. A. (2014). Guillain-Barré syndrome: pathogenesis, diagnosis, treatment and prognosis. *Nature Reviews. Neurology*, *10*(8), 469—482. https://doi.org/10.1038/nrneurol.2014.121

van Doorn, P. A., Ruts, L., & Jacobs, B. C. (2008). Clinical features, pathogenesis, and treatment of Guillain-Barré syndrome. *The Lancet. Neurology*, *7*(10), 939–950. https://doi.org/10.1016/S1474-4422(08)70215-1

Verboon, C., van Doorn, P. A., & Jacobs, B. C. (2017). Treatment dilemmas in Guillain-Barré syndrome. *Journal of Neurology, Neurosurgery, and Psychiatry*, *88*(4), 346–352. https://doi.org/10.1136/jnnp-2016-314862

Vetten, M. A., Yah, C. S., Singh, T., & Gulumian, M. (2014). Challenges facing sterilization and depyrogenation of nanoparticles: effects on structural stability and biomedical applications. *Nanomedicine : Nanotechnology, Biology, and Medicine*, *10*(7), 1391–1399. https://doi.org/10.1016/j.nano.2014.03.017

Wachsmann, P., & Lamprecht, A. (2012). Polymeric nanoparticles for the selective therapy of inflammatory bowel disease. *Methods Enzymol*, *508*, 377–397.

Wachsmann, P., Moulari, B., Béduneau, A., Pellequer, Y., & Lamprecht, A. (2013). Surfactant-dependence of nanoparticle treatment in murine experimental colitis. *Journal of Controlled Release : Official Journal of the Controlled Release Society*, *172*(1), 62–68. https://doi.org/10.1016/j.jconrel.2013.07.031

Waksman, B. H., & Adams, R. D. (1955). Allergic neuritis: an experimental disease of rabbits induced by the injection of peripheral nervous tissue and adjuvants. *J Exp Med*, *102*(2), 213–236.

Walczyk, D., Bombelli, F. B., Monopoli, M. P., Lynch, I., & Dawson, K. A. (2010). What the Cell "Sees" in Bionanoscience. *Journal of the American Chemical Society*, *132*, 5761–5768.

Weerth, S., Berger, T., Lassmann, H., & Linington, C. (1999). Encephalitogenic and neuritogenic T cell responses to the myelin-associated glycoprotein (MAG) in the Lewis rat. *J Neuroimmunol*, *95*(1–2), 157–164.

Weishaupt, A., Gold, R., Hartung, T., Gaupp, S., Wendel, A., Bruck, W., & Toyka, K. v. (2000). Role of TNF-alpha in high-dose antigen therapy in experimental autoimmune neuritis: inhibition of TNF-alpha by neutralizing antibodies reduces Tcell apoptosis and prevents liver necrosis. *J Neuropathol Exp Neurol*, *59*(5), 368–376.

Wu, M. X., Daley, J. F., Rasmussen, R. A., & Schlossman, S. F. (1995). Monocytes are required to prime peripheral blood T cells to undergo apoptosis. *Proc Natl Acad Sci U S A*, *92*(5), 1525–1529.

Xiao, J., Zhai, H., Yao, Y., Wang, C., Jiang, W., Zhang, C., Simard, A. R., Zhang, R., & Hao, J. (2014). Chrysin attenuates experimental autoimmune neuritis by suppressing immuno-inflammatory responses. *Neuroscience*, *262*, 156–164. https://doi.org/10.1016/j.neuroscience.2014.01.004

Xu, J., Wang, J., Qiu, J., Liu, H., Wang, Y., Cui, Y., Humphry, R., Wang, N., DurKan, C., Chen, Y., Lu, Y., Ma, Q., Wu, W., Luo, Y., Xiao, L., & Wang, G. (2021). Nanoparticles retard immune cells recruitment in vivo by inhibiting chemokine expression. *Biomaterials*, *265*, 120392. https://doi.org/https://doi.org/10.1016/j.biomaterials.2020.120392

Yi, C., Zhang, Z., Wang, W., Zug, C., Schluesener, H. J., & Zhang, Z. (2011). Doxycycline attenuates peripheral inflammation in rat experimental autoimmune neuritis. *Neurochemical Research*, *36*(11), 1984–1990. https://doi.org/10.1007/s11064-011-0522-2

Yuki, N., & Hartung, H.-P. (2012). Guillain-Barré syndrome. *The New England Journal of Medicine*, *366*(24), 2294–2304. https://doi.org/10.1056/NEJMra1114525

Zettl, U. K., Mix, E., Zielasek, J., Stangel, M., Hartung, H. P., & Gold, R. (1997). Apoptosis of myelin-reactive T cells induced by reactive oxygen and nitrogen intermediates in vitro. *Cell Immunol*, *178*(1), 1–8.

Zhang, H. L., Zheng, X. Y., & Zhu, J. (2013). Th1/Th2/Th17/Treg cytokines in Guillain-Barré syndrome and experimental autoimmune neuritis. *Cytokine Growth Factor Rev*, *24*(5), 443–453.

Zhang, W., Cao, S., Liang, S., Tan, C. H., Luo, B., Xu, X., & Saw, P. E. (2020). Differently Charged Super-Paramagnetic Iron Oxide Nanoparticles Preferentially Induced M1-Like Phenotype of Macrophages. *Frontiers in Bioengineering and Biotechnology*, *8*, 537. https://doi.org/10.3389/fbioe.2020.00537

Zhang, Y., Hughes, K. R., Raghani, R. M., Ma, J., Orbach, S., Jeruss, J. S., & Shea, L. D. (2021). Cargo-free immunomodulatory nanoparticles combined with anti-PD-1 antibody for treating metastatic breast cancer. *Biomaterials*, *269*, 120666. https://doi.org/https://doi.org/10.1016/j.biomaterials.2021.120666

Zhang, Z. Y., Zhang, Z., Fauser, U., & Schluesener, H. J. (2009). Improved outcome of EAN, an animal model of GBS, through amelioration of peripheral and central inflammation by minocycline. *J Cell Mol Med*, *13*, 341–351.

Zhang, Z., Zhang, Z. Y., Fauser, U., & Schluesener, H. J. (2008). Valproic acid attenuates inflammation in experimental autoimmune neuritis. *Cell Mol Life Sci*, *65*(24), 4055–4065.

Zhu, J., Bai, X. F., Mix, E., & Link, H. (1997). Cytokine dichotomy in peripheral nervous system influences the outcome of experimental allergic neuritis: dynamics of mRNA expression for IL-1 beta, IL-6, IL-10, IL-12, TNF-alpha, TNF-beta, and cytolysin. *Clinical Immunology and Immunopathology*.

Zhu, J., Bai, X., Mix, E., Meide, P. H., Zwingenberger, K., & Link, H. (1997). Thalidomide suppresses T- and B-cell responses to myelin antigen in experimental allergic neuritis. *Clin Neuropharmacol*, *20*, 152–164.

Zhu, J., Bengtsson, B. O., & Mix, E. (1998). Clomipramine and imipramine suppress clinical signs and T and B cell response to myelin proteins in experimental autoimmune neuritis in Lewis rats. *J Autoimmun*, *11*(4), 319–327.

Zhu, J., Mix, E., & Link, H. (1998). Cytokine production and the pathogenesis of experimental autoimmune neuritis and Guillain-Barré syndrome. *J Neuroimmunol*, *84*(1), 40–52.

Zou, L. P., Deretzi, G., Pelidou, S. H., Levi, M., Wahren, B., Quiding, C., Meide, P., & Zhu, J. (2000). Rolipram suppresses experimental autoimmune neuritis and prevents relapses in Lewis ats. *Neuropharmacology*, *39*, 324–333.